Polysaccharide deacetylases from *Bacillus anthracis*

University of Crete

2012

Supervisor: Prof. Vassilis Bouriotis

Part of the experimental work was perfomed at the Institute Pasteur

under the supervision of Dr. Ivo Gomperts Boneca and Dr. Agnes Fouet

Αφιερωμένο στους αγαπημένους μου γονείς

Dedicated to my beloved parents

Ευχαριστίες

«Ευποιίας ης έτυχες, μνημόνευε»
Κλεόβουλος ο Ρόδιος, 6ος π.Χ. αιών, Εκ των 7 σοφών της Αρχ. Ελλάδος

Αρχικά οφείλω ένα μεγάλο ευχαριστώ στον κύριο Μπουριώτη που μου έδωσε την δυνατότητα να ξεκινήσω την ερευνητική μου πορεία στο εργαστήριό του και με εμπιστεύθηκε για να συνεχίσω, υπό την καθοδήγησή του, για την λήψη του διδακτορικού μου. Επιπλέον ένα μεγάλο ευχαριστώ αξίζει στον Dr. Ivo Boneca που με δέχθηκε επανειλλημένως στο εργαστήριο του στο Ινστιτούτο Παστέρ και στην Dr. Agnes Fouet που με έφερε για πρώτη φορά σε επαφή με τα μυστικά του *Bacillus anthracis*.

Ivo, I would like to express my deep gratitude since your support and faith were critical to the completion of my thesis. Agnes, I am especially indebted to you because you inspired me and introduced me to *B. anthracis* world... This thesis wouldn't have been possible if it weren't for your valuable help. Both of you were always so gracious and generous with your time and ideas!

Είναι σημαντικό επίσης να ευχαριστήσω τα μέλη της επταμελούς μου επιτροπής, Κυριάκο Πετράτο, Νίκο Πανόπουλο, Μιχάλη Κοκκινίδη, Κρίτωνα Καλαντίδη, Ιωάννη Βόντα και Τάσο Οικονόμου για τον χρόνο που μου αφιέρωσαν και τις πολύτιμες συμβουλές τους.

Ξεχωριστή μνεία αξίζει στα άτομα του εργαστηρίου τόσο στην Ελλάδα όσο και στην Γαλλία που με βοήθησαν, με ανέχτηκαν, ήταν εκεί να με συμβουλεύσουν, να με συνδράμουν ψυχολογικά, ηθικά και πρακτικά. Πρώτα απ'ολα να ευχαριστήσω την Μαίρη που έχει σταθεί δίπλα μας πρώτα σαν μητέρα και μετά σαν συνεργάτης. Επίσης, όλα τα παιδιά που έχουμε συνεργαστεί όπως η Αλεξάνδρα, η Θάνια, η Σοφία, η Γιούλη, η Δήμητρα, ο Σωτηράκης, που ήταν δίπλα μου και εντός και εκτός εργαστηρίου και αντικατέστησαν την οικογένειά μου εδώ στο Ηράκλειο... Τον Νίκο Τσολάκο για την παροχή του πρωτόκολλου καθαρισμού της BC1974. Την Μαρία την Μαρκάκη και την Κατερίνα Λιαπάκη που πολλές φορές χρειάστηκε να μας συμβουλέψουν ή να μας συνδράμουν σε αναλώσιμα... Τα παιδιά στο Παστέρ στην Γαλλία που με βοήθησαν να ενσωματωθώ στην πόλη αλλά και στο εργαστήριο. Αφιέρωσαν χρόνο και διάθεση σε μένα. Many thanks from the bottom of my heart to

Fred, Mathilde, Meriem, Sophie, Martine, Marine, Alice, Chantal, Willy, Daniel! Επίσης τους φίλους που έκανα στο Παρίσι και ομόρφυναν τις ώρες μου εκεί. Πολλά ευχαριστώ στον Γιώργο, την Τάνυα, τον Άκη, την Ιωάννα, τον Πάνο, τον Christoph, την Maria και την Marta . Είναι όμορφο να ξέρεις ότι μπορείς να εμπιστευθείς ανθρώπους και να μοιραστείς μαζί τους τις προσωπικές σου ανησυχίες και σκέψεις, όταν είσαι τόσο μακρυά από την οικογενειακή σου εστία. Ιδιαίτερη θέση στις ευχαριστίες έχουν δύο φιλικά μου άτομα που μου στάθηκαν τα τόσα χρόνια μου στο Ηράκλειο καλύτερα και από συγγενείς, τον Μαρίνο και τον Μάκη. Ένα ευχαριστώ είναι λίγο.

Τέλος, τίποτα δεν θα είχα καταφέρει στην ζωή μου αν δεν είχα την οικογένεια μου να με στηρίζει ηθικά, ψυχολογικά, υλικά. Δύο γονείς που στερήθηκαν και στερούνται για να έχω εγώ την «πολυτέλεια» να σπουδάζω και έναν αδερφό που στέκεται δίπλα τους βράχος και προσπαθεί να αναπληρώσει και την δική μου απουσία. Σας ευγνωμονώ για όλα...

TABLE OF CONTENTS

LIST OF FIGURES

LIST OF TABLES

LIST OF ABBREVIATIONS

PGNG-dacs	Peptidoglycan N-acetyl-glucosamine deacetylases
PA	Protective antigen
EF	Edema factor
LF	Lethal Factor
PG	Peptidoglycan
SLH	S-layer homology
D-Glu	D-Glutamic acid
D-Ala	D-Alanine
meso-Dap	meso-Diaminopimelic acid
UDP-GlcNAc	Uridine diphosphate N-acetylglucosamine
UDP-MurNAc	Uridine diphosphate N-acetylmuramic acid
GlcNAc	*N*-acetyl glucosamine
MurNAc	*N*-acetylmuramic acid
NADPH	Nicotinamide adenine dinucleotide phosphate
HF	Hydrofluoric acid
HF-PS	Hydrofluoric acid-derived Polysaccharide
Nod protein	Nucleotide-binding oligomerization domain proteins
SCWP	Secondary cell-wall polymers
DPGA	D-poly-γ-glutamate
GluPG	poly-glutamate bound to peptidoglycan
CE4	Carbohydrate Esterase family 4
LysM	Lysozyme M
LysP	Lysozyme P
BMM	Bone marrow-derived macrophages
PGNG-dac	Peptidoglycan N-acetyl glucosamine deacetylase
IPTG	isopropyl-*β*-D-thiogalactoside
Ni-NTA	Nickel-Nitrilotriacetic acid
DMF	Dimethylformamide
HPLC	High Pressure Liquid Chromatography
rp- HPLC	Reverse phase High Pressure Liquid Chromatography
GPGP polylinker	Glycine-Proline-Glycine-Proline polylinker
GFP	Green Fluorescent Protein
Ct	Cycle threshold
LD_{50}s	Fifty percent lethal doses
MALDI-TOF	Matrix Assisted Laser Desorption Ionization - Time of Flight
MALDI-PSD	Matrix Assisted Laser Desorption Ionization - Post-source decay
GMDP	N-Acetyl-D-glucosaminyl-(β 1,4)-N-acetylmuramyl-L-alanyl-D-isoglutamine

ΠΕΡΙΛΗΨΗ

Οι απακετυλάσες *N*-ακετυλογλυκοζαμίνης της πεπτιδογλυκάνης ανήκουν στην οικογένεια των εστερασών υδατανθράκων CE4 η οποία περιλαμβάνει ένζυμα που χαρακτηρίζονται από σημαντική ομολογία και λειτουργικές ομοιότητες. Το μακρομόριο της πεπτιδογλυκάνης αποτελεί σημαντική δομή του κυτταρικού τοιχώματος όλων των βακτηρίων. Πρόσφατες μελέτες έχουν δείξει ότι η *N*-απακετυλίωση του μορίου της *N*-ακέτυλ-γλυκοζαμίνης της πεπτιδογλυκάνης επηρεάζει την αναγνώριση του βακτηρίου από τα κύτταρα του ξενιστή ενώ παρέχει προστασία από παράγοντες της πρωταρχικής ανοσολογικής απόκρισης του ξενιστή, όπως η λυσοζύμη. Αποτελεί εξαιρετικό ενδιαφέρον το γεγονός ότι τα γονιδιώματα του *Bacillus cereus* και του συγγενικού παθογόνου *Bacillus anthracis* (ομολογία >90%) περιέχουν το καθένα 10 γονίδια τα οποία κωδικοποιούν για πιθανές απακετυλάσες πολυσακχαριτών, από τις οποίες 5 αναφέρονται ως πιθανές απακετυλάσες *N*-ακετυλογλυκοζαμίνης της πεπτιδογλυκάνης (*ba1961, ba1977, ba2944, ba3679, ba5436*). Οι αιτίες ύπαρξης τόσο μεγάλου αριθμού γονιδίων που κωδικοποιούν για πιθανές *N*-απακετυλάσες πεπτιδογλυκάνης στο γονιδίωμα του *B.anthracis*, σε αντίθεση με τα γονιδιώματα άλλων παθογόνων βακτηρίων τα οποία διαθέτουν μόνο ένα αντίστοιχο γονίδιο, αποτελεί το βασικό επιστημονικό ερώτημα της παρούσας διδακτορικής διατριβής.

Για την διαλεύκανση του βιολογικού ρόλου των παραπάνω ενζύμων ακολουθήθηκε συνδυασμός βιοχημικών και μοριακών τεχνικών καθώς και κυτταρικός εντοπισμός τους στο βακτήριο *B. anthracis*. Συνοψίζοντας τα αποτελέσματα της παρούσας διατριβής καταλήγουμε ότι 3 από τα 5 ένζυμα (BA1977, BA1961, BA3679) έχουν ενεργότητα *N*-απακετυλίωσης της *N*-ακετυλ-γλυκοζαμίνης της πεπτιδογλυκάνης. Ωστόσο, μόνο το ένζυμο BA1977 παρέχει προστασία στο βακτήριο ενάντια στην εξωγενώς προστιθέμενη λυσοζύμη *in vitro* καθώς και σε ζωϊκό μοντέλο και συνεπώς είναι απαραίτητο για την πλήρη παθογονικότητα του *B. anthracis*. Αντίθετα, τα ένζυμα BA1961 και BA3679 φαίνεται να σχετίζονται με την ρύθμιση της σύνθεσης πεπτιδογλυκάνης πρωταρχικά στα σημεία κυτταρικής διαίρεσης. Τα υπόλοιπα 2 ένζυμα συμμετέχουν στην βιοσύνθεση του ουδέτερου πολυσακχαρίτη του *B. anthracis* καθώς εμπλέκονται είτε στην τροποποίησή του

(BA2944) είτε στην πρόσδεσή του στο μόριο της πεπτιδογλυκάνης και στην αγκυροβόληση των πρωτεϊνών της S στοιβάδας (BA5436).

Τα αποτελέσματα της παρούσας διατριβής παρέχουν καινοτόμα και θεμελιώδη στοιχεία για την λειτουργία των *N*-απακετυλασών των καταλοίπων της *N*-ακέτυλογλυκοζαμίνης της πεπτιδογλυκάνης στον παθογόνο μικροοργανισμό *B. anthracis*. Επιπρόσθετα θέτουν τις βάσεις για την ανάπτυξη νέων αντιβιοτικών που στοχεύουν σε ένζυμα τροποποίησης διάφορων μακρομορίων, δομές οι οποίες είναι απαραίτητες για την κυτταρική ανάπτυξη και την παθογένεια των βακτηρίων.

ABSTRACT

The development of new antibacterial agents to combat the rapidly increasing antibiotic resistance is a priority area in antiinfectives research. Peptidoglycan deacetylases (PGNG-dacs) are required for bacterial evasion to lysozyme and innate immune responses. Interestingly, there is an unusual occurrence of multiple putative polysaccharide deacetylases in *Bacillus anthracis*. The envelope of *B. anthracis* is a dynamic organelle composed of peptidoglycan (PG), a pyruvylated neutral polysaccharide (PS) which anchors SLH-harboring proteins including the S-layer proteins Sap and EA1 and a poly-γ-D-glutamic (PDGA) capsule. Our results provide novel and fundamental insights on the function of polysaccharide deacetylases in a major bioterrorism agent and a framework for the design of novel antibacterial agents targeting enzymes involved in the modification of crucial cell wall polysaccharides for cell growth and virulence.

PGNG-dacs are members of Carbohydrate esterase family 4 (CE4 as defined in the CAZY database http://www.cazy.org/CE4_bacteria.html). Today ten PGNG-dacs and/or their corresponding genes from several bacteria including major pathogens such as *B. cereus*, *S. pneumoniae* and *L. monocytogenes* have been identified and characterized. *B. cereus sensu lato* strains including *B. anthracis* contain ten polysaccharide deacetylase homologues. Five of these homologues have been proposed to be PGNG-dacs.

We have employed a combined biochemical and genetic (knock-out) analysis in order to elucidate the biological roles of the five putative PGNG-dac's. The intrinsic biochemical properties of each deacetylase did not reveal any clear hypothesis for their individual role in *B. anthracis*. To assign such function, we constructed single mutants of all five putative deacetylase encoding genes from *B. anthracis* and compared their major phenotype characteristics. The combination of different phenotypes of each mutant allowed us to propose a role for BA1961, BA1977 and BA3679 in PG metabolism. Instead, BA2944 and BA5436 appear to be involved at two distinct steps in the synthesis of the neutral polysaccharide. BA1977 exhibit similar properties to presently characterized PGNG-dacs (lysozyme sensitivity, reduced virulence of their mutants in mice models) indicating that PG *N*-deacetylation could be a general mechanism used by bacteria to evade the host

immune system. Inhibition of PGNG-dacs would enable the host organism to lyse invading bacteria with lysozyme that is inactive against bacteria with functional enzymes. Transmission electron microscopy (TEM) of the 7702 Δ*ba1961* and 7702 Δ*ba3679* mutant strains reveal local thickenings of their PG mainly in the septa and show a defect in cell separation and a reduced efficiency of spore formation compared to the wild type. While little is known about PG biosynthesis in *B. anthracis*, two enzymatic systems are thought to act in *B. subtilis*, one for lateral cell wall growth and a second for division/septation. If an analogous organization exists in *B. anthracis* our data suggest that BA1961 and BA3679 would interact predominantly with complexes at the septum while BA1977 would associate with lateral PG synthesis. Finally, BA5436 and BA2944, do not act on peptidoglycan. In fact, in the 7702 Δ*ba5436* mutant strain, we were unable to detect the neutral polysaccharide in the cell wall nor the S-layer proteins associated to it. HPLC analysis of 7702 Δ*ba2944* mutant polysaccharide reveal a shift of the peak corresponding to PS of the parental 7702 strain suggesting the polysaccharide as substrate of BA2944. Our results suggest that BA2944 is required to deacetylate the trisaccharide repeating unit, →6)-α-d-GlcNAc-(1→4)-β-d-ManNAc-(1→4)-β-d-GlcNAc-(1→, the building block for the synthesis of the neutral polysaccharide, while BA5436 would modify the proposed linkage unit GlcNAc-ManNAc. Experiments aiming to further elucidate the biological roles of BA5436 and BA2944 are in progress.

PGNG-dacs are validated antibiotic targets as demonstrated by the reduced virulence of mutant strains of various pathogens and RΔ*ba1977* in this study. The identification of additional PGNG-dacs BA1961 and BA3679 in *B. anthracis* with different suggested biological role, offers new targets for the design of inhibitors against this bioterrorism agent. Furthermore, elucidation of the structural requirements for S-layer assembly in Gram+ bacteria may lead to numerous translational applications in industrial processes exploiting the SLH domain and synthetic pyruvylated polysaccharides.

1. INTRODUCTION

1.1 History

Anthrax disease was first recorded in chapter 9 of Exodus in the Bible as the 5th plague of Egypt. Hippocrates (5th century B.C.) was the first who actually assigned the name anthrax describing a disease characterized by the black color of skin lesions and blood [1] while the Roman poet Virgil (70-19 B.C., 3rd Georgic) provided one of the first and most detailed descriptions of an anthrax epidemic, highlighting the ability of this disease to spread to humans [2]. Professors J McSherry and R Kilpatrick refer to anthrax as the cause for the plague of Athens in 430 BC [3].

Anthrax was implicated in the death of animals all over the planet, until the end of the 19th century. In Europe, anthrax was responsible for enormous domestic livestock losses from the 17th to the 19th century. Notably, in the middle of the 18th century, about half of the ovine population in Europe was decimated by the disease [1]. Several outbreaks have occurred in recent history in numerous countries including Iran, South Africa, Namibia, Nepal, China and Australia, between 1940 to 2000 [4].

The identification of the etiological agent of anthrax was first demonstrated by Robert Koch in 1876 when he described the consistent presence of a rod-shaped microorganism that could transform to spores under poor nutrient conditions, in the blood and tissues of diseased animals. This demonstration was further confirmed by Louis Pasteur who verified that the bacterium itself is sufficient to cause disease [5]. Cohn gave the name *Bacillus anthracis* to this bacterium in 1875.

Bacillus anthracis study paved the way for the establishment of modern medical microbiology and vaccinology, since it provided knowledge for the fight against infectious diseases. However, this pathogenic bacterium has also been used for unethical goals such as bioweapon for bacteriological warfare and bioterrorism [5]. Military programs of several countries such as Japan, Great Britain and Soviet Union during the 20th century used *B. anthracis* spores as a weapon for mass destruction. The latest and most known “anthrax attack” was located at the East Coast of the United States during the dawn of 21st century. 22 anthrax cases were confirmed, 11 of those were due to inhalational anthrax (5 people died) and the rest were due to cutaneous anthrax [6]. The American National Institute of Allergy and Infectious Diseases (NIAID) was granted by the American Government a $1,5 billion grant (2,5

greater than that obtained by the same institute between 1985 and 1998 for AIDS research) to initiate studies aiming to prevent or combat bioterrorism.

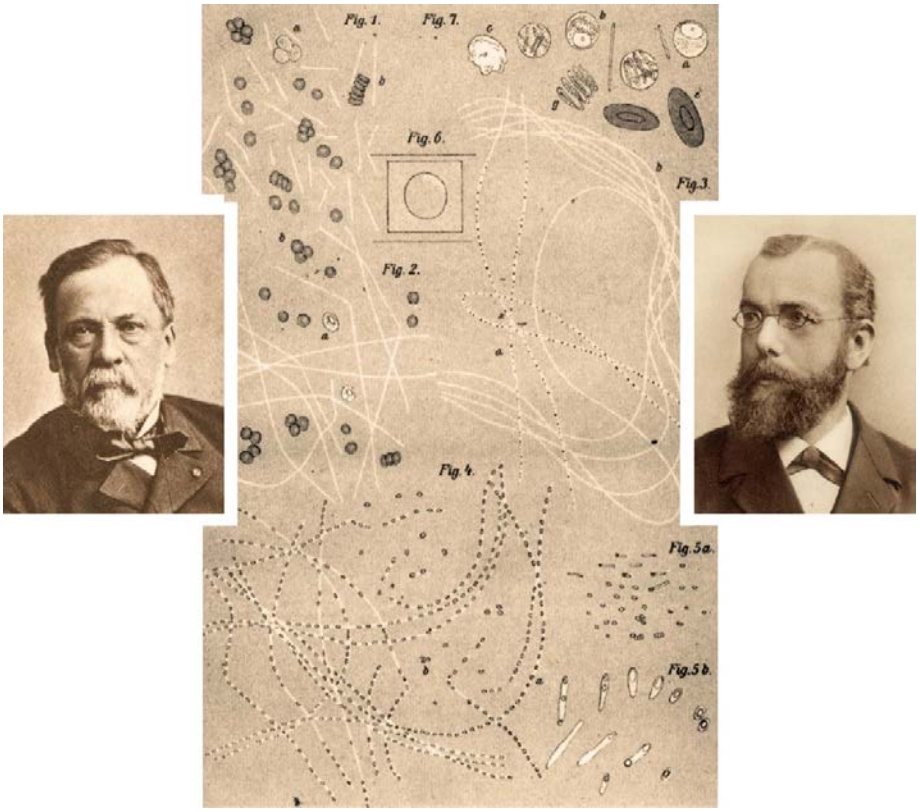

Figure 1. *The discoverers of Bacillus anthracis and fathers of medical microbiology: Robert Koch (1843–1910), right, and Louis Pasteur (1822–1895), left, and inset: drawing of B. anthracis by Robert Koch together with Ferdinand Cohn (1828–1898) made in 1876* [5].

1.2 Bacillus anthracis pathophysiology and life cycle

Bacillus anthracis belongs to the *Bacillus cereus sensu lato* group of bacteria, which also includes *Bacillus cereus*, *Bacillus thurigiensis*, *Bacillus mycoides*, *Bacillus pseudomycoides*, and *Bacillus weihenstephanensis* [7, 8]. All members of the above group share the same characteristics: Gram positive, rod-shaped, spore forming, non motile, aerobic, soil bacteria with similar growth features and natural genetic exchange systems. Among the bacteria of *Bacillus cereus* group there are several

distinguishable species-specific characteristics, including those related to pathogenicity.

Pathogenic *Bacillus anthracis* endospores reach a primary site in the subcutaneous layer (95% in the United States), gastrointestinal mucosa (< 1%), or alveolar spaces (5%). Cutaneous anthrax results from exposure to the spores of *B anthracis* while handling sick animals or contaminated wool, hair, or animal hides. Pulmonary anthrax results from inhaling anthrax spores while gastrointestinal anthrax results from ingesting meat products that are exposed to the bacterium. Anthrax caused by inhalation is usually fatal, and symptoms usually begin days after exposure. This delay makes the initial exposure to *B anthracis* difficult to track. For cutaneous and gastrointestinal anthrax, low-level germination occurs at the primary site, leading to local edema and necrosis. Endospores are phagocytosed by macrophages and germinate. Macrophages containing bacilli detach and migrate to the regional lymph node. Vegetative anthrax bacilli grow in the lymph node, creating regional hemorrhagic lymphadenitis. Bacteria spread through the blood and lymph and increase to high numbers, causing severe septicemia. High levels of exotoxins are produced that are responsible for overt symptoms and death. In a small number of cases, systemic anthrax can lead to meningeal involvement by means of lymphatic or hematogenous spread. In cases of pulmonary anthrax, peribronchial hemorrhagic lymphadenitis blocks pulmonary lymphatic drainage, leading to pulmonary edema. Death results from septicemia, toxemia, or pulmonary complications and can occur one to seven days after exposure [9].

Bacillus anthracis fully virulent strains harbor two plasmids, pXO1 and pXO2. pXO1 plasmid encodes approximately 143 ORFs, which include the structural toxin genes, *pagA*, *lef*, and *cya*; regulatory elements controlling the toxin genes (e.g. *atxA* [10]); *gerX*, a three-gene germination operon [11]. Among the 143 ORFs there is a collection of putative transposases, resolvases, and integrases, suggesting an evolution involving lateral movement of DNA among species [12]. pXO2 plasmid carries the capsule biosynthetic operon (see chapter 1.3.4) [13, 14], as well as the regulatory genes, *acpA* and *acpB* [15, 16]. The regulatory genes, *acpA*, *acpB* and *atxA*, have been reported to control expression of the *Bacillus anthracis* capsule biosynthesis operon *capBCAD*. The *atxA* gene is located on the virulence plasmid pXO1, while pXO2 carries *acpA* and the *cap* genes. *acpA* has been viewed as the major regulator of the *cap* operon because it is essential for capsule gene expression

in a pXO1− pXO2+ strain. *atxA* is essential for toxin gene transcription but has also been implicated in regulation of the *cap* genes [17].

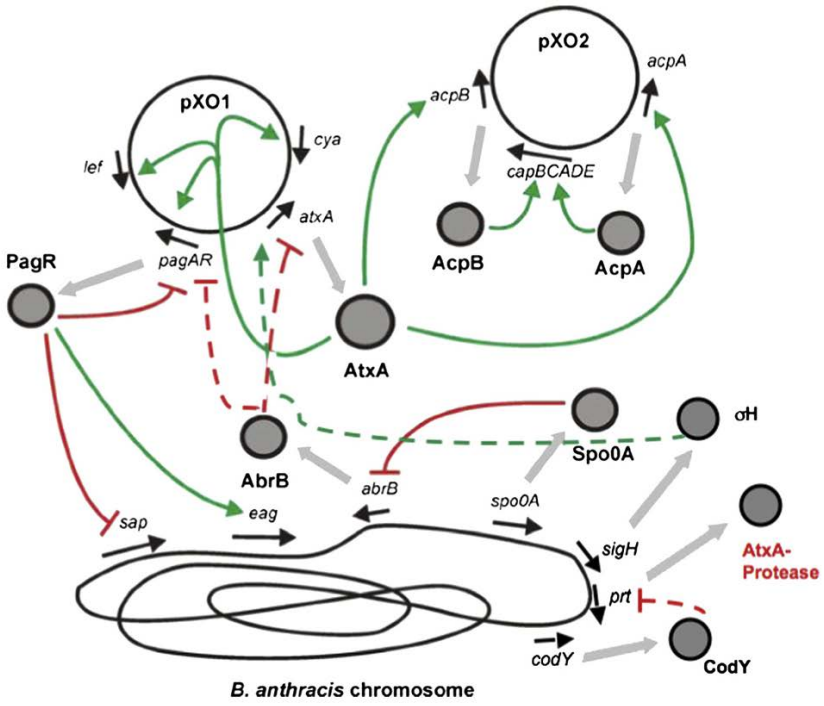

Figure 2. *Schematic representation of known Bacillus anthracis regulatory networks involving AtxA (modified from (Fouet and Mock, 2006)). Black arrows represent genes and gray arrows denote synthesis of the corresponding gene product. Gray circles represent proteins. Green arrows and red lines denote activation and repression of gene expression, respectively. Dotted lines indicate suggested, controversial or hypothetic regulations.* [15].

Bacillus anthracis life-cycle can be divided into two phases: multiplication in the mammalian host and persistence in the soil. Cutaneous, gastrointestinal or respiratory entry of *Bacillus anthracis* spores into mammals may lead to systemic infection and death. Anthrax spores are globally distributed in soils with high calcium levels and a pH above 6.1 [18] and are highly resistant to heat, drying, ultraviolet light, and gamma radiation [9]. After infection, spore germination initiates in macrophages by the *gerH* locus [19] to create vegetative cells that can replicate to

high numbers in virtually all body tissues. Death of the host and contact of infected tissues with oxygen initiates sporulation [11].

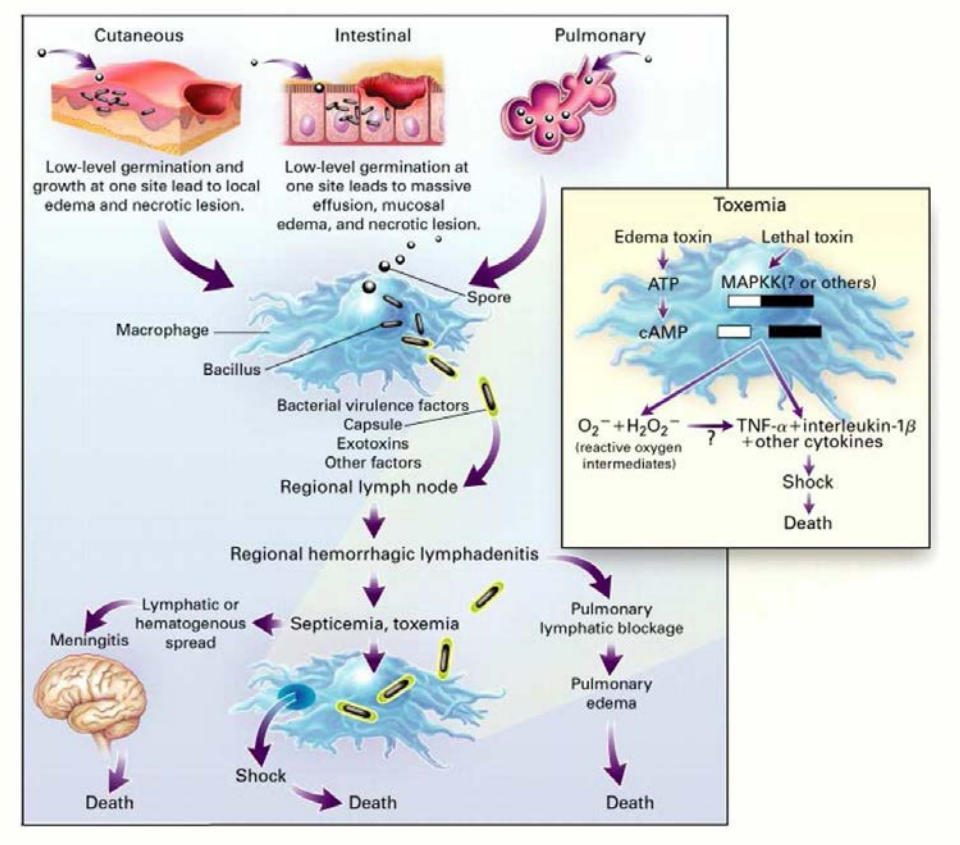

Figure 3. *Pathophysiology of Anthrax* [9].

1.3 Bacillus anthracis toxins

B.anthracis toxins play a key role in the pathogenesis of anthrax and are composed of three proteins acting in binary combinations [20], termed protective antigen (PA), for its ability to elicit a protective immune response against anthrax [21]; lethal factor (LF); and edema factor (EF).

The first step of *B. anthracis* toxin entry into host cells is the highly specific binding of PA to the cell surface receptor. On cell binding, PA is cleaved by furin or a furin-like protease. The proteolytic activation of PA leads to its oligomerization into ring-shaped heptamers and the exposure of the binding site for EF and LF. This is a

critical step in the intoxication. There is evidence that heptameric PA binds a maximum of three molecules of either LF or EF, or a combination of both [22].This step is then followed by the internalization of the hetero-oligomeric complex. At acidic pH, the prepore is converted to a pore and this transition is followed by insertion of the pore into the membrane, allowing the translocation of LF/EF.

EF is an adenylate cyclase converting intracellularATP into cAMP, an activity that is dependent on the eukaryotic protein calmodulin [23]. Edema Toxin therefore provokes a substantial increase in intracellular cAMP levels.

LF is a zinc protease. It has been reported that LF cleaves the N-terminus of all isoforms of mitogen-activated protein kinases (MAPKKs), except for MAPKK-5 [24, 25]. The MAPK pathway relays environmental signals to the transcriptional machinery in the nucleus and thus modulates gene expression via a burst of protein phosphorylation.

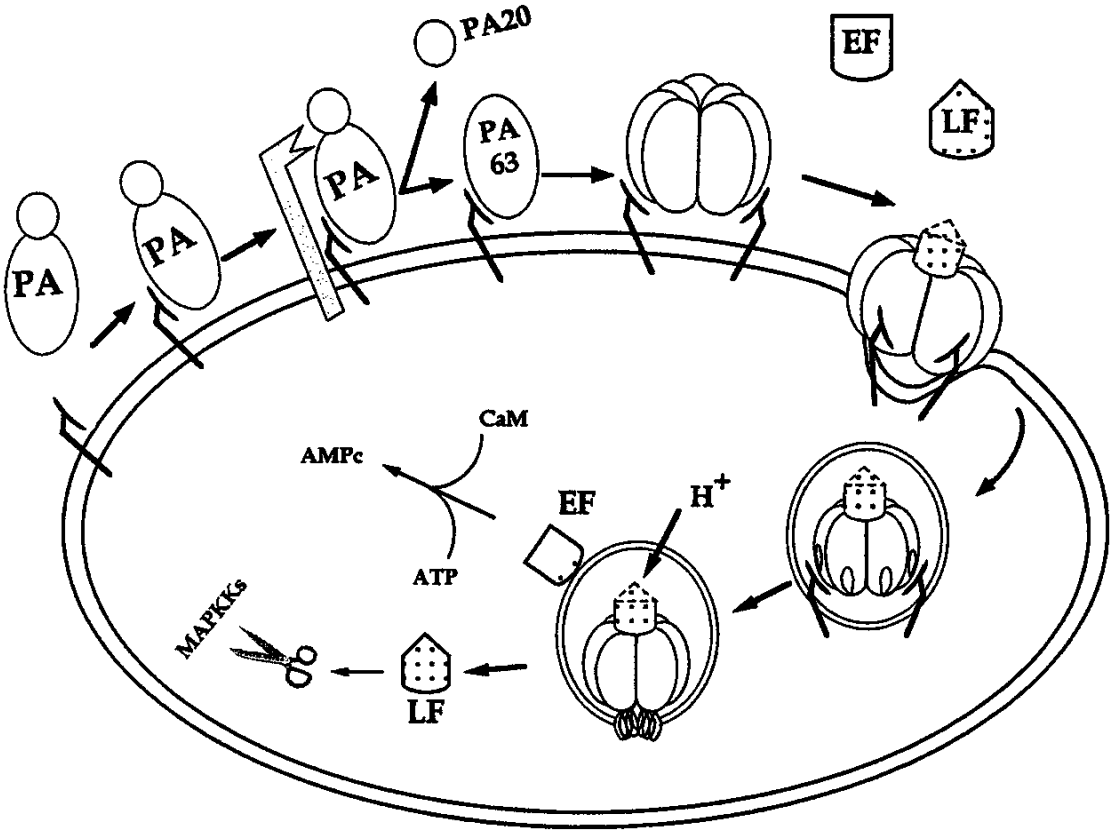

Figure 4. *Cellular model of action of anthrax toxins* [16].

1.4 Bacillus anthracis cell wall

Bacillus anthracis possesses several distinct surface layers namely: peptidoglycan, neutral polysaccharide, S-layer and capsule and are outlined below:

1.3.1 Peptidoglycan

B. anthracis peptidoglycan (PG) is of the A1 γ type according to the chemotaxonomy developed by Schleifer and Kandler [26]. PG is a highly complex and essential macromolecule of *B. anthracis* cell wall that enables the bacterium to resist osmotic pressure. Although it is often regarded as an inert structure, PG is a dynamic macromolecule with tight regulation. PG remodeling allows cell growth and division. *B. anthracis* PG consists of alternating units of *N*-acetylglucosamine and *N*-acetylmuramic acid held together by β(1-4) glycosidic bonds and the stem peptides which are composed by L-Ala, D-Glu, meso-DAP, D-Ala, D-Ala. 32% of the stem peptides are cross-linked between meso-DAP and D-Ala. A variety of different enzymes, including glycosyltransferases, transpeptidases (also known as penicillin-binding proteins), D,D-carboxypeptidases and hydrolases shape the three-dimensional structure of PG, increasing the complexity of this macromolecule [27].

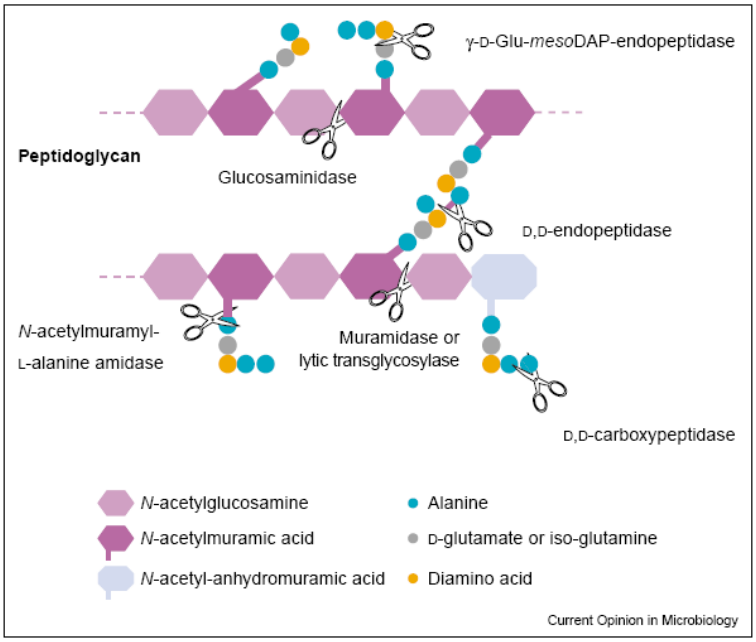

Figure 5. *PG hydrolases. Schematic representation of the PG layer. The scissors indicate the bond that is hydrolyzed by the corresponding PG hydrolase.*

PG biosynthesis is a complex process that can be divided in three sets of reactions depending on which compartment these reactions take place:

(i) *Cytoplasmic reactions* (synthesis of the nucleotide precursors). In the cytoplasm, fructose-6-phosphate is converted to UDP-GlcNAc via a series of cytosolic enzymatic reactions. Subsequently, UDP-GlcNAc is converted to UDP-MurNAc by two enzymatic reactions involving MurA and MurB. MurA catalyses the first step of this transformation by transferring the enolpyruvate moiety of phosphoenolpyruvate (PEP) to the 3-hydroxyl of UDP-GlcNAc. MurB reduces the UDP-GlcNAc-enolpyruvate product using one equivalent of NADPH and a solvent-derived proton. This two-electron reduction creates the lactyl ether of UDP-MurNAc. MurC,D,E,F are responsible for the assembly of the stem peptide leading to UDP-MurNAc-pentapeptide [28].

(ii) *Reactions at the inner side of the cytoplasmic membrane* (synthesis of lipid-linked intermediates). Transferase MraY catalyzes the transfer of the phospho-MurNAc-pentapeptide moiety of UDP-MurNAc-pentapeptide to the membrane acceptor, undecaprenyl phosphate, yielding lipid I. Transferase MurG catalyzes the addition of *N*-acetylglucosamine to the *N*-acetylmuramic acid residue of lipid I leading to the formation of lipid II, the molecule that carries the complete disaccharide-peptide monomer unit: GlcNAc-β-(1-4)-MurNAc-L-Ala-γ-D-Glu-DAP (or L-Lys)-D-Ala-D-Ala [29].

(iii) *Reactions at the outer side of the cytoplasmic membrane* (polymerization reactions). Transfer of lipid II to the outer leaflet, initiates the extracellular steps of PG formation. In a recent study it was demonstrated that the translocation of lipid II through the bacterial membrane requires the integral membrane protein FtsW [30]. Lipid II is subsequently polymerized by a transglycosylation reaction in order to form the immature PG. Transglycosylation is followed by a transpeptidation reaction for PG maturation and cross-bridges formation [31].

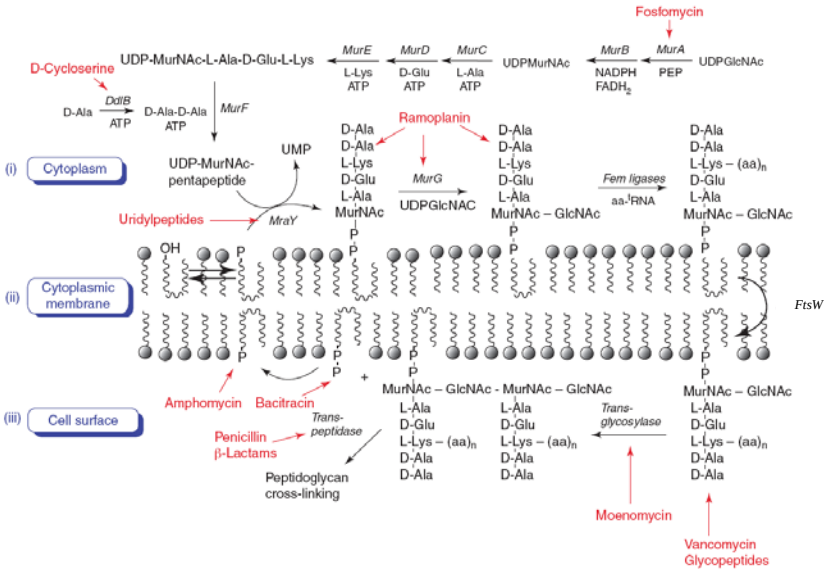

Figure 6. *The PG biosynthetic pathway showing sites of action of natural product inhibitors.*

The innate immune system functions as both the critical first line of defense during infection and as a sensor of non-pathogenic microbiota during steady state conditions. The fundamental part of the adaptive immunity consists of cells with highly specific receptors that can recognize any antigenic molecule.

Bacteria contain numerous ligands that are sensed by host proteins called pattern recognition receptors (PRRs). PRRs have developed to be a sensor for pathogenic and non-pathogenic microbes and are found in diverse eukaryotes including flies, mice and humans [32]. They recognize fundamental parts of microbes and are hardly susceptible to modification. The major families of host receptors that sense bacterial products include the secreted peptidoglycan recognition proteins (PGRPs), the Toll-like receptors (TLRs) and the Nod-like receptors (NLRs). The TLRs are predominantly surface-associated host proteins, NLRs are cytoplasmic proteins while PGRPs are secreted.

PG, the fundamental component of the cell wall in gram-positive and gram-negative bacteria is a typical example of a molecular pattern for the immune system to recognize. It is sensed directly through secreted peptidoglycan recognition proteins (PGRPs). Humans and mice have four PGRPs, PGLYRP-1, PGLYRP-2, PGLYRP-3, and PGLYRP-4 [33]. *Drosophila* immune system detects Gram-positive bacteria by a complex of two pattern recognition receptors: peptidoglycan recognition protein SA

(PGRP-SA) and Gram-negative binding protein 1 (GNBP1), acting upstream of Toll. This recognition step activates the Toll signalling pathway. GNBP1 is involved in the hydrolysis of Gram-positive peptidoglycan producing new glycan reducing ends, which are subsequently detected by PGRP-SA [34]. The minimal structure needed to activate the Toll pathway is a muropeptide dimer with a free reducing end of the N-acetyl muramic acid, essential for activity. Monomeric muropeptides were inactive and inhibitory in combination with dimers [35].

In addition, intracellular peptidoglycan is detected by two host receptors in the NLR family. Nucleotide-binding oligomerisation domain-containing protein 1 (Nod1) is a host intracellular protein that is expressed in virtually all cell types [36]. Nod1 senses fragments of the stem peptide terminating in meso-DAP, with or without MurNAc attached, and may also sense stem peptide fragments terminating in D-Ala in some hosts [37]. Nod2 is a host intracellular protein that is expressed in myelomonocytic cells, such as monocytes, macrophages and neutrophils, and is also expressed by stimulated epithelial cells in culture [38, 39]. Both Nod1 and Nod2 contain nucleotide oligomerisation binding (Nod) domains that define the receptor family, in addition to C-terminal leucine-rich repeat (LRR) domains which sense PG and *N*-terminal caspase recruitment domains (CARD) which interact with adaptor molecules to initiate signaling cascades following receptor activation [36, 38].

In 2003, major advances were made with the identification of the cytosolic receptors (Nod) 1 and (Nod) 2 as sensors of unique muropeptides derived from PG hydrolysis [40-42]. Sensing of muropeptides from Nod-Like receptors initiates multiple proinflammatory pathways for controlling infection and initiating antigen-specific immune responses. Nod1 recognizes GlcNAc-MurNAc-L-alanine-γ-D-glutamate-mesoDAP produced by most Gram-negative bacteria and some Gram-positive bacteria, including *Bacillus* species. Nod2 senses the PG motif GlcNAc-MurNAc-L-alanine-D-glutamate, which is present in nearly all Gram-negative and Gram-positive bacteria.

TLRs are also pattern recognition receptors that can be activated by pathogen associated molecular patterns, which activates transcription factors as NF-κB. These transcription factors in their turn induce pro-inflammatory cytokine and cell-surface protein production [43]. TLR2 and TLR 4 are known to be the most important in bacterial cell wall recognition. Toll-like receptor-2 (TLR-2) senses lipoteichoic acid (LTA) and lipoproteins, which are associated with bacterial membranes [43, 44], and

may also sense PG, although this remains controversial [45, 46]. Each TLR is a type 1 membrane protein with an extracellular leucine-rich domain that functions as the binding domain for the ligand. The intracellular tail of TLRs contain a highly conserved Toll/IL-1R (TIR) homology domain that in case of activation recruits MyD88. MyD88 binds to the tail and then activates an intracellular pathway [47].

Many pathogenic species contain secondary modifications at their glycan strands affecting their recognition by the innate immune system of the host [48]. The three major secondary modifications of PG are: *N*-deacetylation of GlcNAc, *N*-glycolylation of MurNAc, and *O*-acetylation of MurNAc and GlcNAc. Enzymes responsible for *N*-deacetylation of MurNAc have also been identified [49]. *B.subtilis* MurNAc *N*-deacetylase (PdaA) together with CwlD (*N*-acetylmuramoyl-L-alanine amidase) are necessary for muramic δ-lactam production in spore cortex, a PG structure surrounding the protoplasm which is postulated to have a role in attaining protoplast dehydration. PdaA probably carries out both deacetylation of MurNAc residues and δ-lactam ring formation and requires the product of CwlD activity as a substrate [50].

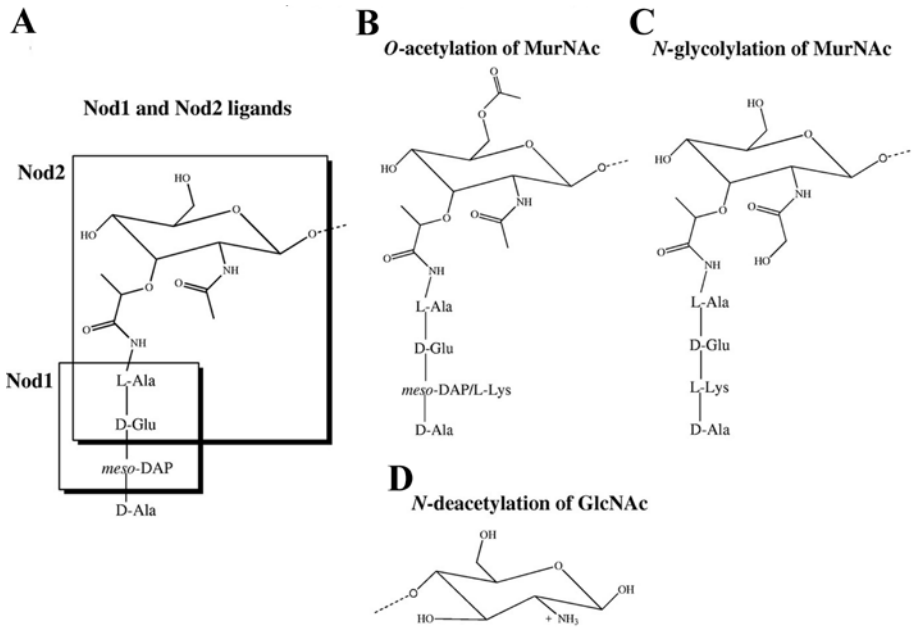

Figure 7. A. *The minimal motifs sensed* by *Nod1 and Nod2 ligands are shown in boxes, depicted on an unmodified, Gram-negative MurNAc residue*. B, C, D. *The three modifications of the glycan backbone discussed in the text* [51].

In all bacterial species the glycan strands of PG are linked to other cell-wall polymers shortly after their insertion into the cell wall. For example, the glycan strands of Gram-positive species attach secondary cell-wall polymers (SCWP) via phosphodiester bonds to their GlcNAc or MurNAc residues of PG. The SCWP can be divided into four groups based on their structural characteristics:

(a) Teichoic acids [52]

(b) Lipoteichoic acids: short phosphate containing polymer chains that can be attached to PG via a lipid anchor [52, 53].

(c) Teichuronic acids: uronic acid-containing heteropolysaccharides [53] and

(d) Neutral and acidic polysaccharides

1.3.2 Neutral Polysaccharide

Whereas *Bacillus anthracis* cell wall is most probably devoid of teichoic acids due to the very low phosphate concentration in the cell wall and to an apparent incomplete biosynthetic pathway [54], it contains a non classical secondary wall polysaccharide that is extracted by hydrofluoric acid treatment. This neutral polysaccharide is covalently attached to PG, has a molecular mass of 12 kDa and consists of galactose, *N*-acetylglucosamine and *N*-acetylmannosamine [55, 56]. Its backbone is composed of multiple trisaccharide repeats of: →6)-α-d-GlcNAc-(1→4)-β-d-ManNAc-(1→4)-β-d-GlcNAc-(1→ and is highly substituted at all GlcNAc residues with α- and β-Gal residues [57]. This polysaccharide is present in both *Bacillus anthracis* vegetative cell wall and spores [58]. An interesting observation is the similarity of glycosyl compositions among SCWP of *B. cereus* strains that have recently been shown to cause severe pneumonia in humans [59] with those of *B. anthracis*. This finding possibly indicates the functional importance of the hydrofluoric acid derived-neutral polysaccharide (and the S-layer homology domain anchoring mechanism) in virulence. One major modification of *B. anthracis* polysaccharide is the addition of a pyruvyl group located exclusively at the terminal β-ManNAc residue of the distal non-reducing end, opposite the end linked to PG. Pyruvylation of the neutral polysaccharide is required for the retention of the SLH-containing proteins to the cell wall, including autolysins that are required for the

bacterium correct septation [60]. Forsberg *et al* reported that the SCWP of *B. anthracis* is also O-acetylated and *N*-deacetylated at specific HexNAc residues, adjacent to the pyruvylated residue [61].

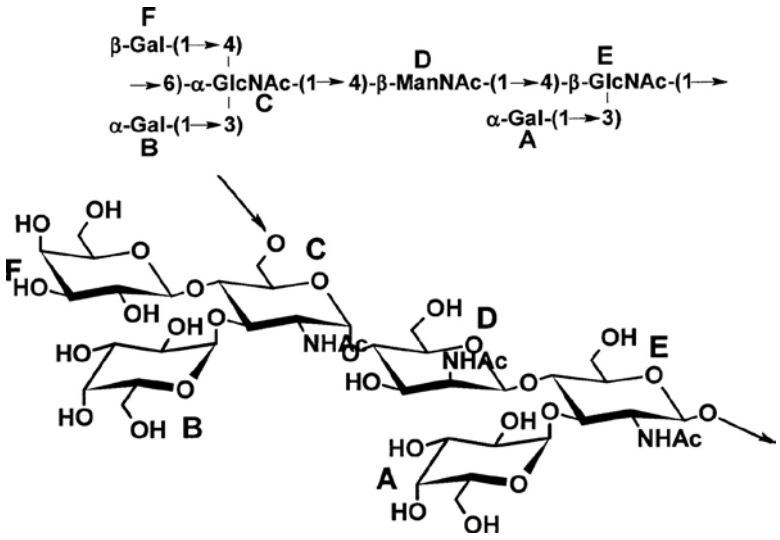

Figure 8: *The structure of the HF-PS repeating oligosaccharide from B. anthracis* [57].

Notably, the SCWP is linked to the peptidoglycan layer via murein linkage units, i.e. a GlcNAc-ManNAc moiety that is linked to the C6 hydroxyl of MurNAc via a phosphodiester bond. [62]

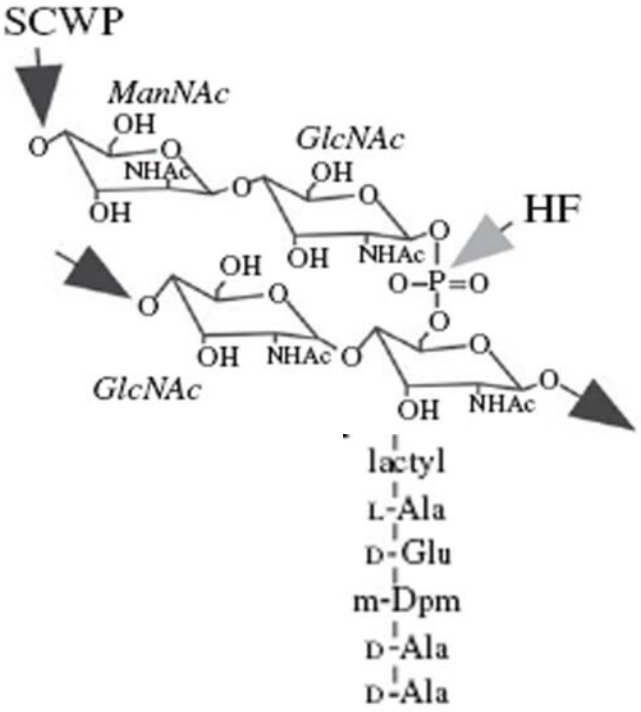

Figure 9. *Structure of the murein linkage unit that tethers the SCWP to the peptidoglycan of bacilli* [62].

1.3.3 S-layer

S-layer proteins self-assemble spontaneously as a bidimensional crystalline array covering the entire cell surface. They are targeted to the cell wall by a domain composed of 3 motifs composed of ~55 residues each and contain 10-15 conserved amino acids referred to as the SLH (S-layer homology) domain [63]. S-layer proteins are attached to the pyruvylated neutral polysaccharide of *B. anthracis* and represent up to 15% of total protein in the bacterium. They can function as protective coats, as structures involved in cell adhesion and as molecule or ion traps. Analysis of the distribution of S-layers in the *B.cereus* group revealed that these structures were present in 51 strains [64]. 16 of these strains were from the *B. anthracis* cluster [8] and all but 2 were either clinical isolates or entomopathogens. These findings suggest that there is a phylogenetic origin for the presence of S-layers and an ecological pressure for the maintenance of such a structure.

B. anthracis possesses two 94 kDa S-layer proteins, namely Sap (surface array protein) and EA1 (extractable antigen 1) [65-67], encoded by the chromosomal genes, *sap* and *eag*. Sap and EA1 are expressed during different developmental stages in *B.*

anthracis. Sap is expressed during exponential growth and EA1 during the stationary phase of growth [65, 68], indicating that S-layers may be growth dependent dynamic structures. Regulation of S-layer protein expression depends on the medium and the strain employed. In conditions that mimic the mammal host, *sap* and *eag* transcription is, respectively, repressed or activated. Expression of the S-layer genes in fully virulent *B. anthracis* strains (pXO1+, pXO2+), is regulated indirectly by AtxA, *B. anthracis* master regulator. This regulation is mediated by PagR, encoded by the second gene of a bicistronic operon coding for a toxin component [69]. It is also well established that AtxA activates transcription of the capsule operon *in vitro* [70] indicating that expression of the S-layer genes is linked to that of the major virulence factors.

Notably, in *B. anthracis* Ames genome, there are 20 chromosomal genes, two genes on plasmid pXO1 and one on pXO2 that carry an SLH-domain [9, 16, 71]. These genes encode various proteins with a range of structural or enzymatic functions. One example of such proteins is AmiA, which is a *B. anthracis* pXO2-encoded peptidoglycan hydrolase [72].

1.3.4 Capsule

B. anthracis capsule is currently considered to be one of its major virulence factors [9, 16]. Although most bacterial capsules are composed of polysaccharides, *B. anthracis* capsule is a polymer of D-glutamic acid, linked by peptide bonds between c-carboxyl and a-amino groups (gamma type). *B. anthracis* capsule synthesis is encoded by its second virulence plasmid pXO2 [73]. Five pXO2 genes, namely *capB, capC, capA, capD* and *capE*, arranged in an operon, are essential for capsule synthesis in *B. anthracis* [13, 74]. These genes encode for membrane proteins which probably constitute a complex. *B. anthracis* capsule is covalently anchored to PG. In a *capD* mutant strain, poly-glutamate is found associated to the surface in a non-covalent way and heating the cells at 65^0C is sufficient to completely release the poly-glutamate filaments into the supernatant [14]. CapD catalyses the amide bond formation between poly-gamma-glutamate and the meso-Dap of PG [75].

The capsule is poorly immunogenic and behaves as a thymus-independent type 2 antigen [76]; this is most probably due to its highly repetitive structure, its enantiomeric content, and the γ linkage of the gammaPDGA filaments. Studies have

shown that the anchored capsule provides an additional virulence mechanism for *B. anthracis*, by mediating retention of bacteria in the liver. It is generally considered that bacteria reach the blood from the initial infection site through the lymphatic system [9, 77] and initially colonize the spleen [77]. Interestingly, the splenic vein connects with the portal vein, which irrigates the liver. Bacilli exiting from the spleen will thus be retained in the liver through interaction of the poly-γ-glutamate capsule with the liver endothelium. *In vitro* experiments have demonstrated that the *B. anthracis* capsule is antiphagocytic, similarly to capsule function in other pathogenic bacteria. Noncapsulated bacilli are readily phagocytosed by tissue culture macrophages while capsulated bacilli are rarely phagocytosed [78, 79]. It has been hypothesized that the capsule enables the bacterium to avoid demise in the host because a strong humoral immune response is not generated against the outer surface of the bacteria.

When the poly-glutamate is bound to a carrier component, such as PG that is naturally linked to (GluPG), it becomes immunogenic and anti poly-glutamate antibodies are observed in patients with anthrax. GluPG, by itself, is able to partially protect mice against infection with an encapsulated non-toxinogenic strain of *B. anthracis*. GluPG in combination with PA protects mice against a fully virulent strain, probably by inhibiting bacilli multiplication and toxemia [80].

1.4 Polysaccharide deacetylases

1.4.1 Characterization

Bacterial peptidoglycan deacetylases are members of the carbohydrate esterase family 4 (CE4) (CAZY database, http://www.cazy.org/). CE4 esterases are metal dependent enzymes that catalyze the hydrolysis of either *N*-linked acetyl group from GlcNAc residues (chitin deacetylase, NodB, and peptidoglycan GlcNAc deacetylase), or O-linked acetyl groups from O-acetylxylose residues (acetylxylan esterase, xylanase) [81-83]. The first gene encoding a peptidoglycan *N*-acetylglucosamine deacetylase (*pgdA*) was identified in *Streptococcus pneumoniae* [84]. So far, ten peptidoglycan *N*-acetylglucosamine deacetylases or their corresponding genes have been studied namely: PgdA from *S.pneumoniae* [84], PdaA from *Bacillus subtilis*

[49], BC1960 and BC3618 from *Bacillus cereus* [85], PgdA from *Listeria monocytogenes* [86], PgdA from *Lactococcus lactis* [87], PgdA from *Streptococcus suis* [88], SfPgdA from *Shigella flexneri* [89], PdaC from *Bacillus subtilis* [90] and *Enterococcus faecalis* (*pgdA*) (Benachour *et al.*, 2012).

Furthermore, three recent reports focus on putative polysaccharide deacetylases which do not act on PG but their substrates have not been identified [91-93]. *Streptococcus mutants pgda* gene encodes for a metal-dependent CE4 esterase that plays a role in tuning cell surface properties and in interactions with (salivary) agglutinin, an essential component of the innate immune system, most likely through deacetylation of an as-yet-unidentified polysaccharide [91]. *Streptococcus iniae* genome encodes for a polysaccharide deacetylase (*pdi* gene) that is involved in adherence and invasion, lysozyme resistance and survival in fish blood while it plays a role in the pathogenesis of the bacterium [92]. Finally, *Staphylococcus epidermidis* possesses the surface-attached protein IcaB that is responsible for deacetylation of its exopolysaccharide. This enzymatic reaction is essential for key virulence mechanisms of *S. epidermidis*, namely biofilm formation, colonization, and resistance to neutrophil phagocytosis and human antibacterial peptides [93].

1.4.2 Structure

CE4 enzymes contain a conserved NodB homology domain, and adopt a distorted $(\alpha/\beta)_8$ barrel fold, with the active site lying in a groove. Most of the structures contain a divalent ion in the active site that is essential for enzyme activity and which is coordinated by highly conserved histidine and aspartate residues.

The first structure of a CE-4 family member that has been reported was peptidoglycan deacetylase (BsPdaA) from *Bacillus subtilis* [94]. BsPdaA deacetylates peptidoglycan *N*-acetyl muramic acid residues, leading to the formation of δ-lactam structures [49]. The BsPdaA NodB homology domain appears to adopt an $(\alpha/\beta)_8$ fold, with a 30 Å groove running over the surface of the protein harboring the majority of the conserved residues and the two of the conserved histidines come together in the bottom of the active site. The observed groove is compatible with the fact that all members of the CE-4 family recognise multimeric substrates.

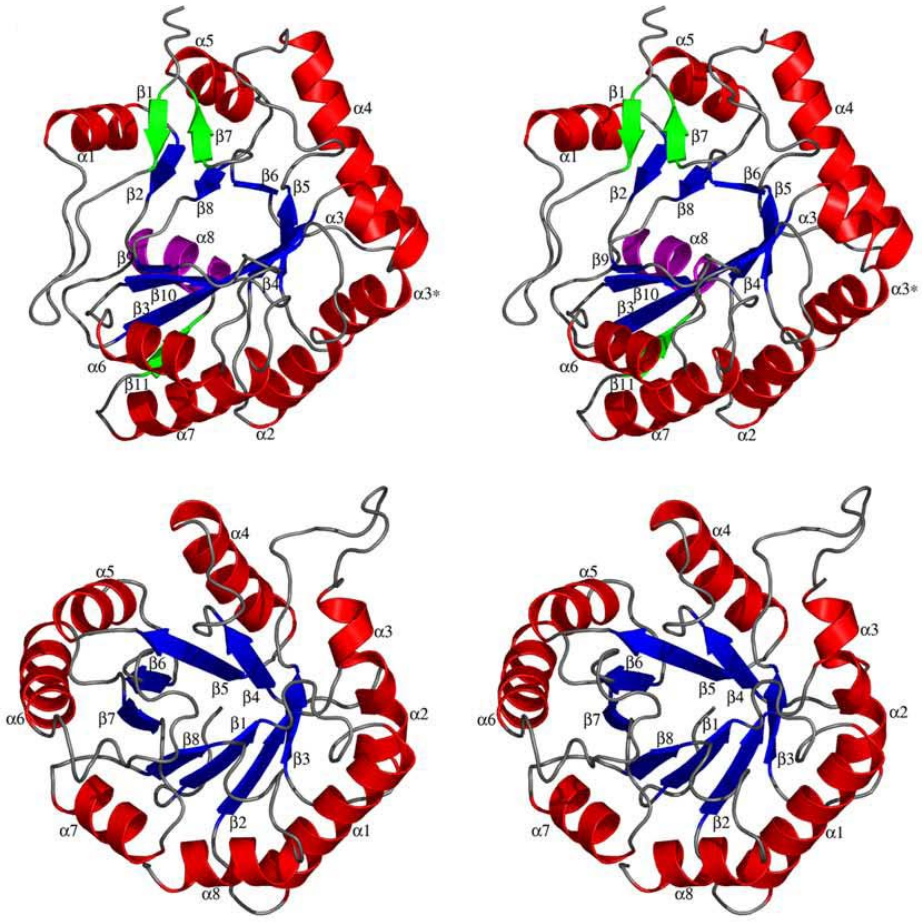

Figure 10. *Stereo images of PdaA and the canonical TIM barrel (β/α)$_8$ fold. PdaA secondary structure elements without equivalents in the TIM barrel fold are coloured green (strands) or magenta (helix).*

Blair et al, solved the structure of a GlcNAc peptidoglycan deacetylase from *Streptococcus pneumoniae* (SpPgdA) demonstrating a unique three-domain structure. Strikingly, structural comparison with the structure of *B. subtilis* PdaA, showed that, although the overall fold of the catalytic core is the same, there are significant topological differences. In this study, they proposed a reaction mechanism for CE4 enzymes using structural, mutagenesis, and in silico data [95]. SpPgdA catalyzes the removal of an *N*-acetyl group by binding a water molecule on its tightly bound zinc. The catalytic base, Asp-275, abstracts a proton from this water molecule, creating a nucleophile to attack the carbonyl carbon in the substrate to produce a tetrahedral

oxyanion intermediate. The charge on this intermediate is stabilized by the metal and the Tyr-367 backbone nitrogen. His-417 then protonates this intermediate on the nitrogen, generating a free amine and also the acetate product on the zinc, as observed in the crystal structure.

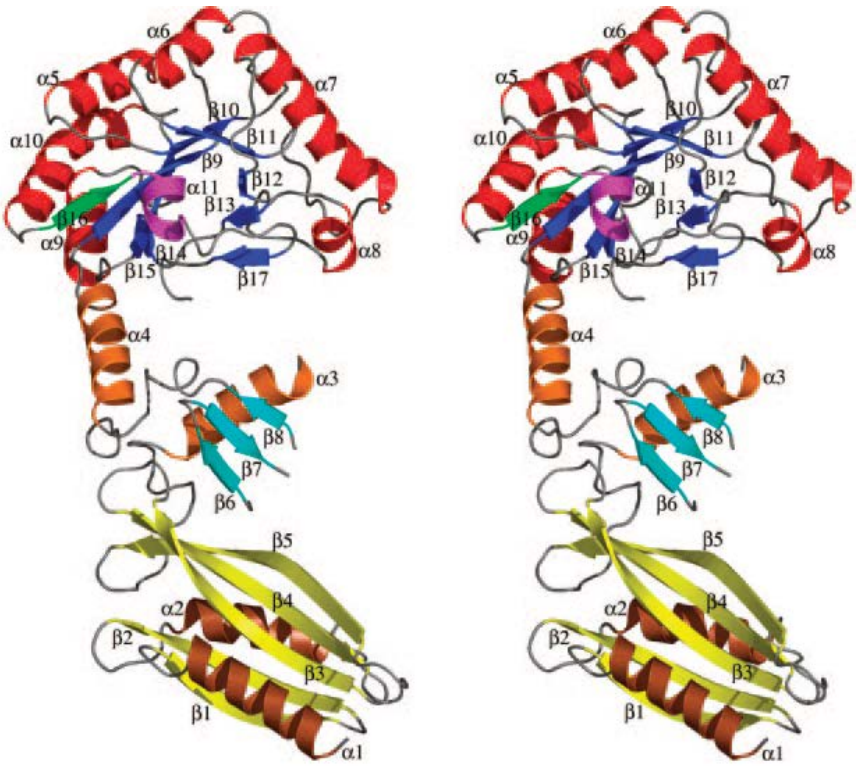

Figure 11. *Stereo image of the SpPgdA (SpPGDA) structure. In the SpPgdA N-terminal domain, helices are colored brown and strands, yellow. In the SpPgdA middle domain, helices are colored orange and strands, cyan. In the catalytic domains, helices are colored red and strands, blue, except for the helices (magenta) and strands (green) that do not fit the canonical* $(\beta/\alpha)_8$ *fold.*

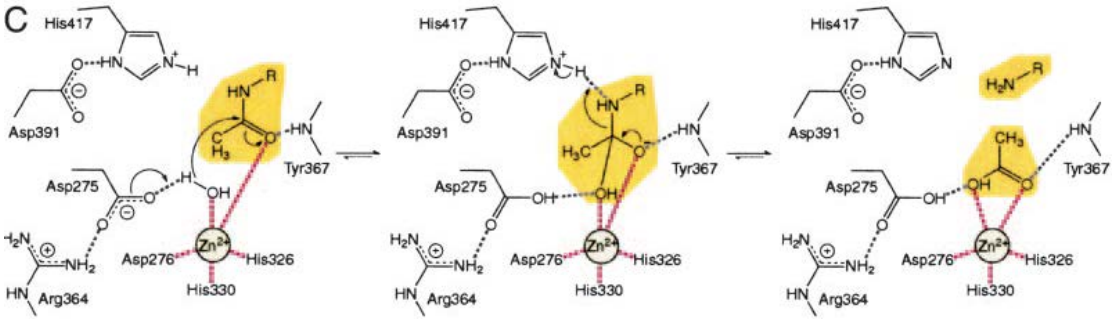

Figure 12. *Proposed catalytic mechanism for Carbohydrate Esterases Family 4 enzymes*

Recently, a new structure of a MurNAc deacetylase from *B. anthracis* (BaCE4) was solved revealing the lack of an otherwise conserved aspartate residue, which coordinates the metal ion in other CE4 structures [96]. In its place, BaCE4 possesses an asparagine residue which points away from the active site metal ion into the core of the protein. Alignments with a number of CE4 sequences indicate that although aspartate is common at this position, asparagine as well as hydrophobic residues, are also observed. The structural studies of CE4 enzymes with different residues at this position may provide information about substrate specificity. It is possible that since BaCE4 deacetylates *N*-acetyl muramic acid, utilizes the extra space provided by the lack of an aspartate residue to bind the bulky group at the O3 position of the muramic acid.

Figure 13. *Ribbon representation of BaCE4, color-ramped from N- (blue) to C- (red) terminus. Acetate and cacodylate ions are shown in ball-and-stick representation, and zinc ions are shown as spheres.*

1.4.3 Biological role

Due to the abundance of lysozyme in both epithelial secretions and professional phagocytes, many pathogens have evolved lysozyme resistance to prevent peptidoglycan hydrolysis. Lysozyme resistance is especially important for Gram-positive pathogens, which rely on a thick peptidoglycan layer to provide structural integrity for the cell. Mechanisms involved in lysozyme resistance include:

a) modification of PG backbone structure via either deacetylation of GlcNAc residues or O-acetylation of the C-6 hydroxyl moiety of the MurNAc residues

b) covalent linkage of other cell wall polymers such as D-alanylation of teichoic acids and

c) production of lysozyme inhibitors such as the periplasmic lysozyme inhibitor Ivy (inhibitor of vertebrate lysozyme) produced by *Escherichia coli* [97] and Sic (streptococcal inhibitor of complement) from *Streptococcus pyogenes* [98] identified as an extracellular virulence factor inhibiting lysozyme.

Lysozyme is a PG *N*-acetyl muramoyl hydrolase that is found in animals, plants, insects, viruses and bacteria [99]. It hydrolyses the β-1,4 glycosidic bond between the C-1 carbon of *N*-acetylmuramic acid (MurNAc) and the C-4 carbon of *N*-acetylglucosamine (GlcNAc) residues of the PG backbone. Due to its cationic nature, lysozyme closely adheres to bacteria via electrostatic interactions with negatively charged teichoic, lipoteichoic acids and phospholipids. In the bacterial surface this interaction can result in bacterial lysis by:

i) the enzymatic properties of lysozyme hydrolyzing β-glycosidic bonds between GlcNAc and MurNAc residues [99]

ii) autolysins, which are activated upon displacement of cell surface divalent cations by lysozyme. Furthermore, increasing evidence suggests that the nonenzymatic function of lysozyme is particularly critical for its bactericidal activity against both Gram+ and Gram- organisms *in vivo* [100, 101]. It has been demonstrated that a 9aa cationic antimicrobial peptide within the protein is capable of disrupting bacterial membranes in the absence of enzymatic activity.

iii) release of bacterial products resulting from degradation of PG and recognized by the host which enhance inflammation and indirectly stimulate bacterial clearance. These inflammatory mediators may include muramoyl dipeptide (MDP) which signals through the Nod2 cytoplasmic pathway.

Two lysozyme genes, those encoding lysozymes M and P, are expressed in mice, while only a single lysozyme gene is expressed in humans [102]. Lysozyme M (LysM) is the only predicted ortholog of human lysozyme and is the predominant form expressed in most cells, including bone marrow-derived macrophages (BMM) [51]. Previous studies have demonstrated that disruption of LysM in mice resulted in increased susceptibility to some bacterial infections [103, 104]. The role of lysozyme appears to be multifaceted. It has been shown that lysozyme activity can kill bacteria and stimulate inflammation, although other studies have shown that it inhibits inflammation [105]. Thus one role of lysozyme may be to degrade potentially proinflammatory peptidoglycan fragments associated with commensal or nonpathogenic bacteria which may be a strategy to avoid mounting an inappropriate inflammatory response. However, lysozyme also serves to generate PG fragments that are important immunostimulatory ligands during infection.

Listeria monocytogenes is a Gram+ intracellular pathogen that is naturally resistant to lysozyme. *L. monocytogenes* peptidoglycan is deacetylated by the action of *N*-acetylglucosamine deacetylase (Pgd) and acetylated by *O*-acetylmuramic acid transferase (Oat). Δ*Pgd,* Δ*Oat* and double mutants were characterized to determine the specific role of *L.monocytogenes* PG acetylation and deacetylation in conferring lysozyme sensitivity during infection of macrophages and mice [106]. Δ*Pgd* and Δ*pgd* Δ*oat* double mutant were attenuated approximately 2 and 3.5 logs respectively *in vivo*. Lysozyme-sensitive *L.monocytogenes* strains were severely attenuated in a mouse model of listeriosis. However, the loss of virulence was not rescued in *lysM*$^{-/-}$ mice. The most likely explanation is a compensatory and redundant mechanism of LysP. LysP compensation in *lysM*$^{-/-}$ mice has been reported. It was shown that LysP mRNA is typically not expressed in the alveolar space in wild-type mice but is upregulated significantly in *lysM*$^{-/-}$ mice [107].

Several studies indicate that PG modification may be differentially regulated to confer lysozyme resistance during infection and that in different infection models, upregulation of one modification may be sufficient to provide resistance, whereas in other models more than one modification may be necessary [51]. The proportion of modified residues may also vary under different conditions or between organisms and should be considered when determining the importance of a particular modification.

Peptidoglycan deacetylase mutants examined so far have been shown to exhibit lysozyme sensitivity in the stationary phase of growth [85, 86, 108]. Several

studies have focused on the transcriptional regulation of PG- modifying enzymes. The *S.suis pgda* gene was upregulated during interactions with neutrophils, which could be a result of oxidative stress [88]. In some organisms, both deacetylation at the C-2 residue of GlcNAc and acetylation at the C-6 residue of MurNAc contribute to lysozyme resistance. A mutant strain of *S.pneumoniae* lacking both modifications was hypersensitive to lysozyme and was attenuated during colonization of the nasopharynx in the presence but not in the absence of lysozyme [109]. An *Enterococcus faecalis* mutant lacking both an O-acetyltransferase gene, *oatA* and an *N*-acetylglucosamine gene, *pgdA*, was also hypersensitive to lysozyme [110]. This mutant strain had impaired survival following phagocytosis, a phenotype described for other lysozyme-sensitive pathogens in both macrophages [86] and neutrophils [88]. However, for both pneumococcal and enterococcal infection models, it seems that one of the two modifications played a predominant role in lysozyme resistance. This may be due in part to differences in expression of the PG-modifying enzymes.

2. MATERIALS AND METHODS

2.1 Ethics Statement.

Animals were housed in animal facilities at the Institut Pasteur, Paris which is accredited by the French Ministry of Agriculture to perform experiments on live rodents (accreditation B 75 15-01), in compliance with the French and European regulations on the care and protection of laboratory animals (EC Directive 86/609 and the French Act #2001-486, issued on June 6, 2001). Protocols were approved in by the veterinary staff of the Institut Pasteur animal facility (CHSCT protocol n° 03-86) and were performed in compliance with the terms of the NIH Animal Welfare Assurance #A5476-01, issued on 02/07/2007.

2.2 Materials

cDNA clones of *B. cereus* ATCC14579 were from Integrated Genomics Inc (Chicago, IL). Primers were synthesized by the Microchemistry Facility of the Institute of Molecular Biology and Biotechnology, FORTH (Table 1). Expression vectors pET-26b, pET-24a, pRSETa and the *E. coli* strains BL21 DE3, BL21(DE3)pLys, DH5a were from Novagen. The strains and plasmids used in this study are listed in Table 2. All chromatographic materials were from Amersham Biosciences. Ni-NTA agarose, PCR and gel extraction kits were from Qiagen and plasmid purification kit from Macherey Nagel GmbH. Restriction and DNA modifying enzymes were from Minotech Biotechnology, New England Biolabs GmbH and ROCHE. Substrates and common reagents were purchased from Sigma-Aldrich, Seikagaku Corporation and Merck. Fluorescamine and Brain-heart infusion (BHI) were purchased from Sigma-Aldrich. FM 4-64 dye and anti-GFP rabbit serum (polyclonal antibody) were from Molecular probes. SYBR Green PCR master mix was from Applied Biosystems. Trizol reagent was from Invitrogen.

2.3. Methods

2.3.1 Cloning and Expression of bc2929, bc5204 and bc1974 genes of B. cereus

The genes were amplified from cDNA clones of *B. cereus* ATCC14579 using DNA polymerase chain reaction. Primers were synthesized to incorporate an NdeI at the start and an XhoI site at the end of the *bc2929* gene and a blunt end at the start and an XhoI site at the end of *bc5204* and *bc1974* genes (Table 1). The amplified genes were purified, digested with the corresponding enzymes and ligated into appropriate vectors. The resulting products were in-frame C-terminal His_6 tag-fused constructs in pET-26b vector for *bc2929*, pET-24a vector for *bc5204* and a non His_6 tag-fused construct in pRSETa for *bc1974* gene, placing the PGNG-dac's genes under the transcriptional control of the T_7 *lac* promoter. All constructs were transformed into BL21 DE3 *E. coli* strains. 20 mL of saturated culture of each of the transformed deacetylase expression strains were inoculated into 1 L of LB medium containing 30 mg ml^{-1} kanamycin (for bc2929 and bc5204) or 100 mg ml^{-1} ampicillin (for *bc1974*) as antibiotic and incubated at 37^{o}C on a shaker incubator to an A_{600} of 0.6. BC2929 *E. coli* culture was incubated to 20^{o}C after addition of 5 mM KCl and 1 mM isopropyl-*β*-D-thiogalactoside (IPTG), BC5204 *E. coli* culture to 30^{o}C after addition of 1 mM $ZnSO_4$ and 1 mM IPTG and BC1974 *E. coli* culture to 30^{o}C after addition of 0.2 mM $CoCl_2$ and 0.5 mM IPTG.

oligonucleotides	Sequence (5'→3')	Source or reference
Construction of *B. anthracis* mutants		
SPC-H^{+1c}	TTTTAGTTGACTTCATTTATATTTTCCTCCTTAGCCTAATTGAGAGAAGTTTCTAT	(6)
SPC-H^{+2c}	TTTTAGTTGACTCATTTATATTTTCCTCCTTAGCCTAATTGAGAGAAGTTTCTAT	(6)
SPC-H^{+3c}	TTTTAGTTGACCATTTATATTTTCCTCCTTAGCCTAATTGAGAGAAGTTTCTAT	(6)
ba2944up5	CGCTCCGTGGTTTTTATACGTTTTACGATTTTGT	this study
ba2944up3	CCCGGGGGAGCTTCTTTCGGTGCAAGAGATGATTGA	this study
ba1977up5	CCTGGTGAATAAGGTGAGTTAGCACATAGT	this study
ba1977up3	CCCGGGCCCAATTGCTACTGCTGCAATCGCTATTAA	this study
ba1961up5	CCAGCAGATGAAGACGGGAAG	this study
ba1961up3	CCCGGGCCACGATCCACGTTCATCAGC	this study
ba3679up5	CCCATGTCTGCCATTGCTTTACGAAGC	this study
ba3679up3	CCCGGGGGGCAAATCCAGGGGTTGAAT	this study
ba5436up5	GCACTGGAACAGCTATCATTTTAC	this study
ba5436up3	CCCGGGGCGTAGTATATTTGTTTG	this study
Ba2944down5	CCCGGGGGTGCAAACAAGCCGACCAGAAGTTATCCTT	this study
Ba2944down3	GCCCTGGTATTTTTAGCAACCAAACGACAA	this study
Ba1977down5	CCCGGGGGGTTATGAGTTTGAAGCTTATCATGAAGAAAGTC	this study
Ba1977down3	GCTGCCTATCTATCCCGATGAATAATCCTA	this study
Ba1961down5	CCCGGGCATTTGCAAGGGTCCGTAGAG	this study
Ba1961down3	GCTCCACTTATATGGGATATTACT	this study
Ba3679down5	CCCGGGGGTACTTCCCATGTTACATAG	this study
Ba3679down3	CAGTTACATTTGGTACATCTG	this study
Ba5436down5	CCCGGGCGACTGGAAAAGCTATGA	this study
Ba5436down3	TTCATGTGCTTTTTCAATTAACCC	this study
PR-5	AATTGGGCCCGACGTCGCATG	this study
PR-3	GAGCTCTCCCATATGGTCGAC	this study
Spec-40	GGAGAGTGTGATGATAAGTGGG	[111]

Spec-30	CGCTGTTAATGCGTAAACCACC	[111]
Construction of *gfp*-fusions		
gfpmut1frw	CCCGGGATGAGTAAAGGAGAAGAACTTTTC	this study
gfpmut1rev	GGGTTAGAATTCCTATTTGTATAGTTCATCCATGCC	this study
ba1961frw	GGGTTAGGATCCATGTATTATTTTTATTCACCAGAA	this study
ba1961rev	CCCGGGGGCCCGGGCCCGTTTTCTTTCTTTTGATGTCTG	this study
ba1977frw	GGGTTAGGATCCATGGAAAAAGCTTTTAAAATTAAA	this study
ba1977rev	CCCGGGGGCCCGGGCCCGCATACGGTTATCATGCCAGAT	this study
ba2944frw	GGGTTAGGATCCATGACAACTTTAATGAAAAGG	this study
ba2944rev	CCCGGGGGCCCGGGCCCGCATACGATTATCATGCCAGAA	this study
ba3679frw	GGGTTAGGATCCACAAGCAGAAAATGCATTTAA	this study
ba3679rev	CCCGGGGGCCCGGGCCCGATGTTTATAACGTAATAATTC	this study
ba5436frw	GGGTTAGGATCCATGATCAAGCGAGTATTTCAA	this study
ba5436rev	CCCGGGGGCCCGGGCCCGCAATCTTGTGTCTTTCCAAAA	this study
Cloning for expression		
bc2929frw	GGAATTCCATATGATGAGTACAGAGGATGAAGCA	this study
bc2929rev	CCGCTCGAGCATACGATTATCATG	this study
bc5204frw	ATGACAACTGTTATTCCTGCT	this study
bc5204rev	CCGCTCGAGTTACAATCTTGTGTCTTTCCA	this study
bc1974frw	ATGTTTCAATCAATTACTTCACCA	this study
bc1974rev	CCGCTCGAGTTACATACGGTTATCATGCCA	this study
qRT-PCR oligonucleotides		
rpoBF	CAGGCGGTTCCGTTAATGA	this study
rpoBR	TCTTTTGCTGATACGTACTCCATACC	this study
GBAA1961F	CTTGGTGAAAACGCAGAAAAGTT	this study
GBAA1961R	CATGCCCTTCATTCGCAATA	this study
GBAA1977F	GCAACAAAACCACAAGAAGTCATT	this study

GBAA1977R	TGGCACAGCAGCTACTGATTG	this study
GBAA2944F	AATCGCTGGCGTTCTAGGTAAA	this study
GBAA2944R	TGGCATTGAGCCGTAAGATG	this study
GBAA3679F	CGAAAGAAGCTGGTTATCAAACTG	this study
GBAA3679R	TGCCCAATCACGTGGATCT	this study
GBAA5436F	CCCTGCTGAACATCATCCAA	this study
GBAA5436R	TCATCAAATGTTAAGTACGCGATTTT	this study

Table 1. *List of oligonucleotides used in the present study*.

Table 2 Strains and Plasmids used in this study

Strains, plasmids or oligonucleotides	Description or sequence	Source or reference
Strains		
E. coli		
TG1	*supE hsd*Δ*5 thi* Δ *(lac-proAB)* F' [*tra*D36 *proAB*$^{+}$ *lacl*^{q} *lacZ*ΔM15]	[112]
DH5α	*F- hsdR17 recA1 thi-1* Δ *(lacIZYA-argF) deoR gyrA96 supE44 (φ80dlac*Δ*(lacZ)M15)*	Novagen
HB101	*F- hsd-20 recA13 ara-14 proA2 lacY1 galK2 rpsL20 (Str) xyl-5 mtl-1 supE44*	[113]
B. anthracis		
7702 [7]	Sterne strain; pXO1^{+}, pXO2^{-}	[114]
RPG1 [R]	pXO1^{+} (*cya lef*), pXO2^{+}	[115]
RPLC2	pXO1^{+} Tox^{-} (lef^{-} cya^{-}), pXO2^{-}	[116]
B. cereus		
ATCC14579		Integrated Genomics Inc (Chicago, IL)
Plasmids		
pGEM T-easy	Cloning vector	Promega
pAT113	Conjugative suicide plasmid used for gene inactivation in *B. anthracis*	[117]
pET-26b	Cloning vector	Novagen
pET-24a	Cloning vector	Novagen
pATΔ28S	Conjugative suicide plasmid used for gene inactivation in *B. anthracis* Spc^{r}	[118]
pNF8	pAT18Ω (PdltΩgfp-mut1)	[119]
pSPCH^{+1}, $^{+2}$, $^{+3}$	pUC19 carrying a non-polar mutagenic Spc^{R} cassette	[60]

Table 2. *Strains, Plasmids and oligonucleotides used in this study*

2.3.2 Purification of BC2929, BC5204 and BC1974

BC2929: Cells were harvested by centrifugation and resuspended in 50 mM Tris-Cl buffer, pH 7.6, 300 mM NaCl (buffer A). After sonication the soluble fractions were collected by centrifugation and loaded onto Ni-NTA agarose equilibrated with buffer A. Proteins were eluted using a step gradient of imidazole (150 mM). Active fractions were dialyzed in buffer A, concentrated and then applied onto a Sephacryl S200 HR column previously equilibrated in buffer A. Active fractions were collected, concentrated and stored at 4^0C.

BC5204: Cells were harvested by centrifugation and resuspended in 50 mM Tris-Cl buffer, pH 7.6, 300 mM NaCl, 1 mM dithiothreitol and 0.3 mg/mL lysozyme. After 150 min incubation at 4^oC suspension was centrifuged, soluble fractions were collected and loaded onto a Q Sepharose Fast Flow chromatography column equilibrated with 25 mM Tris-Cl buffer, pH 8. Proteins were eluted using a step gradient of NaCl (370 mM). Active fractions were loaded onto a Zn-NTA column equilibrated with 25 mM Tris-Cl pH 8, 370 mM NaCl. BC5204 was eluted using a step gradient of imidazole (150 mM). Active fractions were dialyzed in 25 mM Tris-Cl buffer, pH 7.6, 300 mM NaCl and applied onto a Sephacryl S200 HR column previously equilibrated in the same buffer. Active fractions were collected, concentrated and stored at 4^0C.

BC1974: Cells were harvested by centrifugation and resuspended in 25 mM Mes-NaOH pH 6.5, 200 mM NaCl, 1 mM dithiothreitol, 0.3 mg/mL lysozyme. After 150 min incubation at 4^oC, suspension was centrifuged; soluble fractions were collected and loaded onto an S Sepharose Fast Flow chromatography column equilibrated with 25 mM Mes-NaOH pH 6.5. Proteins were eluted using a linear gradient of NaCl (0-1M). Active fractions were collected, dialyzed in 25 mM Mes-NaOH pH 6.5, reloaded onto an S Sepharose Fast Flow and eluted as described above. After dialysis in 25 mM Mes-NaOH pH 6.5, 200 mM NaCl active fractions were further applied onto a Sephacryl S200 HR column previously equilibrated in the same buffer, collected, concentrated and stored at 4^0C.

2.3.3 Preparation of Radiolabeled Substrates

Labeling of glycol chitin and peptidoglycan was performed using [^{3}H] acetic anhydride according to Araki and Ito [120].

2.3.4 Enzyme assays

Enzyme assays were performed in a mixture containing

BC2929: 25 mM Tris-Cl pH 7.0, 1 mM $CoCl_2$ and 5 µl of substrate (1 mg/mL). Incubation time was 2.5 h at 37^{o}C.

BC5204: 25 mM MES-NaOH pH 5.6, 1 mM $CoCl_2$ and 5 µl of substrate (1 mg/mL). Incubation time was 2.5 h at 50^{o}C.

BC1974: 25 mM Tris-HCl, pH 8, 1 mM $CoCl_2$ and 5 µl of substrate (1 mg/mL). Incubation time was 1 h at 50^{o}C.

We have employed two different assays for determining polysaccharide deacetylase activity.

(i) A radiometric assay: deacetylase activity was estimated using as substrate partially *O*-hydroxyethylated chitin (glycol chitin) and peptidoglycan radiolabeled in *N*-acetyl groups [120].

(ii) An assay based on fluorogenic labeling with fluorescamine, which labels the free amines generated by the enzymatic deacetylation of *N*-acetyl-chitooligosaccharides. This allowed miniaturization of the assay to 50 µL volumes suitable for a 96-well format [95].

Kinetic properties of BC2929, BC5204 and BC1974 toward *N*-acetylchitooligosaccharides were determined as below. The reactions were performed with various concentrations of $GlcNAc_{4–6}$ in a total volume of 50 µl at the best reaction conditions for each enzyme as mentioned above. Borate buffer (pH 8.5) was then added and free amines were labeled with 20 µl of 2 mg/ml fluorescamine in dimethylformamide (DMF) for 10 min at room temperature. The labeling reaction was terminated by the addition of 150 µl of DMF/H2O (1:1). Fluorescence was quantified by using FLUOstar Galaxy Microplate Fluorescence Reader (BMG Laboratories), with excitation and emission wavelengths of 390 and 460 nm,

respectively. The production of free amine was quantified with a glucosamine standard. All measurements were performed in triplicates.

2.3.5 Analysis of enzymatic reaction products

BC1960, BC1974, BC2929, BC3618 and BC5204 were incubated, at optimum reaction conditions for each enzyme, with the following substrates: a commercially available muropeptide *N*-acetyl-D-glucosaminyl-(*β*-1,4)-*N*-acetylmuramyl-L-alanyl-D-isoglutamine (GMDP), $GlcNAc_6$ and peptidoglycan precursors: UDP-GlcNAc, UDP-MurNAc, UDP-MurNAc-L-Ala-D-Glu, UDP-MurNAc-L-Ala-D-Glu-meso-DAP, UDP-MurNAc-L-Ala-gamma-D-Glu-meso-Dap-D-Ala-D-Ala, UDP-MurNAc-L-Ala-gamma-D-Lys-Dap-D-Ala-D-Ala and Lipid II. Reaction products were separated and analysed by HPLC as previously described [121, 122]. Reaction products from $GlcNAc_6$ and GMDP enzymatic reactions were further analyzed by MALDI-TOF and MALDI-PSD.

2.3.6 Construction of B. anthracis 7Δba1961, 7Δba1977, 7Δba2944, 7Δba3679 and 7Δba5436 mutants, complemented strains and gfp fusions

DNA fragments containing the sequence upstream and downstream of *ba1961, ba1977, ba2944 ba3679* and *ba5436* were generated by PCR using the proper oligonucleotides (Table 1). Each fragment was cloned into pGEM vector. The constructs were then digested with SmaI/PstI in order to ligate the upstream and downstream fragments of each gene in the same plasmid. The proper cassettes that give resistance to spectinomycin [123] from $pSPCH^{+1}$, $^{+2}$, $^{+3}$ were incorporated in frame between the upstream and downstream fragments of each gene [60]. After digestion, the whole construction (upstream fragment- spectinomycn cassette-downstream fragment) was ligated to pAT113 vector [123]. The final constructs were used to generate the deletion mutants *7Δba1961, 7Δba1977, 7Δba2944, 7Δba3679* and *7Δba5436* by filter mating [114, 124] *B. anthracis* 7702 [114] with *E. coli* HB101 carrying the plasmid pRK24 and each of the appropriate recombinant plasmids [117].

7*Δba1961*, 7*Δba1977*, 7*Δba2944*, 7*Δba3679* and 7*Δba5436* in *B. anthracis* were confirmed by PCR amplification and spectinomycin resistance.

Complemented strains were constructed as follows: The full-length sequence of each gene plus 700 bp upstream were PCR amplified (Table 1) and the products ligated into the pAT113 vector. The resulting recombinant plasmids were transformed into *E. coli* HB101(pRK24) and then introduced into *B. anthracis* mutant strains by filter mating, selecting for erythromycin resistance. Integration of the recombinant plasmids occurred via single-crossover events, at the original locus and was confirmed by PCR amplification.

To construct the strains that express the genes of this study fused with *gfp*, the *gfp-mut1* gene was amplified from pNF8 [119] with specific primers, digested with SmaI and EcoRI and ligated into the plasmid pATΔ28S [118]. Then, each gene (lacking the stop codon) was amplified from *B. anthracis* 7702 chromosomal DNA with the appropriate primers in order to incorporate at the C terminal the polylinker GPGP. The amplicon was digested with BamHI and SmaI and ligated in frame to the 5' end of *gfp-mut1*. HB101(pRK24) *E. coli* cells were then transformed with the resulting plasmids and the *gfp* expressing strains were produced by single recombination after heterogamic conjugation experiments with both *B. anthracis* 7702 and RPG1 [115] strains. Transconjugants and recombinants were selected and tested as above.

2.3.7 Transduction experiments

Transduction of the deletions, from 7*Δba1961*, 7*Δba1977*, 7*Δba2944*, 7*Δba3679 and* 7*Δba5436* deletion mutants to RPG1 strain of *B. anthracis* (generating R*Δba1961*, R*Δba1977*, R*Δba2944*, R*Δba3679 and* R*Δba5436* deletion mutants) were performed with phage CP51 as described by Green et al. [73]. RPG1 strain is ideal for testing *B. anthracis* virulence in mice models. Furthermore, we have employed RPG1 strain in order to reveal if pXO2 plasmid affects the regulation of PGNG-dacs directly or indirectly.

2.3.8 Peptidoglycan and neutral polysaccharide purification

PG from parental *B. anthracis* 7702 and mutants was prepared from exponentially growing bacteria as well as from spores and purified as previously described [125, 126]. Muropeptides from the native PG were generated using the muramidase mutanolysin M1, separated by HPLC, purified, and analyzed by MALDI PSD as previously described [121].

PS was extracted from cell walls as described by Ekwunife *et al.* [56].

2.3.9 Site- directed mutagenesis

D77N BC1974 was constructed by a two step-four primer overlap/extension PCR method. The sequences of the primer pairs were: D77Nfrw (5'- ACATTTGAC *AAT* GGGCCAGGGA-3') and D77Nrev (5'- CCTGGCCC *ATT*G TCAAATGTAA-3'). Engineered codons are in italic. The amplified product was subcloned in pRSETa vector.

2.3.10 Real time PCR studies in B. anthracis

RPLC2 *B. anthracis* strain cultures were grown in R medium (minimal medium) [127] supplemented with 0.6 % sodium bicarbonate under elevated CO_2 levels (>5 %) at temperatures 30 ^{o}C and 37 ^{o}C. RNA was isolated at the exponential and stationary phase of the bacteria cell cycle. Total RNA extraction procedure was adapted from the protocol described by Guillouard et al. for *B. subtilis* [128]. The quality of RNA preparations was analyzed on an RNA NanoLabChip. 2 μg of RNA was reverse transcribed using an AMV reverse transcriptase and random hexamers from Amersham, according to the manufacturer's instructions. All Real-Time PCR reactions were performed in a 25 μl mixture in a 96-well plate, containing 40 ng of cDNA preparation, 1 X power SYBR Green PCR master mix, 2 μM of each primer (final concentration). As reference gene was used *rPOB*, a gene that encodes for the β subunit of RNA polymerase. The method used to analyze the data from real time PCR was the relative quantification, relating the PCR signal of the target transcript that was

treated with reverse transcriptase to that of the sample that was untreated and to the reference gene. Three individual experiments were performed for each gene. For each experiment, each individual sample was run in triplicate wells and the Ct of each well was recorded at the end of the reaction. The average and standard deviation (SD) of the three Cts was calculated and the average value was accepted if the SD was lower than 0.05.

2.3.11 Autolysis Assay

Ten mL cultures in SPY [67] medium of the parental (7702 and RPG1) and the mutant strains at an A_{600} 0.5 were centrifuged and the bacterial pellet was concentrated ten times in SPY medium devoid of sucrose to which 10 mM NaN_3 was added (final concentration). The decrease in optical density of each culture was monitored for 240 min taking samples every 30 min.

2.3.12 Analysis of Cell Surface and Supernatant Proteins

For this analysis, we used the method described by Foster [129]. The protein samples were run on 10% acrylamide gel, then fixed and stained using Coomassie Brilliant Blue.

2.3.13 Fluorescence microscopy of vegetative cells

B. anthracis cultures of the parental strains (7702 and RPG1) and the mutant strains were inoculated from fresh overnight plates to an initial A_{600} of 0.1 and grown to stationary phase as liquid cultures in SPY medium.

For membrane visualization, the FM 4-64 fluorescent dye was added to a final concentration of 1 μg/mL. Cells were examined by fluorescence microscopy and the pictures were obtained without fixation on an inverted epifluorescence microscope Axio Observer (Zeiss), using the Axiovision software.

2.3.14 Western Blot Analysis

Bacterial cell lysates during the time points at which GFP-fluorescence signal was obtained were separated by SDS-PAGE, blotted, and probed with the following antibodies: polyclonal rabbit anti-GFP primary antibody diluted 1:1000 and polyclonal goat anti-rabbit IgG horseradish peroxidase secondary antibody diluted 1:10000.

2.3.15 Transmission electron microscopy

Spores and vegetative cells were initially fixed with glutaraldehyde 2.5% in cacodylate buffer 0,1M pH 7 and postfixed in 1% osmium tetroxide in water. Samples were pelleted and embedded in low melting point 2% agar. Blocks of agar containing samples were transferred in 0.5% uranyl acetate/ H_2O and then dehydrated through a series of ethanol washes. Finally, samples were embedded in epoxy resin.

2.3.16 In vitro lysozyme sensitivity

In order to test the sensitivity of the mutants in the presence of exogenous added lysozyme, they were grown in SPY liquid broth at 37^{o}C. Ten mL of each culture were grown to an A_{600} of 0.5 (exponential phase of growth), centrifuged and resuspended to a buffer containing 20% sucrose, 20 mM Tris pH 8, 1 mM EDTA, 50 mM NaCl (buffer B). Ten μg/mL hen egg lysozyme (final concentration) or 10 u mutanolysin were added to half of the resuspension and both cultures were incubated for 30 min. Cells before and after the addition of lysozyme or mutanolysin were observed by optical microscopy. Another 10 mL of the initial culture at A_{600} of 1.2 (stationary phase of growth) were centrifuged and resuspended to buffer B. Cells were treated as previously described with lysozyme or mutanolysin at different time points (15 min, 45 min, 75 min) and observed by optical microscopy.

2.3.17 Mice experiments

OF/1, BALB/c (6- to 8-week-old females, Charles-Rivers, Arbresle, France) and BALB/c *lysM*$^{-/-}$ outbred mice (backcrossed at least eight generations in the BALB/c background) [130] were injected subcutaneously with different amounts of spores of the RPG1 *Δba1977* mutant or parental RPG1 strain, as previously described [114]. Fifty percent lethal doses (LD_{50}s) were estimated using the method of Reed and Muench [131] with eight animals per spore dose. Drawing of Kaplan-Meier survival curves and log rank analysis for evaluating survival differences between the groups were performed with Graph- Pad Prism 4 software (GraphPad Software, San Diego, CA).

Spore stocks for the animal experiments were obtained by growing *B. anthracis* RPG1 cultures on NBY agar for 7 days at 30°C. Spores were harvested and washed twice in distilled water, heated for 20 min at 65°C to kill vegetative cells, and washed again with distilled water. Spores were then re-suspended in distilled water and stored at 4°C before use.

3. RESULTS

3.1 Computational analysis

Ten coding sequences (CDS) found in *B. anthracis* belonging to the polysaccharide deacetylase family CE4 are identical in size and exhibit more than 90% identity to their homologues from *B. cereus sensu stricto*. Among these 10 CDS, Table 3 lists the 5 CDS encoding putative PGNG-dac's of *B. cereus* ATCC14579 alongside the orthologues members of *B. anthracis*.

B. cereus **ATCC14579**	***B. anthracis*** **str. Ames**	**Identity %**	**Similarity %**
NP_831730 (275) (BC1960)	NP_844369 (275) (BA1961)	94	97
NP_833348 (213) (BC3618)	NP_845942 (213) (BA3679)	97	100
NP_832677 (275) (BC2929)	NP_845280 (275) (BA2944)	94	97
NP_834868 (245) (BC5204)	NP_847604 (245) (BA5436)	93	96
NP_831744 (273) (BC1974)	NP_844383 (273) (BA1977)	98	99
NP_832887 (280) (BC3146)	-		

Table 3. *The five orthologous coding sequences from B. cereus and B. anthracis. Values in parentheses refer to the number of amino acids in the respective open reading frame. (-) indicates the absence of the corresponding gene in B. anthracis genome. Possible function has been assigned to these enzymes by ERGO-light data base (http://www.integratedgenomics.com/).*

Moreover, through computational analysis we explored the possible operon-like arrangement of the 5 genes that encode for the putative 5 PGNG-dacs of the present study. Figure 14 illustrates the neighbouring genes of the 5 PGNG-dacs.

Figure 14. *Gene organization of polysaccharide deacetylases on B. anthracis str. Ames genome. ba1961 (panel A), ba1977 (panel B), ba2944 (panel C), ba3679 (panel D) and ba5436 (panel E). Arrows indicate open reading frames. Genes of interest are highlighted in red. These clusters of genes are highly conserved in B. cereus ATCC14579 genome.*

3.2 Enzyme purification and characterization of B. cereus deacetylases

Purification and characterization of BC1960 and BC3618 has been described in a previous study [85].

In addition to *bc1974*, *bc2929* and *bc5204* genes we have also tried to express the remaining putative GlcNAc deacetylase gene *bc3146*. However, we were unable to demonstrate enzymatic activity of this gene product toward various chitin and peptidoglycan substrates tested.

BC2929 and BC5204 were produced containing a C-terminal His_6-tag and purification was achieved in a two step procedure employing affinity (Ni-NTA) and gel filtration chromatography (S200-HR). BC1974 was produced without a His_6-tag and purified employing a three step procedure using two S Sepharose Fast Flow and one S200-HR gel filtration chromatographic columns (Fig. 15).

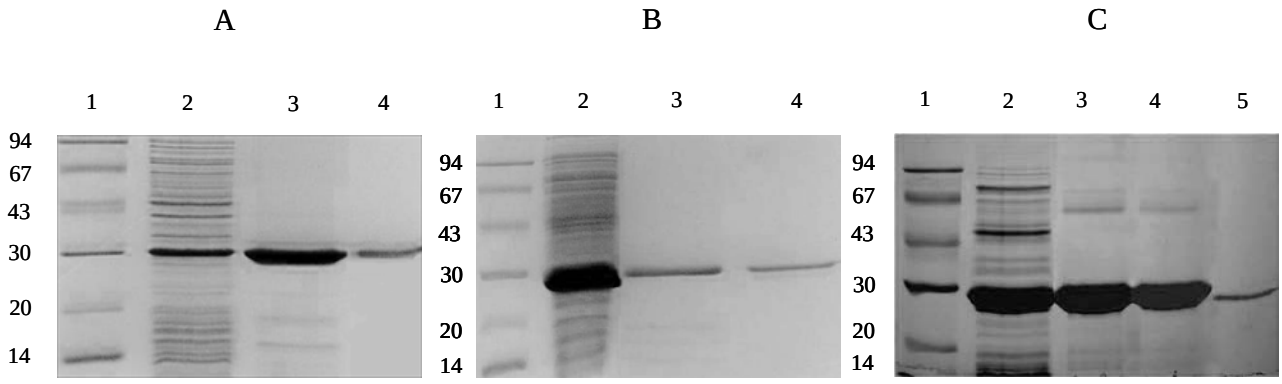

Figure 15. *SDS-PAGE of the purified polysaccharide deacetylases BC2929, BC5204 and BC1974. (panel A) BC2929: lane 1, molecular weight markers; lane 2, crude extract; lane 3, Ni-NTA eluate; lane 4, gel filtration eluate. (panel B) BC5204: lane 1, molecular weight markers; lane 2, crude extract; lane 3, Zn-NTA eluate; lane 4, gel filtration eluate. (panel C) BC1974: lane 1, molecular weight markers; lane 2, crude extract; lane 3, first S Sepharose eluate; lane 4, second S Sepharose eluate; lane 5, gel filtration eluate. Samples were electrophoresed on a 12% polyacrylamide gel under denaturing and reducing conditions. Protein bands were visualized by staining with Coomassie Brilliant Blue R.*

All recombinant enzymes appear to be monomers according to SDS-PAGE and gel filtration chromatography and exhibit molecular masses of ~30 kDa (BC2929), ~29 kDa (BC5204) and ~28 kDa (BC1974) in agreement with the masses estimated from the nucleotide sequences (30,821, 28,390 and 30,675 kDa respectively).

All three enzymes were inhibited by the presence of 1 mM Cu^{2+} and Zn^{2+} tested as chlorides, whereas they were not inhibited by other divalent or monovalent metals (Mg^{2+}, Ca^{2+}, Mn^{2+}, K^{+}, and Na^{+}) tested up to 10 mM concentration, using glycol chitin as substrate. A maximum 60 % increase in activity of all three enzymes was observed by the addition of 0.5 mM $CoCl_2$ in the assay buffer. Interestingly, BC5204 activity increased up to 60 % by the addition of 0.5 mM $NiCl_2$ using glycol chitin as substrate. BC2929 and BC5204 were inhibited by acetate at concentrations starting from 5 mM in contrast to BC1974 which was not inhibited even at concentration of up to 100 mM. The purified recombinant enzymes exhibited different pH, temperature optima, and thermal stability, as determined by using radiolabeled glycol chitin as substrate (Table 4).

	BC2929	**BC5204**	**BC1974**	**BC3618¶**	**BC1960¶**
Molecular weight (kDa)	30	29	29	28	30
Number of subunits	1	1	1	1	1
Optimum pH values	7	6	7-8	8	6
Optimum temperature (°C)	37	50	50	37	50
Activation by metal ions (0.5 mM)	Co^{2+}	Co^{2+}, Ni^{2+}	Co^{2+}	Co^{2+}	Co^{2+}
Inhibition by metal ions (1 mM)	Cu^{2+}, Zn^{2+}	Cu^{2+}, Zn^{2+}	Cu^{2+}, Zn^{2+}	Cu^{2+}, Zn^{2+}	Cu^{2+}, Zn^{2+}
Signal peptide	Yes	Yes	Yes	No	No
Inhibition by acetate (5 mM)	Yes	Yes	No	No	No

Table 4. *Comparison of biochemical properties of polysaccharide deacetylases from B. cereus. BC1974, BC2929 and BC5204 were biochemically characterized using optimum reaction conditions for each enzyme and radiolabeled glycol chitin as substrate.*

¶ *BC1960 and BC3618 have been previously characterized* [85].

All polysaccharide deacetylases were highly promiscuous enzymes as they were active on peptidoglycan and radiolabeled glycol chitin as well as on *N*-acetyl chitooligosaccharides and the synthetic muropeptide GMDP (except BC2929). PG precursors were also examined as possible substrates because two of the enzymes of the present study (BC1960 and BC3618) do not possess a signal peptide. Interestingly, only BC5204 and BC2929 were active using lipid II as substrate while BC5204 was also active toward UDP-GlcNAc. All other enzymes (BC1960, BC1974 and BC3618) were inactive toward all PG precursors (Table 5).

	BC1960	**BC1977**	**BC2944**	**BC3679**	**BC5436**
Insoluble PG (HP26695/BC14579)	+	+	+	+	+
Glycol Chitin	+	+	+	+	+
GMDP	+	+	-	+	+
UDP-GlcNAc	-	-	-	-	+
lipid II	-	-	+	-	+
$GlcNAc_{1-6}$	$GlcNAc_{3-6}$	$GlcNAc_{3-6}$	$GlcNAc_{4-6}$	$GlcNAc_{3-6}$	$GlcNAc_{2-6}$
GlcNAc-6P	-	+	-	-	-

Table 5. *Substrate specificity of the recombinant enzymes BC1960, BC1974, BC2929, BC3618 and BC5204. Substrate specificity was examined using optimum reaction conditions for each enzyme. (+) indicates enzyme activity, (-) indicates that the corresponding enzyme is inactive on the substrate examined. GlcNAc: N-acetyl glucosamine.*

Kinetic parameters for $GlcNAc_{4–6}$ were obtained from Lineweaver-Burk plot analysis, and the enzyme reaction rates for these substrates seemed to follow Michaelis-Menten kinetics (Table 6). BC2929 exhibited the highest k_{cat}/K_m value toward $GlcNAc_4$ and $GlcNAc_6$ and the lowest K_m for $GlcNAc_4$ among these

substrates. BC5204 exhibited the highest k_{cat}/K_m value toward $GlcNAc_6$ and the lowest K_m for $GlcNAc_5$. BC1974 exhibited the highest k_{cat}/K_m value toward $GlcNAc_5$ and the lowest K_m for $GlcNAc_5$ and $GlcNAc_6$. The resulting k_{cat}/K_m ratios combined with K_m values indicated that the favorable substrate for each enzyme was $GlcNAc_4$ for BC2929, $GlcNAc_6$ for BC5204 and $GlcNAc_5$ for BC1974.

Substrate	BC2929			BC5204			BC1974		
	K_m	V_{max}	K_{cat}/K_m	K_m	V_{max}	K_{cat}/K_m	K_m	V_{max}	K_{cat}/K_m
	μM	*μmole/ sec/μg*	$\mu M^{-1}\ sec^{-1}$	*μM*	*μmole/ sec/μg*	$\mu M^{-1}\ sec^{-1}$	*μM*	*μmole/ sec/μg*	$\mu M^{-1}\ sec^{-1}$
$GlcNAc_4$	4.72±0.165	0.418±0.015	0.08±0.002	27.5±1.65	0.435±0.022	0.41±0.021	67.65±3.585	0.79±0.038	5.88±0.305
$GlcNAc_5$	16.96±0.678	0.329±0.016	0.014±0.001	5.92±0.296	0.366±0.017	0.81±0.042	10.11±0.515	0.881±0.037	21.78±1.11
$GlcNAc_6$	7.6±0.38	0.9±0.045	0.082±0.004	14.4±0.748	0.537±0.025	6.21±0.329	10.07±0.483	0.13±0.005	9.347±0.458

Table 6. *Kinetic properties of BC2929, BC5204 and BC1974 toward $GlcNAc_{4–6}$. Enzyme assays were performed as described at "Material and Methods". The k_{cat} values were derived from the expression V_{max}/ enzyme concentration.*

Since all five enzymes presented rather promiscuous substrate specificity, we wondered whether using $GlcNAc_6$, a substrate mimic of the glycan backbone of the PG, the different enzymes would show different specificity for the GlcNAc residues deacetylated. The three enzymes, BC1974, BC2929 and BC5436 (homologues of BA1977, BA2944 and BA5436 from *B. anthracis* respectively) were incubated with $GlcNAc_6$ for 1h and the reaction products were separated by HPLC and analysed by MALDI-TOF and MALDI-PSD techniques (Fig. 16). BC2929 generated one single peak which corresponded to the deacetylation of one single GlcNAc in the entire $GlcNAc_6$ substrate (1219 m/z). BC5204 presented a similar pattern of deacetylation (1219 m/z) although a small fraction of the products also had two glucosamine residues (1177 m/z). In contrast, BC1974 was able to deacetylate most of the central GlcNAc residues (1135 m/z). Interestingly, the three enzymes did not deacetylate the reducing and non-reducing terminal GlcNAc residues of $GlcNAc_6$ but only the intermediate ones with different combinations.

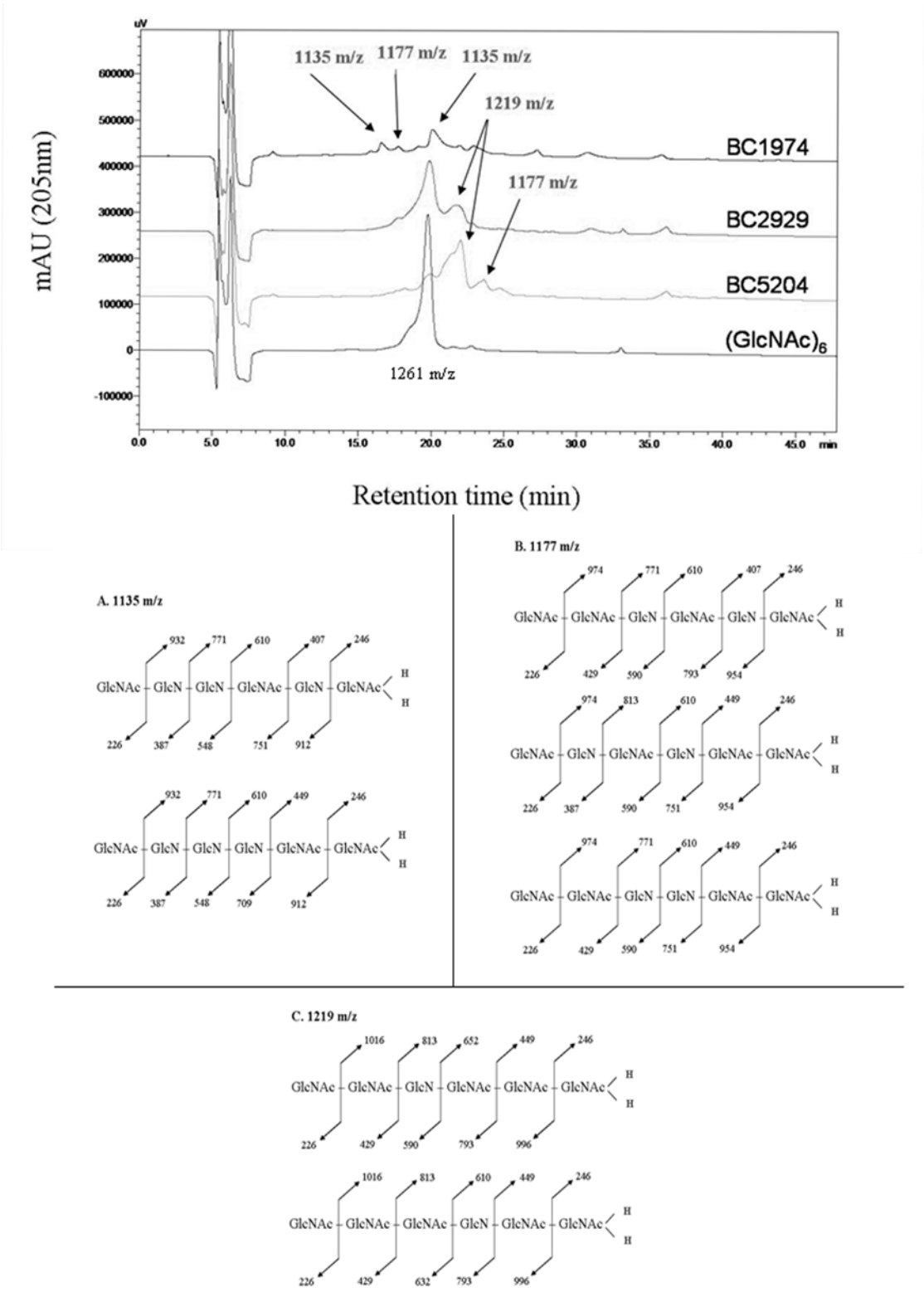

Figure 16: *Analysis of enzymatically deacetylated oligomer $GlcNAc_6$. $GlcNAc_6$ was incubated with BC1974, BC2929 or BC5204 for 1 h at optimum reaction conditions and the resulting oligosaccharides were separated by HPLC and analyzed by*

MALDI-TOF and MALDI-PSD. BC1974 produced three new peaks that exhibited molecular masses of 1135 m/z, 1177 m/z, BC2929 produced a new peak that exhibited molecular mass of 1219 m/z and BC5204 revealed two new peaks that exhibited molecular masses of 1219 m/z, 1177 m/z.

The synthetic muropeptide GMDP was also incubated with the three deacetylases. Two of the three enzymes (BC5204 and BC1974) converted GMDP in a new muropeptide (peak 1, Fig. 17). The new species were purified by high pressure liquid chromatography and analyzed by MALDI-TOF. The new muropeptide had molecular mass of 678 and differed from GMDP (m/z 720.2915) by m/z 42, which corresponds to the loss of an acetyl group. Subsequently, we performed MALDI-PSD on peak 1 to determine which moiety of GMDP was modified by both deacetylases (Fig. 17). Interestingly PSD analysis of peak 1 revealed that only the *N*-acetylglucosamine residue had lost the *N*-linked acetyl functional group and that no modification of the *N*-acetylmuramic acid residue had occurred. Indeed, a major fragment (m/z 517.4) corresponds to the loss of glucosamine (m/z 161). Fragmentation from the C-terminal end of the deacetylated GMDP generates a and b type ions. For example, a_1-NH_3 ion m/z 504.2 is further converted into m/z 343.2 corresponding to the loss of m/z 161, therefore, a glucosamine residue. Finally, the presence of the ion m/z 318.2, which corresponds to the *N*-acetylmuramic acid alone, clearly excludes deacetylation of the *N*-acetylmuramic acid residue. Furthermore, no fragments corresponding to the loss of *N*-acetylglucosamine were observed (loss of m/z 203). BC2929 and the mutated enzyme BC1974* seemed to convert GMDP to a new muropeptide (peak 2, Fig. 17) but further MALDI-TOF and MALDI-PSD analysis revealed no evidence of deacetylation. Peak 2 may correspond to a non reduced state of GMDP.

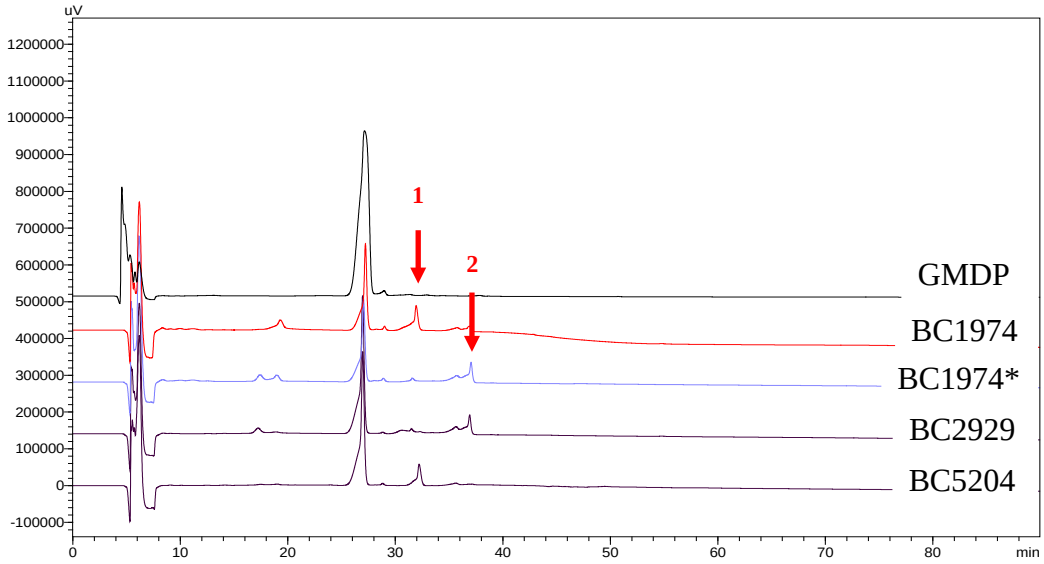

Figure 17. *HPLC analysis of GMDP. GMDP (control) was treated with BC2929, BC5204, BC1974 and enzyme variant BC1974 D77N and the resulting muropeptides (peak 1 and peak 2) were separated by HPLC and analyzed by MALDI-TOF.*

3.3 Site Directed mutagenesis of BC1974

Most of the known structures of peptidoglycan deacetylases contain a divalent cation that is necessary for enzyme activity. This ion is coordinated by a metal-binding triad (two His and one Asp) that is conserved throughout the CE4 family. Alignments with a number of CE4 sequences with BC1974 indicated that Asp^{77} is common at this position in PG *N*-acetylglucosamine deacetylases contrary to PG *N*-acetyl muramic acid deacetylases that present at the same position an asparagine, or other hydrophobic residues such as alanine or valine [96].

In order to investigate the role of Asp^{77} in substrate specificity of the enzyme BC1974, it was mutated to an asparagine. The mutated enzyme was tested using as substrates radiolabeled glycol chitin, peptidoglycan from *H. pylori* and the synthetic muropeptide GMDP. D77N mutation resulted in a dramatic decrease of the enzyme activity for all substrates examined.

3.4 Expression of ba1961, ba1977, ba2944, ba3679 and ba5436 mRNA transcripts.

Expression profiles of *ba1961, ba1977*, *ba2944*, *ba3679* and *ba5436* at two different developmental stages (exponential and stationary phase of growth) of *B. anthracis* RPLC2 strain, at two different temperatures, are depicted in Figure 18.

Bergman *et al*. suggested that the five deacetylase genes are expressed at different developmental stages of *B. anthracis* life cycle [132]. In particular, *ba1961* is expressed at the phase of sporulation, *ba3679* and *ba5436* at the early sporulation phase, *ba2944* at the early stationary phase and *ba1977* at the exponential phase of growth. We examined the expression profile of the five genes at exponential and stationary phase of growth of the bacterium life cycle. Significant difference was detected in the expression of *ba1977* gene both at the exponential and even greater at the stationary phase. *ba1977* was upregulated compared to all the other genes of interest. Increase in transcriptional levels of *ba2944* was also detected compared to the rest of the genes but it was less than *ba1977* transcriptional level. *ba1961, ba3679* and *ba5436* showed insignificant differences at their expression levels. Possibly, they were either downregulated or inactive during the developmental stages tested.

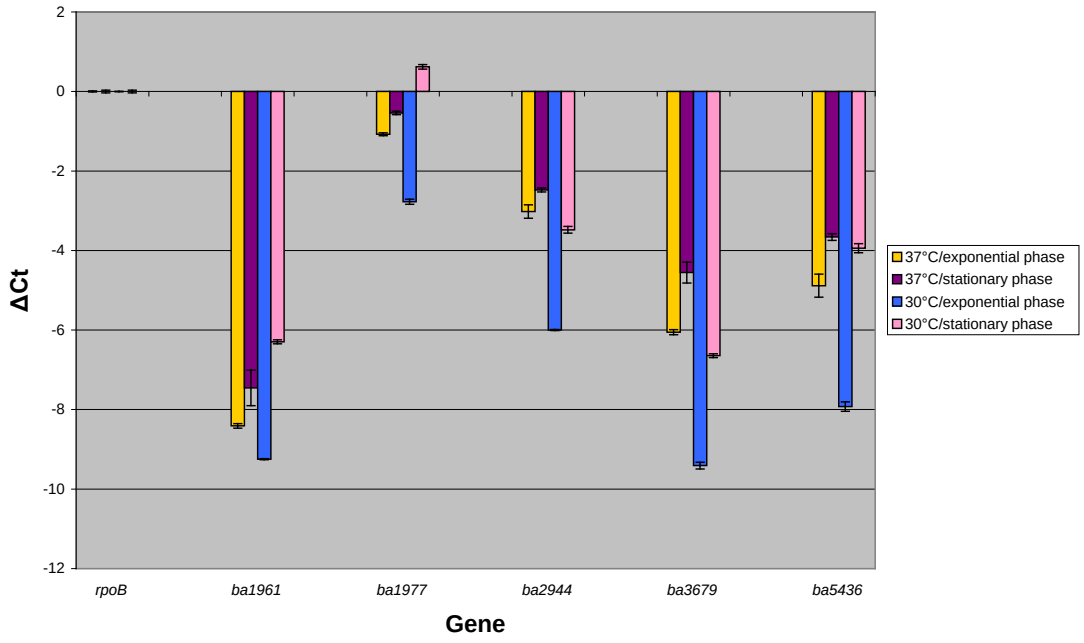

Figure 18. *Expression profiles of ba1961, ba1977, ba2944, ba3679 and ba5436 as measured by quantitative realtime PCR. The mRNA expression levels of the five*

deacetylase genes and rpoB were measured at two developmental stages (exponential and stationary phase of growth). Differences were calculated as ΔCt with rpoB as a reference gene. Vertical bars represent the mean SD.

3.5 Localization of B. anthracis deacetylases

Since biochemical characterization and kinetics of the recombinant enzymes did not reveal any particular substrate specificity, to gain some insight on the physiological role of each putative PGNG-dac, we decided to study the subcellular localization of these enzymes. SignalP and TatP (http://www.cbs.dtu.dk/services/) signal peptide analysis revealed that BC1974, BC2929 and BC5204 (homologues of BA1977, BA2944 and BA5436 from *B. anthracis* respectively) have a signal peptide. BC1960 and BC3618 (homologues of BA1961 and BA3679 from *B. anthracis* respectively) that have been characterized in a previous study [85] do not have a signal peptide that targets them either to the Sec or the TAT translocation pathway. LocateP database (http://www.cmbi.ru.nl/locatep-db/cgi-bin/locatepdb.py) predicted BC1974 to be an *N*-terminally anchored membrane protein whereas BC2944 and BC5204 were predicted to be secreted through the Sec-(SPI) pathway. BC1960 and BC3618 were predicted to have an intracellular localization using the same database.

In order to investigate the subcellular localization of the five deacetylases of *B. anthracis* in the 7702 and RPG1 strains, we constructed C-terminal *gfp* fusions of *ba1961*, *ba1977*, *ba2944*, *ba3679* and *ba5436* genes. To visualize the GFP fusion proteins in living cells, the *B. anthracis* strains producing these fusions were grown in BHI or SPY medium and examined by fluorescence microscopy (Fig. 19). Fluorescent signal was obtained for every deacetylase of the present study during the stationary phase of growth and the expression of the GFP-fused enzymes was confirmed by western blot analysis (Fig. 19F). BA1977 and BA5436 fusions were partially cleaved potentially releasing GFP in the cytoplasm. Fluorescence signals for all deacetylases were identical in both genetic backgrounds except BA2944 which appeared to have a more enhanced phenotype in the R genetic background.

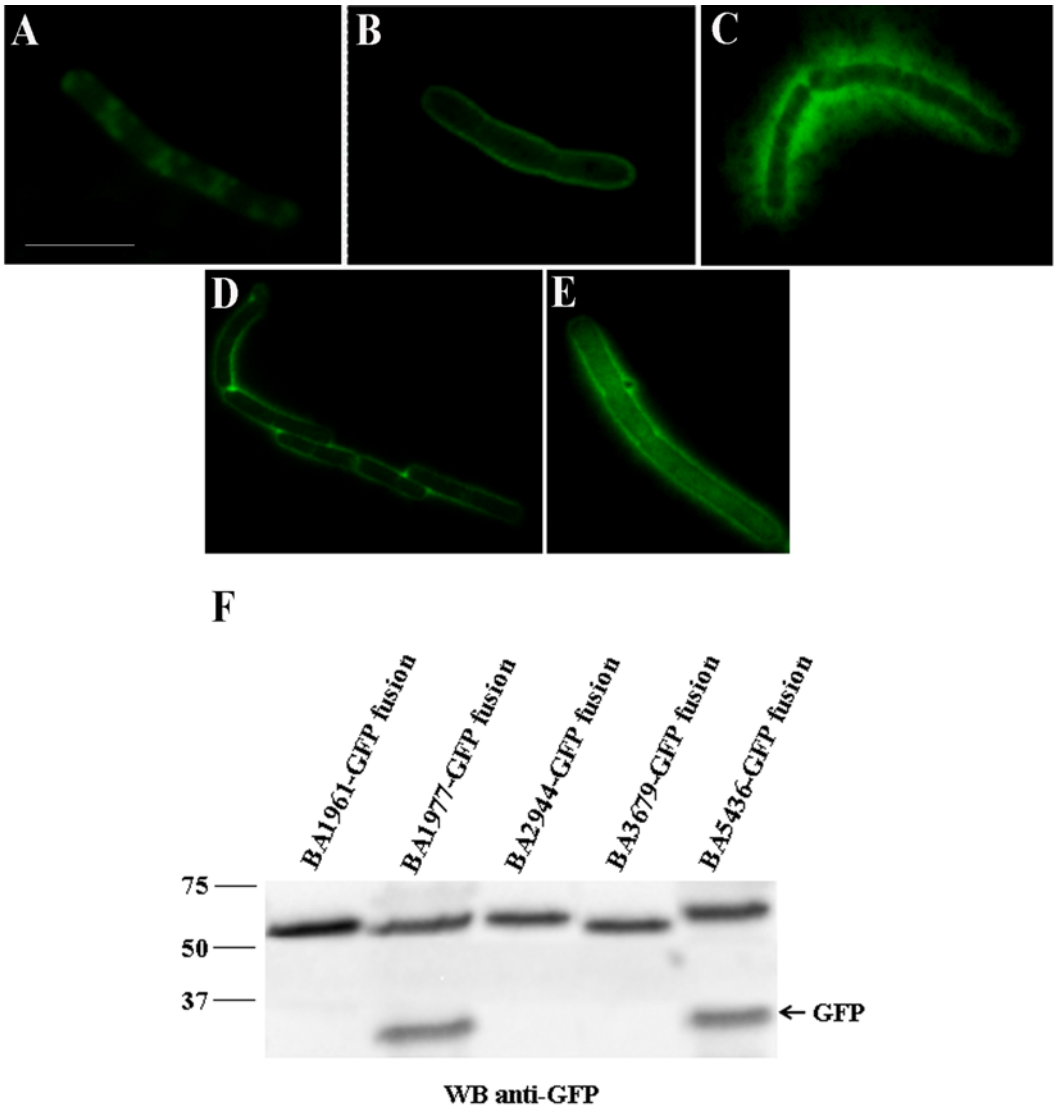

Figure 19. *Localization of BA1961, BA1977, BA2944, BA3679 and BA5436. BA1961-GFP fusion appeared to localize as a helical pattern (panel A), BA1977-GFP fusion distributes at the cell membrane (panel B), BA2944-GFP fusion localizes outside the cell envelope (panel C), BA3679-GFP fusion appears both around the cell envelope and the septa (panel D) and BA5436-GFP fusion reveals diffused localization both near cell envelope and to a lower degree in the cytoplasm (panel E). Scale bars, 5 μM. Panel F displays western blot analysis of each GFP-fusion strain, using a polyclonal anti-GFP antibodies. Partial cleavage of GFP is only observed in BA1977-GFP and BA5436-GFP fusion-harboring strains.*

In more detail BA1961 appeared to localize as X pattern at the septa (Fig. 19A). BA1977 displayed a different pattern of localization, with fluorescent labeling distributed at the cell membrane, which appeared excluded from the septum (Fig. 19B). Despite the partial cleavage of the BA1977-GFP fusion (Fig. 19F), we did not observe any residual cytoplasmic labeling (Fig. 19B). BA2944 produced a unique localization pattern as fluorescence was observed outside the bacteria (Fig. 19C). BA3679 displays a combination of patterns, with fluorescence distributed both around the cell envelope and the septa (Fig. 19D). Finally, subcellular distribution of BA5436-GFP fusion revealed diffuse localization both near the cell membrane and to a lower degree to the cytoplasm probably due to partial cleavage of GFP (Fig. 19E). Hence, besides BA2944, all putative PGNG-dacs seemed to be associated with the cell envelope. Their localization was compatible with PG as a native substrate. In contrast, BA2944 localization clearly on the cell surface distant from the cell membrane suggested that the native substrate of BA2944 is another polysaccharide.

3.6 Construction, characterization and complementation of B. anthracis ba1961, ba1977, ba2944, ba3679 and ba5436 mutants

To elucidate the biological role of BA1961, BA1977, BA2944, BA3679 and BA5436, the corresponding genes were inactivated in *B. anthracis* 7702 ($pXO1^+$, $pXO2^-$) strain (7 genetic background). The mutations were also transduced to *B. anthracis* RPG1 ($pXO1^+$, Tox^-, $pXO2^+$) strain (R genetic background). All mutants as well as their respective parental strains grew in different liquid medium (BHI broth, SPY medium), indicating that their inactivation had no effect on the growth of *B. anthracis* (Fig. 20). Interestingly, when analyzed by phase contrast microscopy, these strains produced long twisted chains of daughter cells that had abnormal shape under light microscope. Furthermore, deletion of *ba1961* and *ba3679* in both backgrounds, produced bacilli that could not sporulate (sporulation efficiency <1%) either on normal sporulation medium (NBY medium) or on SPY agar medium unless the concentration of Mg^{2+} was reduced to 0.5 mM. Complemented strains fully recovered the wild type phenotypes (Fig. 21).

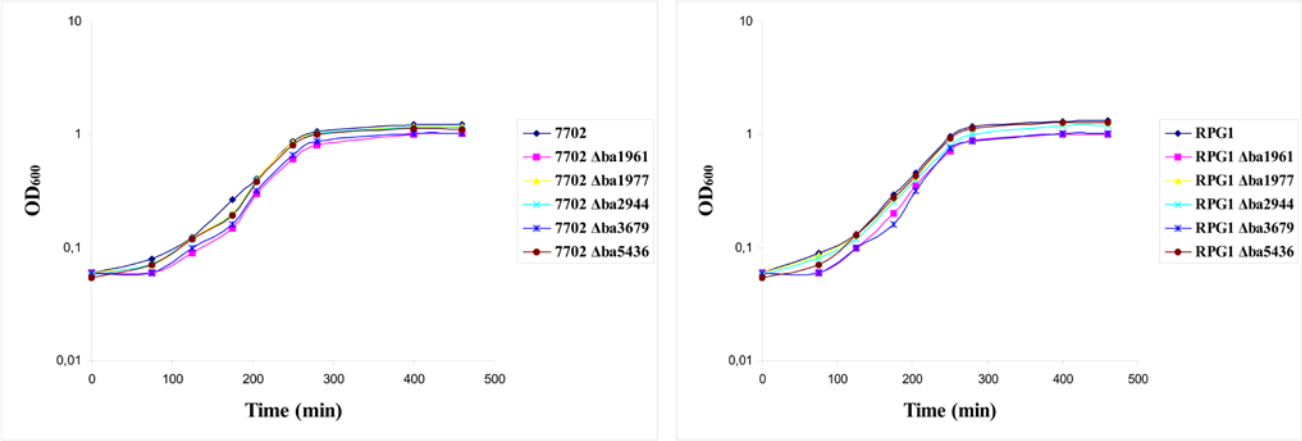

Figure 20. *Growth curves of B. anthracis 7702 and mutant strains. Cultures were prepared in SPY liquid broth and grown at 37^{0}C.*

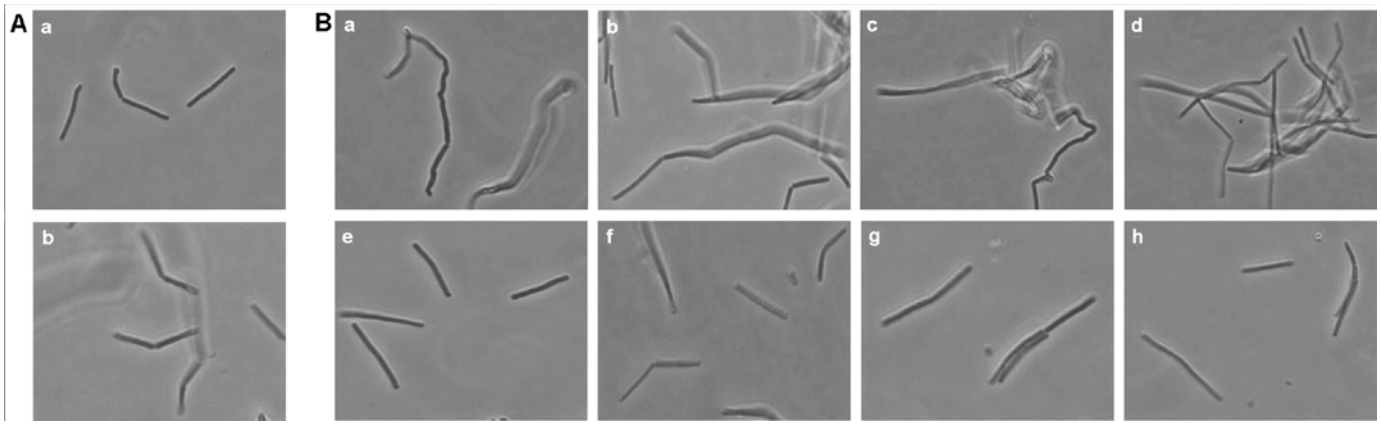

Figure 21. *Complemented strains under phase contrast microscopy. Panel A shows parental 7702 (a) and RPG1 (b) strains. Panel B compares the phenotype of 7Δba1961 (a), 7Δba2944 (b), 7Δba3679 (c) and 7Δba5436 (d) mutant strains with the corresponding complemented ones (e, f, g, h).*

In order to examine and visualize the morphological phenotype of all mutants, we used the lipophilic styryl dye FM 4-64 that stains membranes and observed them under fluorescence microscopy (Fig. 22A). Only the 7 and R*Δba1977* mutants presented “wild-type” morphology (Fig 22A, panel b). Instead, the 7 and RΔ*ba5436* mutants produced extremely long chains of septated daughter cells unable to separate (Fig. 22A, panel e). The 7 and RΔ*ba1961* and 7 and RΔ*ba3679* mutants appeared as twisted long chains of daughter cells with abnormal shape (Fig 22A, panels c and d). Interestingly, the last mutation, Δ*ba2944*, yielded a different phenotype depending on the *B. anthracis* genetic background. The RΔ*ba2944* mutant produced long chains of septated cells (Fig. 22A, panel h) while 7Δ*ba2944* behaved like the wild-type 7702 strain (Fig. 22A, panel g).

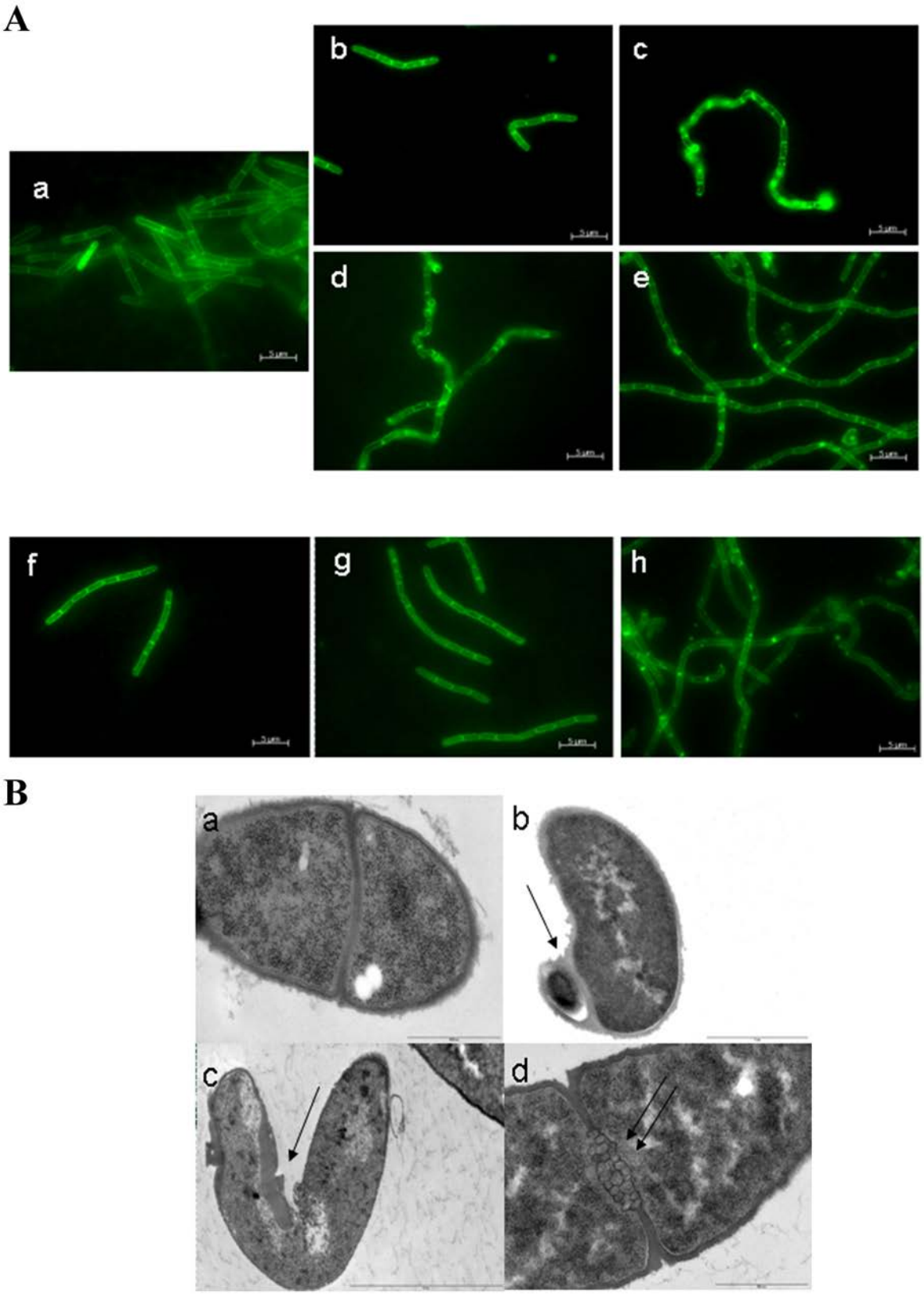

Figure 22. *Phenotype analysis of parental and mutant strains. A. Fluorescence microscopy using FM4-64 staining. (panel a) parental B. anthracis 7702 strain,*

(panel b) 7Δba1977, (panel c) 7Δba1961, (panel d) 7Δba3679, (panel e) 7Δba5436 and (panel f) 7Δba2944 mutant strains. (panel g) parental B. anthracis RPG1 strain. 7Δba2944 had the same phenotype as the parental strain 7702, whereas RΔba2944 produced long chains of septated cells (panel h). B. Transmission electron micrographs of 7702 and 7Δba1961, 7Δba3679, 7Δba5436 mutant strains during vegetative growth. (panel a) parental B. anthracis 7702 strain. The black arrows point to peptidoglycan thickenings at the region of septation for 7Δba1961 (panel b) and at some surface areas for 7Δba3679 (panel c) or to "mesosomic structures" at the septa for 7Δba5436 mutant strain (panel d).

Mutants exhibiting the strongest phenotypes in terms of morphology (7Δ*ba1961*, 7Δ*ba3679* and 7Δ*ba5436*) were selected for analysis by transmission electron microscopy (Fig. 22B). Analysis of 7Δ*ba5436* revealed some vesicular structures which appeared near the septum and the internal part of the membrane. These structures usually are related to artifacts (mesosomes) induced by chemical fixation. However, we observed these structures in three independent preparations with this strain and not in the 7702 strain suggesting a change in the composition of the septum cell-wall. Analysis of 7Δ*ba1961* and 7Δ*ba3679* showed that the mutants exhibited peptidoglycan thickenings at the septa (Fig. 22B, panel b) and at some locations of the lateral wall of the bacilli (Fig. 22B, panel c), which induced torsion of the bacterial cells.

The spores of all the mutant strains, even the 7 and RΔ*ba1961* and 7 and RΔ*ba3679*, that can sporulate only after the decrease of Mg^{2+} concentration, appeared to have the same morphology as wild-type spores (Fig. 23).

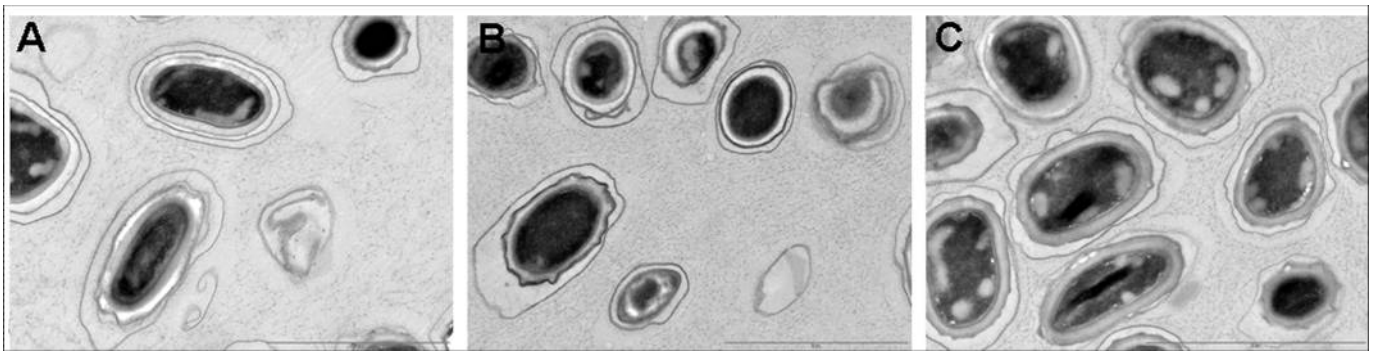

Figure 23. *Trasmission electron microscopy of 7702 wild-type spores (A), 7Δba1961 spores (B) and 7Δba3679 spores (C). Sporulation of 7702Δba1961 and 7702Δba3679 mutant strains occurred after decreasing* Mg^{2+} *concentration to 0.5 mM in culture medium.*

3.7 B. anthracis deacetylases affect the muropeptide composition and the neutral polysaccharide biosynthesis

Since all five enzymes are active on PG *in vitro*, four out of five localize in proximity to the cell envelope, two affect cell morphology and sporulation (BA1961 and BA3679) and two appear to be involved in cell daughter separation (BA2944 and BA5436), we decided to analyze the muropeptide composition of the PG of each mutant. The PG structures of both the vegetative form and the spores of 7Δ*ba1961*, 7Δ*ba1977*, 7Δ*ba2944*, 7Δ*ba3679* and 7Δ*ba5436* mutants were analysed and compared to those of parental strain 7702. After PG digestion with the muramidase mutanolysin, the resulting muropeptides were separated by HPLC (Fig. 24, 25A and 25B). Muropeptide profiles derived from the vegetative form of all mutant strains were identical to those of the parental strain. In contrast, 7*Δba1977* mutant appeared to give completely different peptidoglycan profile at the stage of spores as compared to the spore peptidoglycan profile of the wild type strain (Fig. 24). Interestingly, *Δba1961* and *Δba3679* produced almost identical PG profile between them and to the vegetative PG profile of the parental strain. Accordingly, the most abundant delta-

lactam modified muropeptides (Fig 25B, peaks ** and ***) were absent from the PG of the mutant spores, which instead accumulated a partially deacetylated dimer (Fig 25C, peak 3a).

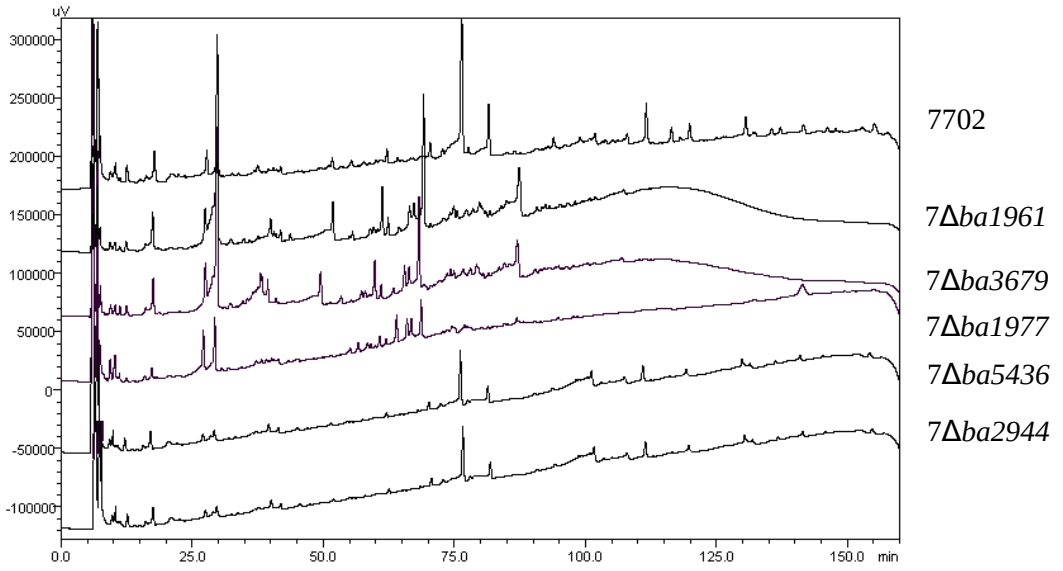

Figure 24. *HPLC analysis of the muropeptide composition of B. anthracis spore PG of WT 7702 strain and mutant stains. Δba1977, Δba1961 and Δba3679 mutant strains showed completely different peptidoglycan profile at the stage of spores compared to the spore peptidoglycan profile of the wild type strain. Δba2944 and Δba5436 showed identical PG profile to the wild type.*

Since, only three of the five enzymes (BA1977, BA1961 and BA3679) appeared to be involved in PG deacetylation and that BA2944 localized on the cell surface distant from the cell membrane, we decided to study the PG linked neutral polysaccharide. *B. anthracis* 7702 and mutant strains cell-walls, free of protein, lipid, and nucleic acid contaminants, were further extracted with hydrofluoric acid, yielding only PG-linked polysaccharides (HF-PS). Extracts were then subjected to rpHPLC in order to obtain chromatographically pure compounds for analysis (Fig. 25D). HF-PS from *7Δba1961*, *7Δba1977* and *7Δba3679* mutant strains displayed similar

chromatograms (A_{206}) to that of the parental strain and revealed one peak. In contrast, HF-PS extracted from 7*Δba2944* mutant strain displayed one peak eluting later than that of the wild-type HF-PS. Interestingly, when purified HF-PS from the 7Δ*ba2944* mutant was treated enzymatically with recombinant BC2929, the HF-PS eluted as wild-type HF-PS (Fig 25D). Three independent experiments using three independent cell-wall preparations revealed the inability of extracting even traces of the HF-PS from 7*Δba5436* mutant strain from the cell-wall (Fig 25D).

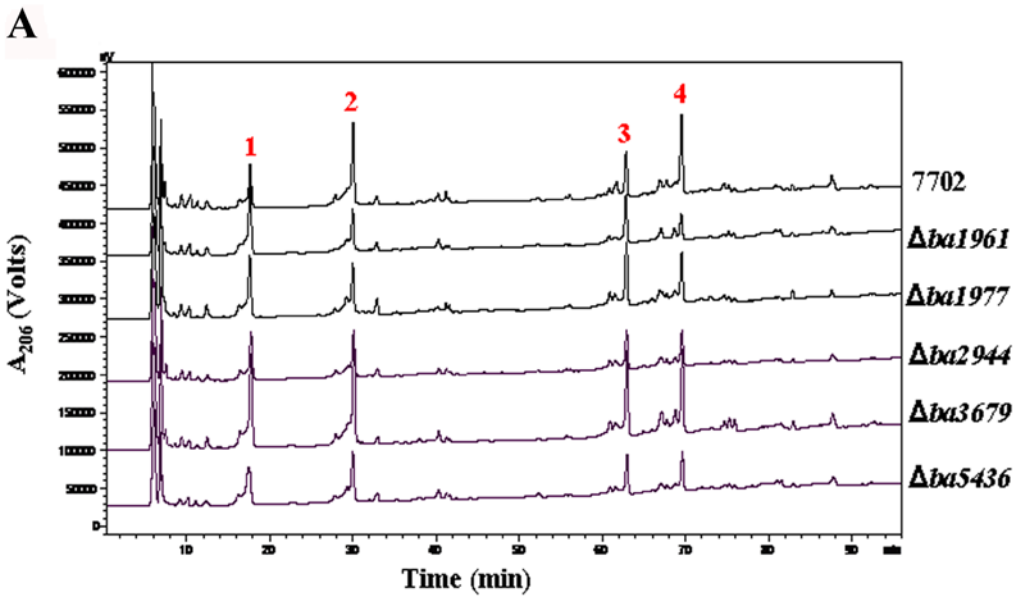

B

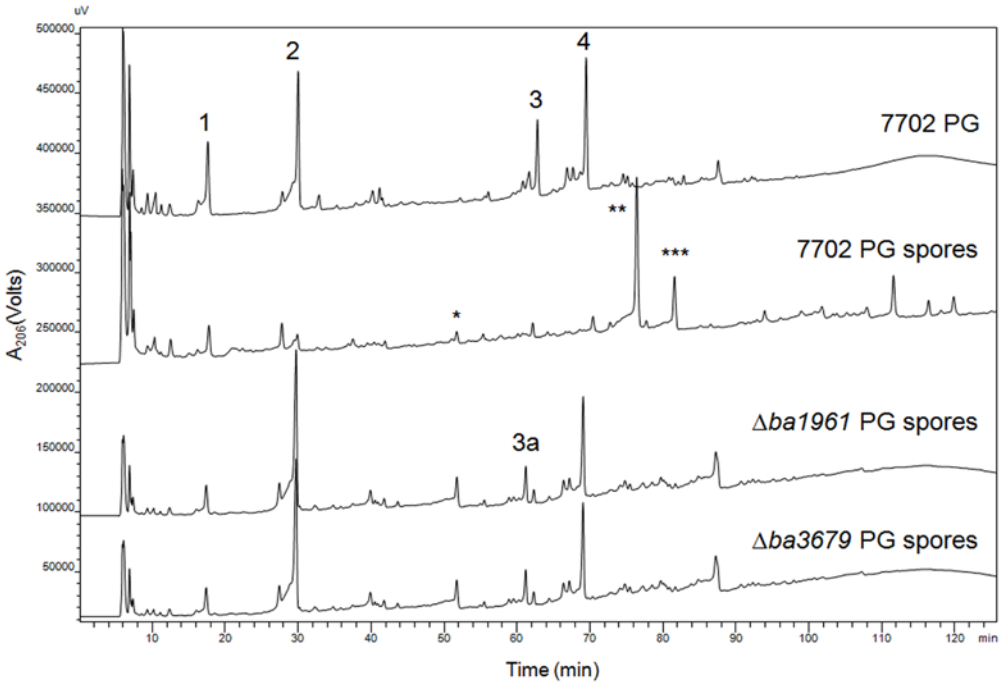

C

Muropeptide peak identification

***B. anthracis* muropeptide**	**Structure**	***m/z***
1	[GlcNAcM-TriP+Na]$^+$	893.092
2	[GlcNAcM-TetraP+Na]$^+$	964.466
3	GlcNM-TriP-GlcNM-TetraP	1732.736
4	GlcNM-TetraP-GlcNM-TetraP	1801.805
3a	[GlcNAcM-TriP-GlcNM-TetraP+Na]$^+$ or [GlcNM-TriP-GlcNAc-TetraP+Na]$^+$	1774,960
*	GlcNAc-reduced lactam-GlcNAcM-Ala	971.802
**	GlcNAc-lactam-GlcNAcM-TetraP	1382.732
***	GlcNAc-lactam-GlcNAcM-Ala	1010.538

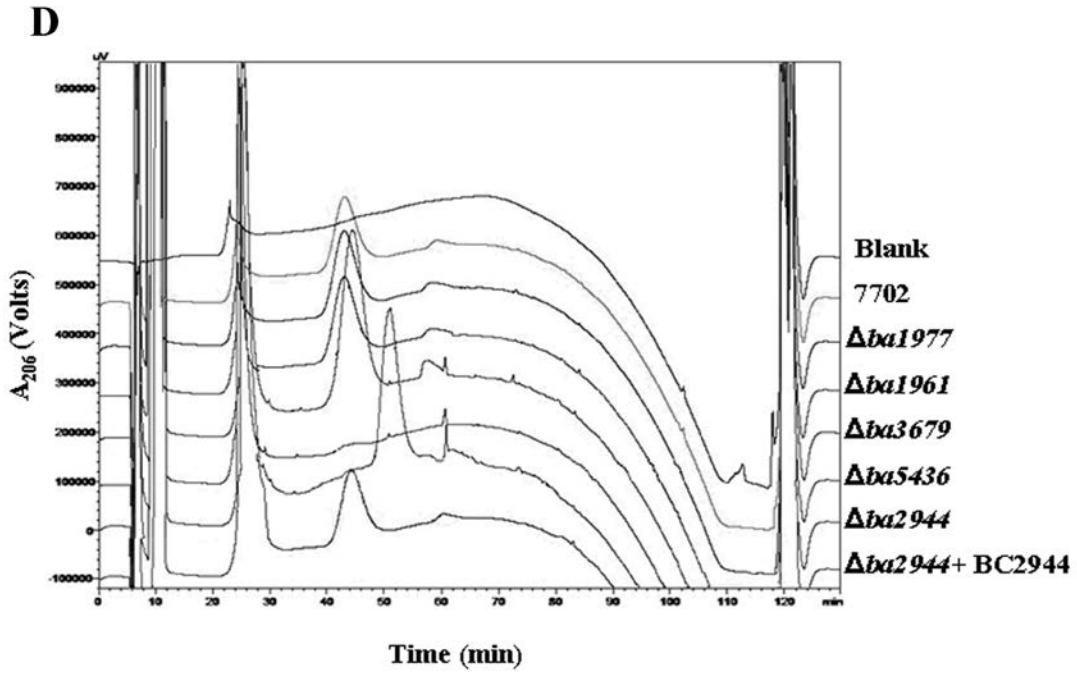

Figure 25. *HPLC analysis of PG and HF-PS of B. anthracis 7702 and mutant strains. A. Muropeptide composition of B. anthracis vegetative PG and mutant strains. Individually each deacetylase has only marginal impact on the muropeptide composition during vegetative phase of growth. B. Muropeptide composition of spore PG of parental and Δba1961 and Δba3679. Δba1961 and Δba3679 mutant strains showed completely different PG profile at the stage of spores compared to the spore PG profile of the parental strain. C. Muropeptide peak identification. D. rpHPLC chromatograms (A_{206}) of HF-PS extracts from 7702 and 7Δba1977, 7Δba1961 and 7Δba3679 mutant strains revealed a single predominant peak. rpHPLC chromatogram of HF-PS purified from 7Δba2944 mutant revealed one peak eluting later than the parental 7702 PS. Incubation of BC2929, ortholog of BA2944, with material corresponding to this peak results in a shift of the peak eluting as wild-type HF-PS. PS could not be detected in the 7Δba5436 mutant.*

3.8 B. anthracis deacetylases interfere with anchoring of S-layer proteins and autolysis

Since *B. anthracis* is known to produce an S-layer comprised of two proteins namely Sap and EA1 [65, 129] as well as other proteins harboring S-layer homology (SLH) domains, which are anchored to the neutral pyruvylated polysaccharide [60, 133] we decided to analyze the effect of deacetylases in anchoring of the two proteins to the cell wall. Under the growth conditions tested, S-layer proteins were found to be mostly cell-associated with only a minor fraction detected in the extracellular milieu of the parental 7702 strain. This pattern of localization was identical for all the mutants constructed in the present study except 7Δ*ba5436* mutant strain whereby S-layer proteins could not be detected associated to the cell-wall (Fig. 26), consistent with the absence of PG anchored neutral polysaccharide in this mutant.

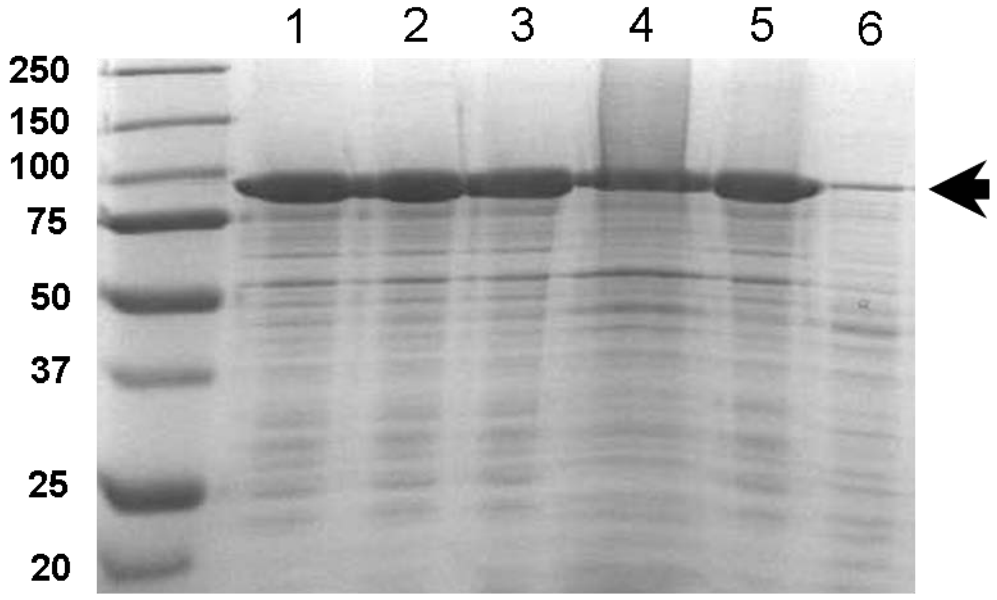

Figure 26. *SDS-PAGE of cell-associated proteins. Lanes (1) parental 7702 strain; (2) 7702Δba1961; (3) 7702Δba1977; (4) 7702Δba2944; (5) 7702Δba3679 and (6) 7702Δba5436. Molecular weight markers are indicated on the left in kDa. The arrow indicates S-layer proteins.*

Fluorescence and electron microscopy revealed an inability of all mutant strains except 7*Δba1977*, 7*Δba2944* and R*Δba1977* in cell separation of the daughter cells after cell division; yet, these deletions had no effect on the PG composition of the vegetative cells. Cell daughter separation is driven by autolysins. We therefore tested the autolytic activity of 7702 and RPG1 strain and the putative polysaccharide deacetylase mutants by addition of sodium azide, a known inducer of autolysis to growing cultures [60].

The 7Δ*ba1961*, 7Δ*ba3679*, 7Δ*ba5436* and RΔ*ba1961*, RΔ*ba3679*, RΔ*ba2944* and RΔ*ba5436* mutant strains did not display autolysis under these conditions, as the optical density of the cultures did not change after 140 min of incubation (Fig. 27A and B). In contrast, cultures of the *B. anthracis* 7*Δba1977* and 7*Δba2944* and R*Δba1977* mutant strain underwent autolysis at a level comparable to that of the parental strain. Noteworthy, the differential behavior of the 7Δ*ba2944* and RΔ*ba2944* mutants correlated perfectly with the differential cell daughter separation phenotype.

3.9 The BA1977 deacetylase affects lysozyme sensitivity

Most PGNG-dacs described so far have been mainly known to contribute to lysozyme resistance of many bacteria [86]. Thus, all five mutants in the 7702 background were grown in SPY medium and tested for lysozyme sensitivity during the exponential (Fig. 24C, panels a, b, c and e) and stationary phases (Fig 27C, panels c and f) of growth by light microscopy. Sensitivity to lysozyme was observed only in the stationary phase of growth of the 7Δ*ba1977* deletion mutant and resulted in cell rounding (Fig. 27C, panel f) while the parental strain remained rod-shaped (Fig 27C, panel c). The other mutants did not display any increased sensitivity to lysozyme compared to the wild-type strain (Fig. 28).

A

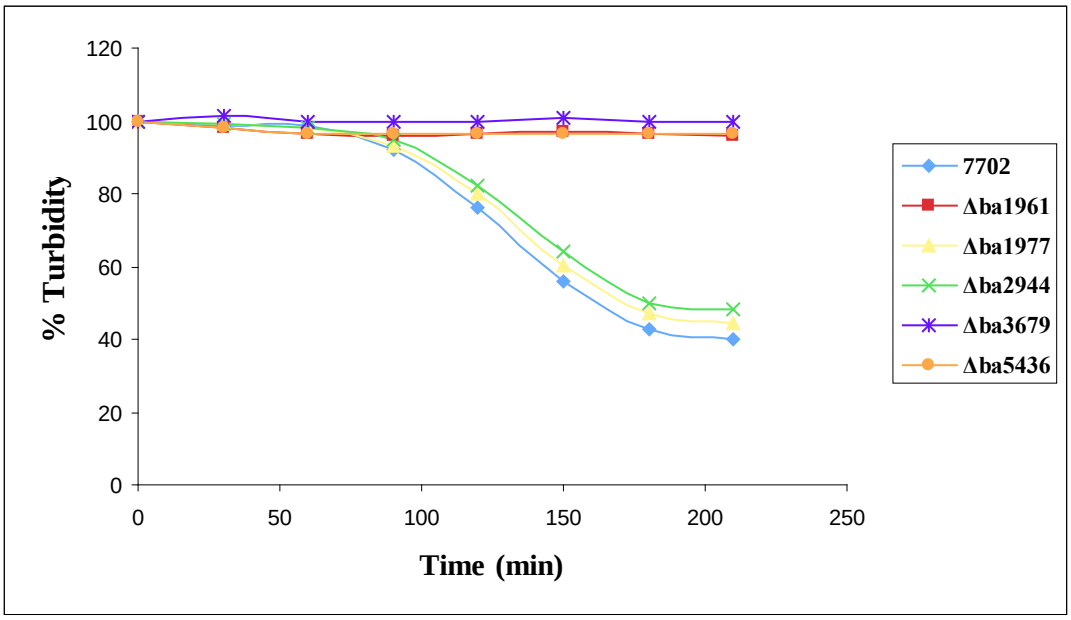
120
100
80
60
40
20
0
% Turbidity
0
50
100
150
200
250
Time (min)
7702
Δba1961
Δba1977
Δba2944
Δba3679
Δba5436

B

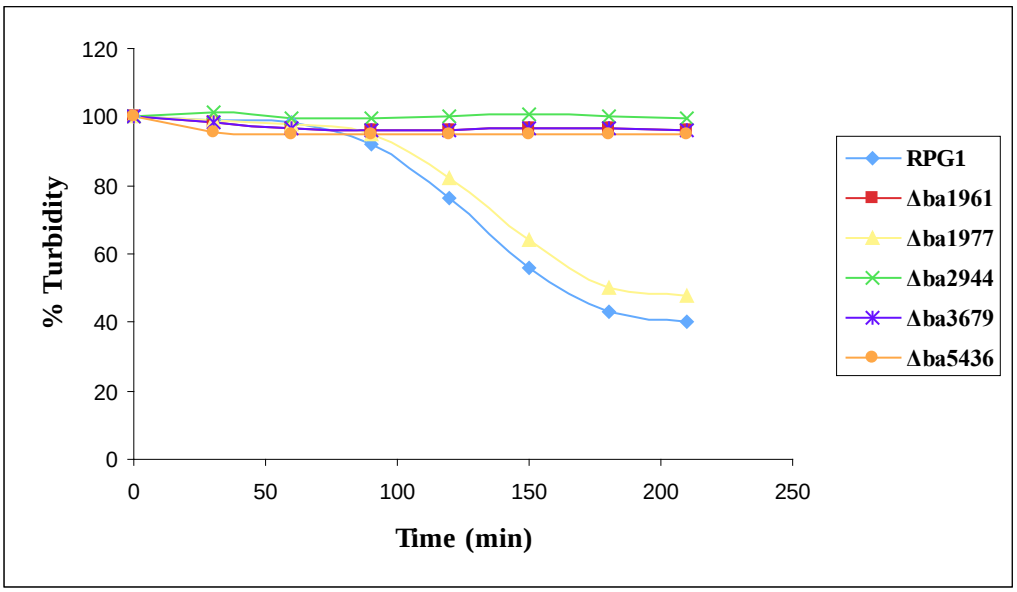
120
100
80
60
40
20
0
% Turbidity
0
50
100
150
200
250
Time (min)
RPG1
Δba1961
Δba1977
Δba2944
Δba3679
Δba5436

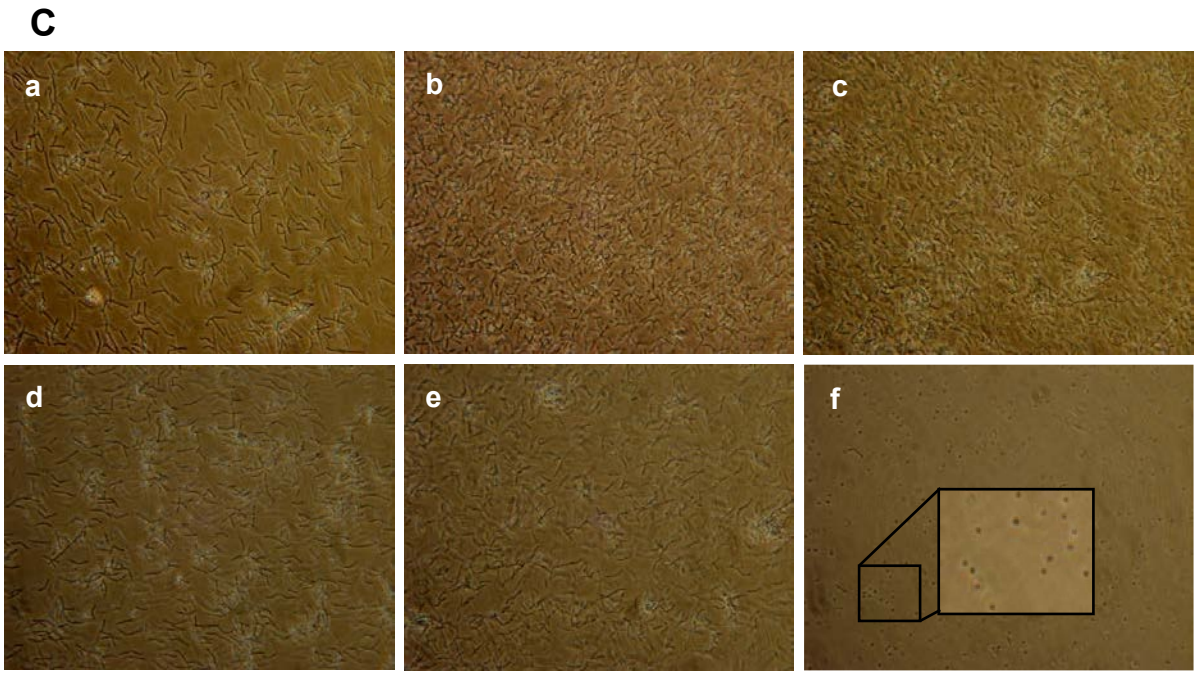

Figure 27. *Autolysis and lysozyme sensitivity of parental and mutant strains. A, B. Autolysis of B. anthracis 7702 and RPG1 mutant strains. Autolysis was induced by the addition of 10 mM sodium azide to cultures of B. anthracis 7702 and RPG1 parental strains and Δba1977, Δba2944, Δba1961, Δba3679 and Δba5436 derivative strains. Cell lysis was monitored by loss of absorbance at* A_{600}*. C. Morphology of B. anthracis 7702 strain and 7Δba1977 in the absence or presence of lysozyme. Both strains had normal bacillary morphology in SPY medium as observed by light microscopy (parental, panel a and 7Δba1977, panel d). Addition of lysozyme in exponential phase of growth had no effect either on wild-type (panel b) or the mutant strain (panel e). Addition of lysozyme during the stationary phase of growth had no effect on the wild-type strain (panel c) but resulted in cell rounding of the 7Δba1977 mutant (panel f). The samples were observed by light microscopy at a magnification of ×400.*

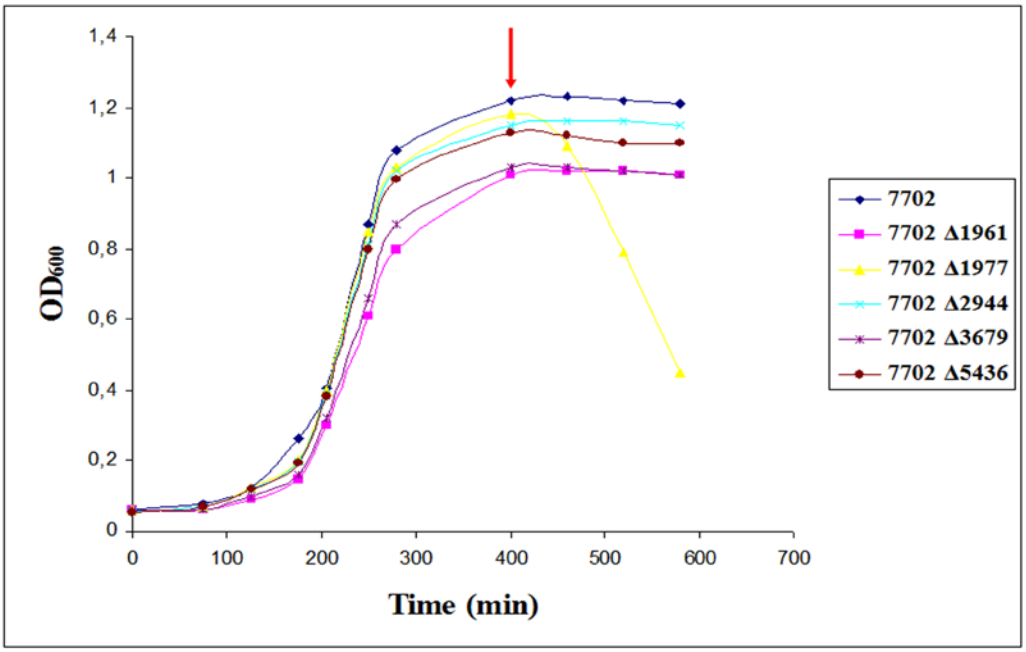

Figure 28. *Effect of lysozyme on 7702 and mutant strains. Strains were grown in SPY liquid broth at 37°C. Red arrow indicates the time point of lysozyme addition.*

3.10 RΔba1977 displays lysozyme-dependent attenuated virulence

As noted above Δ*ba1977* is the only mutation yielding strains that exhibits lysozyme sensitivity while retaining a normal wild-type morphology and response to induced autolysis. As a result, we tested the virulence of this mutant in a sub-cutaneous mouse model of infection in comparison to the parental RPG1 strain (Fig. 29A, B, C, D). The R*Δba1977* mutant was significantly attenuated after subcutaneous injection to OF/1 and BALB/c mice in comparison to the wild type strain. Injection of $5x10^3$ parental spores led to 100% death in OF/1 mice and 80% death in BALB/c mice. In contrast, the mutant strain was not virulent enough at the same dose to kill any mouse in the OF/1 and killed only 20% in the BALB/c background. In order to further define the virulence effects of the attenuated mutant, LD_{50}s were determined for the parental and R*Δba1977* mutant strain. Groups of mice (n=8) were infected by subcutaneous injection with three doses of spores. LD_{50}s revealed a ~10^2-fold decrease in virulence of the RΔ*ba1977* mutant in the OF/1 background and a ~10^4-fold decrease in virulence in the BALB/c background (Fig. 29G). Next, we tested

whether the attenuated *in vivo* phenotype of the RΔ*ba1977* mutant was related to the *in vitro* sensitivity to lysozyme. Since spores germinate, at least in part, in macrophages and that mouse macrophages produce only lysozyme M [51], we performed infection by subcutaneous injection of BALB/c *lysM*$^{-/-}$ mice with $5x10^3$ and $5x10^4$ mutant and RPG1 spores. The results indicated an increase in virulence of the RΔ*ba1977* mutant strain compared to that in OF/1 and BALB/c mice (Fig. 29E, F). We also estimated the LD_{50} of the RPG1 and the RΔ*ba1977* mutant in BALB/c *lysM*$^{-/-}$ mice (Fig. 29G). Interestingly, there was almost 100-fold increase in virulence for R*Δba1977* mutant strain when it was injected in *lysM*$^{-/-}$ mice; however, it did not entirely match the LD_{50} of the RPG1 strain.

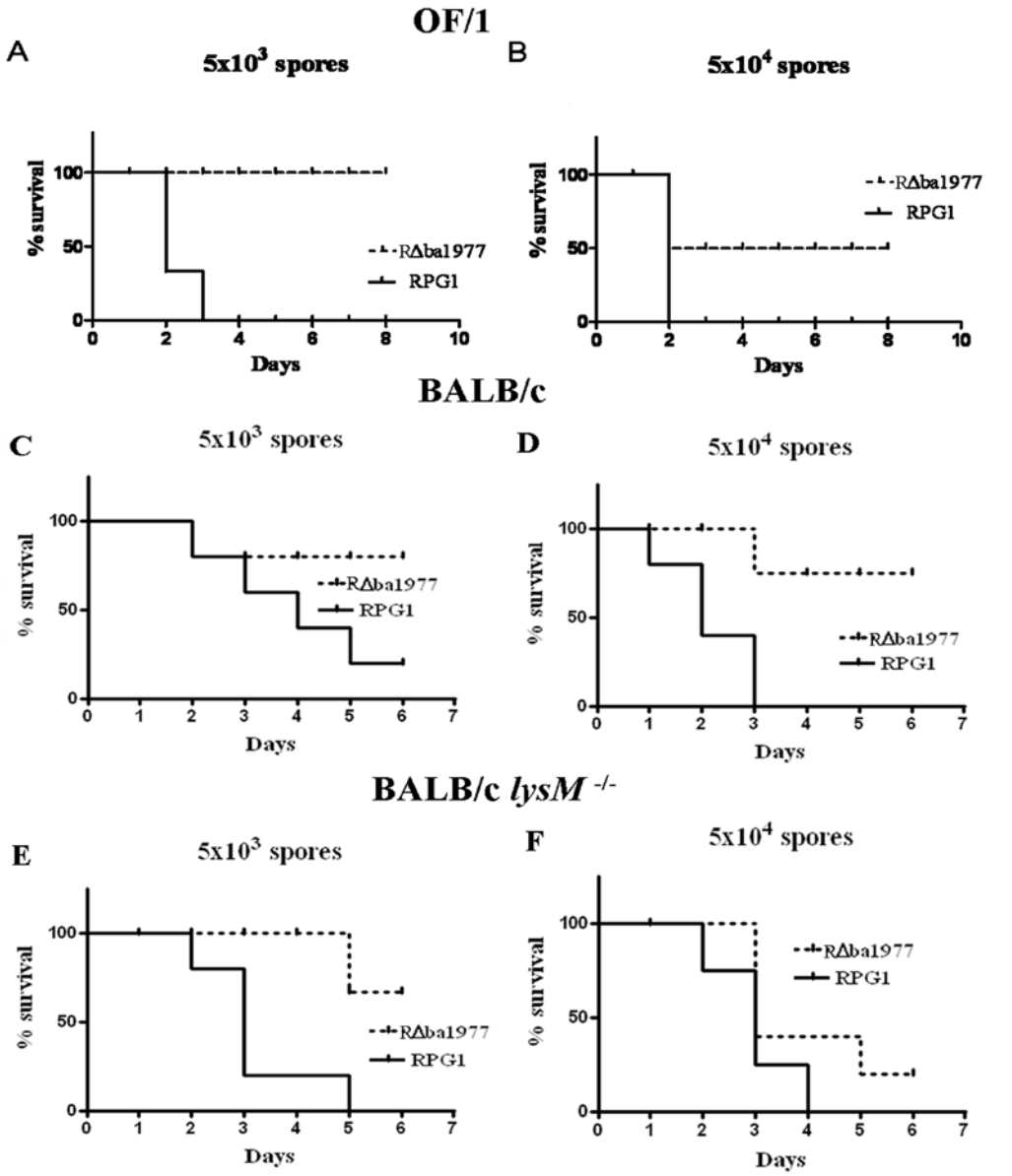

G

	LD_{50}
RPG1 OF/1	$1.23x10^2$
RPG1 BALB/c	$1.20x10^2$
RPG1 BALB/c *lysM*$^{-/-}$	$1.80x10^2$
RΔ*ba1977* OF/1	$1.39x10^4$
RΔ*ba1977* BALB/c	$8.81x10^5$
RΔ*ba1977* BALB/c *lysM*$^{-/-}$	$1.04x10^4$

Figure 29. *Survival of mice after injection with different doses of RPG1 and RΔba1977 spores. Injection of $5x10^3$ spores of RPG1 and RΔba1977 mutant in OF/1 mice (diagram A) or in BALB/c mice (diagram C). Injection of $5x10^4$ spores in OF/1 mice (diagram B) or in BALB/c mice (diagram D). Infection by subcutaneous injection of BALB/c lysM$^{-/-}$ mice with $5x10^3$ (diagram E) and $5x10^4$ (diagram F) mutant and RPG1 spores. LD_{50}s were determined (panel G). Experiments were performed with three doses per strain and groups of 8 mice.*

4. DISCUSSION

The ability to evade host immune surveillance is a critical virulence determinant for any pathogenic microorganism. One of the strategies that microorganisms use to evade the host innate immune system is de-*N*-acetylation of their cell surface glycans. In *Staphylococcus epidermidis*, exopolysaccharide deacetylation was shown to be crucial for biofilm formation, surface colonization, resistance to neutrophil phagocytosis and cationic antimicrobial peptides [93]. In S*treptococcus pneumoniae* and *Listeria monocytogenes*, mutagenesis studies revealed that cell surface peptidoglycan deacetylaces (*pgdA*s) play a role in protection against host defenses by de-*N*-acetylating *N*-acetylglucosamine (GlcNAc) residues of the peptidoglycan cell wall [27, 86, 108].

Peptidoglycan, the peptide-linked heteropolymer of GlcNAc and *N*-acetylmuramic acid, is one of the main protective barriers in the bacterial cell wall. In mammalian cells a set of hydrolytic enzymes fragment and destroy the peptidoglycan layer. Muropeptides, the bacterial peptidoglycan degradation products are sensed by a group of pattern recognition molecules (Nod proteins), initiating innate immune responses [27]. However, bacteria have developed defense mechanisms against the mammalian hydrolases by modifying peptidoglycan so that it is no longer recognized by these enzymes [27, 134, 135]. Peptidoglycan modification, specifically *N*-deacetylation, is a highly efficient strategy used by pathogenic bacteria to evade innate host defenses. For example, de-*N*-acetylation of peptidoglycan GlcNAc residues confers resistance to lysozyme, an exogenous muramidase, upon several bacterial species, such as *S. pneumoniae* [84], *B. cereus* [85, 136], *L. monocytogenes* [86] and *L. lactis* [87].

Bacterial peptidoglycan deacetylases are members of the carbohydrate esterase family 4 (CE4) (CAZY database, http://www.cazy.org/CAZY/). CE4 esterases are metal dependent enzymes that catalyze the hydrolysis of either *N*-linked acetyl group from GlcNAc residues (chitin deacetylase, NodB, and peptidoglycan GlcNAc deacetylase), or O-linked acetyl groups from O-acetylxylose residues (acetylxylan esterase, xylanase) [81-83]. Boneca *et al.* [86] studied the PgdA from *L. monocytogenes* and demonstrated for the first time that peptidoglycan *N*-deacetylation has an important role in virulence and evasion of host defense [86].

The genomes of *B. cereus* and its closest relative *B. anthracis* contain 11 putative polysaccharide deacetylase homologues. Six of these homologues have been proposed to be peptidoglycan GlcNAc deacetylases (PGNG-dacs). The unusual presence of multiple putative PGNG-dacs in *Bacillus* sp. genomes especially *B. cereus sensu lato*, including *B. anthracis* possibly indicates the different roles of these enzymes in the cellular, developmental or environmental biology of these bacteria e.g. sporulation, germination, microbe-host interactions. Given the laboratory safety precautions necessary for working with highly infectious agents and the recent concerns and proscriptions related to *B. anthracis* as a potential bioweapon (class A agent, Center for Disease Control) the *B. cereus* enzymes offer themselves as suitable models for studying the corresponding proteins of *B. anthracis*. A non-pathogenic strain of *B. anthracis*, *B. anthracis* 7702 (pXO1+, pXO2-), is also available when safety precautions are not available. Inhibition of these enzymes is extremely attractive in the quest for preventing proliferation of these highly infectious organisms.

In light of the unusual occurrence of multiple putative PGNG-dac's, we employed a combined biochemical and genetic (knock-out) analysis in order to elucidate the biological role of these enzymes. BC1974, BC2929 and BC5204, as well as BC1960 and BC3618 purified and characterized in a previous study [85], were highly promiscuous enzymes as they were active on a wide range of substrates such as PG from the Gram-positive *B. cereus* ATCC14579 and the Gram-negative *H. pylori* 26695, *N*-acetylchitooligomers ($GlcNAc_{4-6}$), GMDP (except BC2929) and glycolchitin. In addition, BC2929 was active on lipid II and BC5204 on lipid II and UDP-GlcNAc.

The intrinsic biochemical properties of each deacetylase did not reveal any clear hypothesis for their individual role. To assign such function, we constructed single mutants of all five putative deacetylase encoding genes from *B. anthracis* and compared their major phenotype characteristics (Table 7). The combination of different phenotypes of each mutant allowed us to propose a role for BA1961, BA1977 and BA3679 in PG metabolism while BA2944 and BA5436 appear to be involved at two distinct steps in the synthesis of the neutral polysaccharide. This is in agreement with the measured kinetic parameters of their three homologues from *B. cereus* BC3618, BC1974 and BC1960 that exhibited similar K_{cat}/K_m values on *N*-acetylchitooligosaccharides $GlcNAc_{4-6}$ but ~4 fold higher than those estimated for

BC5204 and ~270 fold higher for BC2929 (Table 5). The kinetic parameters for BC1960 and BC3618 on *N*-acetylchitooligomers have been previously reported [85]. Accordingly, the glycan strand backbone of PG is chemically similar to linear oligo-GlcNAc chains. The distinct kinetic parameters between the first group of deacetylases BC3618, BA1974 and BC1960, and the second group BC2929 and BC5204, suggest that the enzymes exhibit different substrate specificity *in vivo* (Table 6).

***B. anthracis* mutations**	***Δba1977***	***Δba1961***	***Δba3679***	***Δba5436***	***Δba2944***
***B. cereus* ortologous proteins**	BC1974	BC1960	BC3618	BC5204	BC2929
Cell separation	Normal	Defect	Defect	Defect	Defect[‡]
Cell division	Normal	Normal	Normal	Normal	Normal
Cell shape	Normal	Defect	Defect	Normal	Normal
PG layer	Normal	Thick	Thick	Normal	Normal
Sporulation[§]	Yes	No	No	Yes	Yes
PG profile (vegetative cells)	Identical to Wt	Identical to Wt	Identical to Wt	Identical to Wt	Identical to Wt
PG profile (spores)	Different from Wt	Different from Wt	Different from Wt	Identical to Wt	Identical to Wt
PS profile	Identical to Wt	Identical to Wt	Identical to Wt	-	Different from Wt
Lysozyme sensitive	Yes	No	No	No	No

Table 7. *Comparative table of the major phenotypic characteristics induced by Δba1961, Δba1977, Δba2944, Δba3679 and Δba5436 mutations. Phenotypes were examined by light, fluorescence and transmition electron microscopy as well as HPLC analysis. (-) Peak corresponding to PS was not observed.*

[‡]*Observed only in RΔba2944*

§Sporulation for 7Δba1961 and 7Δba3679 was only obtained after decreasing Mg^{2+} concentration to 0.5 mM.

Among the mutations constructed only Δ*ba1977* yielded sensitivity to lysozyme during the stationary phase of growth (Fig. 27C), while it had no effect on the growth and morphology of the mutant strain (Fig. 22B). In contrast to all other mutants it was affected to a similar degree as the wild-type by the induction of autolysis (Fig. 27A, 27B). Furthermore, RΔ*ba1977* was significantly attenuated after subcutaneous injection in mice indicating that BA1977 contributes to *B. anthracis* virulence *in vivo* (Fig. 29). Experiments using BALB/c *lysM*$^{-/-}$ mice showed significant increase in the virulence of RΔ*ba1977* mutant strain highlighting the lysozyme dependent contribution of BA1977 to *B. anthracis* virulence. However, the increase in virulence of the mutant did not reach the parental strain levels possibly due to the presence of lysozyme P which is still expressed in *lysM*$^{-/-}$ mice [51].

PGNG-dacs with similar properties to BA1977 (lysozyme sensitive, reduced virulence of their mutants) from other bacteria have been previously reported [86, 88, 108] indicating that BA1977 is the *bona fide* PG *N*-deacetylation PgdA of *B. anthracis*. Inhibition of PGNG-dacs would enable the host organism to lyse invading bacteria with lysozyme that is inactive against bacteria with functional enzymes. Using computational structure-based virtual screening followed by biochemical evaluation inhibitors of PgdA from *S. pneumoniae* were recently identified [137]. Paradoxically, despite the high degree of deacetylation of the PG of *B. anthracis*, inactivation of *ba1977* did not lead to any measurable change in the levels of deacetylation.

The localization of BA1977-GFP fusion at the cell membrane and the prediction that it is an *N*-terminally anchored protein, suggests that it has only access to the stress bearing PG layer contrary to other PgdA homologues. Thus, only a minor but crucial layer of the PG would be modified by BA1977 explaining the lack of measurable changes in the level of PG deacetylation but yet major consequences to the action of lysozyme. Furthemore, RT-PCR experiments of its homologue *ba1977* revealed that BA1977 is strongly expressed especially at the stationary phase of growth as compared to the rest of the PGNG-dac's homologues as well as *rpoB*.

7*Δba1961* and 7*Δba3679* mutant strains were not sensitive to lysozyme and showed a defect in cell separation. TEM revealed local thickenings of PG mainly in the septa and in different parts of the cell wall (Fig. 22C). The defect in cell separation observed could be the result of a failure of one or more of the *B. anthracis* autolysins to properly target and/or interact with PG at the septum in the absence of *N*-deacetylation. The cell wall thickening and torsion could be also the result of aborted septa or assymmetrical septa that were unable to complete cell division and proceed with cell elongation. This observation is reminiscent of the role of D,D-carboxy- and endopeptidases in regulation of cell division in *E. coli* [138].

Accordingly, strains lacking functional *ba1961* or *ba3679* were unaffected by the induction of autolysis suggesting a mechanism of impaired substrate recognition by PG hydrolases that are crucial for autolysis and cell division (Fig. 27A, 27B). Both mutants also showed a significantly reduced efficiency for spore formation compared to the wild type. The absence of the muramic delta-lactam residues containing muropeptides suggested a role in regulating PG maturation during cortex formation. However, the lactam moiety requires deacetylation of the muramic acid while BA1961 and BA3679 are involved in GlcNAc deacetylation. Hence, their role in lactam generation is probably indirect. In *B. subtilis*, this function is performed by PdaA that requires the prior action of the dedicated CwlD amidase to remove the stem peptide [50]. We propose that BA1961 and BA3679 deacetylate PG generating the optimal substrate of an amidase working in tandem with *B. anthracis* PdaA (BA0424). In the absence of the proper substrate, the amidase is unable to generate the substrate of PdaA impairing sporulation. Interestingly, sporulation was significantly enhanced when Mg^{2+} concentration in the medium was reduced. The phenotype of Mg^{2+} dependence, associated with a shape defect appears to be characteristic of genes involved in shape determination and cell wall synthesis [139].

BA1961 and BA3679 are not predicted to have a signal peptide therefore we examined PG precursors as potential substrates. However, none of these proteins was active on all PG precursors examined (Table 4). Two homologues of the SecA gene were identified in the *B. anthracis* genome suggesting that this bacterium has an alternative secretion pathway which may be responsible for secretion of some of the signal-less proteins [140]. While little is known about PG biosynthesis in *B. anthracis*, two enzymatic systems are thought to act in *B. subtilis* one for lateral cell wall growth and a second for division/septation [141, 142]. If an analogous

organization exists in *B. anthracis* our data suggest that BA1961 and BA3679 would interact predominantly with complexes at the septum while BA1977 is more associated with lateral PG synthesis.

Surprisingly, the two additional deacetylases were involved in the biosynthesis of the neutral polysaccharide of *B. anthracis*. 7, RΔ*ba5436* mutants were as resistant as the parental strains to lysozyme and to the induction of autolysis (Fig. 27A, 27B). Although they exhibited parental-like cell morphology, they showed a defect in cell daughter separation (Fig. 22B). The results from muropeptide analysis, lysozyme sensitivity test and the default in cell separation observed for 7, RΔ*ba5436* mutants prompted us to examine the neutral polysaccharide from *B. anthracis* as an alternative substrate. Interestingly, in the 7Δ*ba5436* mutant strain, we were unable to detect the neutral polysaccharide and the S-layer proteins associated to the cell-wall (Fig. 28). Defect in cell septation linked to polysaccharide modification has been previously reported for the *ΔcsaB* mutant, in which the neutral polysaccharide is no longer pyruvylated and consequently the SLH-harboring proteins, including autolysins, are no longer anchored [60]. Here, we show that the S-layer proteins are no more anchored suggesting that the SLH-harboring autolysins are also absent.

Recently, a series of reports have elucidated the structure of the major neutral polysaccharides of *B. cereus* and *B. anthracis* [57, 58, 60, 142]. Interestingly, the gene encoding BA5436 is present immediately upstream of *tagO*, although not in an operon-like arrangement (Fig. 14) [133]. It has been recently shown that TagO-mediated assembly of linkage units tether pyruvylated neutral polysaccharide to the *B. anthracis* envelope thereby enabling S-layer anchoring. The absence of the neutral polysaccharide could explain the formation of mesosomes revealed by TEM indicating reduced integrity of the cell wall (Fig. 22C). We propose at this stage BA5436 to be involved in the synthesis of the linkage unit GlcNAc-ManNAc required for tethering of the neutral polysaccharide [143]. Therefore, *B. anthracis* Δ*ba5436* mutant strains synthesize an unmodified linkage unit leading to the complete absence of the neutral polysaccharide and consequently in a defect in anchoring of SLH-harboring proteins, as exemplified by S-layer proteins (Fig 28).

At least 31 proteins identified in the secretome of *B. anthracis* are highly homologues to proteins strongly related to virulence in other pathogenic bacteria [140]. *B. anthracis* secretes, in addition to its “classic” lethal toxin and edema toxin, a

large repertoire of proteins which may be essential for its virulence. Chitlaru *et al*. proposed that BA2944 is among the secreted proteins that are relevant with virulence of pathogenic bacteria [140]. The only observable phenotype associated with Δ*ba2944* mutants was a modification in the neutral polysaccharide (Fig 25D) and an RPG1-background specific cell daughter separation phenotype (Fig. 22B). AmiA is a *B. anthracis* pXO2-encoded peptidoglycan hydrolase [72]. The N-terminal domain of AmiA is composed of three SLH repeats of about 50 residues each, involved in the cell wall targeting and non-covalently anchoring of several surface proteins in Gram-positive bacteria [125]. Therefore we can hypothesize that the modification of neutral polysaccharide by BA2944 prevents pXO2-encoded autolysin to target cell-wall and to further hydrolyze PG. In the absence of pXO2, another autolysin lacking an SLH domain might replace the function of AmiA, explaining the different phenotypes of the two genetic backgrounds.

Alternatively, it suggests that pXO2 carries a regulator that prevents complementation of AmiA by this second autolysin. *amiA* expression is controlled by AcpA, which also controls expression of *acpB*, encoding a regulator playing a significant role in virulence [144, 145] These regulators are good candidates for that function.

BC5204 and BC2929 homologues of *B. anthracis* BA5436 and BA2944 respectively, were promiscuous enzymes and their intrinsic biochemical properties did not elucidate their real substrate *in vivo*. One possible explanation for this observation is that the extent of deacetylation and substrate preference of the enzymes *in vitro* and *in vivo* should vary and depends on the location of the enzymes, access to substrates and stimulatory effects of cellular components that are not present in the *in vitro* system. Proteomic analysis studies identified BA2944 in the secretome of *B. anthracis* [140, 146] consistent with the localisation of the BA2944-GFP fusion and its substrate, the neutral polysaccharide.

In conclusion, the increased threat of anthrax in biowarfare created an urgent need to characterize new antibacterial targets from *B. anthracis*. The development of new agents to combat worsening antibiotic resistance is a priority in anti-microbial research. The most important medical countermeasures for anthrax prophylaxis and treatment include vaccines, antibodies, antibiotics and antitoxin agents. Antibiotics are effective against *B. anthracis* only if given at the very early stage of infection when symptoms are non specific and diagnosis is difficult. As a result, there is an

urgent need for antibiotics to provide improved therapy in combination with an anthrax antitoxin [147]. Antibiotics are active only against germinated spores; therefore dormant spores can germinate and cause disease once therapy has been discontinued.

The biosynthesis of the peptidoglycan (PG) layer of bacterial cell walls is a well-proven target for antibacterial action because it is the site of action of the clinically important penicillin/β-lactam and vancomycin/glycopeptide classes of antibiotics. β-lactams share the same mode of action, inhibiting synthesis of the bacterial cell wall by covalently binding with nucleophilic active site serine residues in D,D-transpeptidases (also called penicillin-binding proteins) which are involved in extracellular assembly of bacterial PG, the essential component of the cell wall. The disaccharide-pentapeptide PG structure is common to Gram-negative and Gram-positive bacteria; therefore, PG biosynthesis is an attractive target for the development of broad spectrum agents. The unique nature of the cell wall of bacteria and its lack in eukaryotic cells, allows in specific inhibitors to be used therapeutically with only a few side-effects to the patient.

Although the enzymes involved in the biosynthesis of PG have been extensively studied and enzyme inhibitors developed, there is limited information on PG modifying enzymes and their examination as new drug targets. However recently published data on these enzymes are very exciting, e.g. hypersensitivity of mutant strains to lysozyme, defects of mutant strains in cell separation, necessitating their assessment as new drug targets.

In light of the fact that effective inhibition of bacterial enzymes is a well known mechanism by which several currently available drugs elicit their antibacterial activity, enzymes continue to draw attention as potential targets for new antibacterial compounds. Currently several approaches are being pursued to study and utilize enzymes for the purpose of antibacterial drug discovery. Genomic approaches are being used to discover previously unknown enzymes that could serve as potential targets. With the advent of genomic and proteomic technologies, it is now possible to simultaneously identify numerous genes and their enzyme products that could be potential targets for new antibacterial compounds.

In this study, we report for the first time the presence of two PGNG-dac's namely BA1961 and BA3679 exhibiting different properties from PGNG-dac's currently characterized from other bacteria and BA1977 characterized in this study.

These two enzymes have a direct role in proper assembly of the PG layer, particularly, during cell division. Furthermore, we present the characterization of two novel polysaccharide deacetylases which do not act on PG and either affect the attachment of the neutral polysaccharide to PG and anchoring of proteins harboring an S-layer homology domain (BA5436) or modify the neutral polysaccharide (BA2944).

In many studies it has been demonstrated that PGNG-dacs genes are validated antibiotic targets as demonstrated by the reduced virulence of mutant strains of various pathogens [86, 88, 108] and RΔ*ba1977* in this study. The identification of additional PGNG-dacs BA1961 and BA3679 in *B. anthracis* of different suggested biological roles offers new targets for the design of inhibitors against this bioterrorism agent. Furthermore, elucidation of the structural requirements for S-layer assembly in Gram-positive bacteria may lead to numerous translational applications in industrial processes exploiting the SLH domain and synthetic pyruvylated polysaccharides.

5. PERSPECTIVES

5.1 New antibacterial agents/ design of deacetylase inhibitors

The crystallization and structural determination of the PGNG-dac's of the present study and the cocrystallization of enzyme-substrate complexes are of special interest for their functional characterization. From the already determined structures deposited in the Protein Data Bank it is known that these enzymes adopt the α/β barrel motif conformation, their active site contains an ion (possibly Zn^{2+}) and the residues involved in catalysis are conserved. Virtual screening methods are increasingly used to identify potential new lead compounds in drug discovery [148, 149] and have also been successfully used on antibacterial targets [150].

Using computational structure-based virtual screening followed by biochemical evaluation, Bui *et al.* were able to identify two promising inhibitors of PgdA (peptidoglycan deacetylase from *Streptococcus pneumoniae*) with IC_{50} values of 584 mM and 130 mM [137].

Furthermore, Ape1 (O-Acetylpeptidoglycan esterase) from *N. gonorrhoeae* was screened against a subset of compounds of the Canadian Compound Collection, using 4-methylumbelliferyl-acetate as substrate and developing a fluorogenic assay amenable for the high-throughput screening for potential inhibitors [151]. Seven compounds were identified as true inhibitors of Ape1 and dose response curves were generated leading to the identification of five of these compounds with IC values ranging between 0.3 μM and 23 μM. Among these, purpurin, a natural red/yellow dye found in the madder plant, was selected for further analysis and it was found to inhibit the growth of both Gram-positive and Gram-negative bacteria that produce both O-acetylated PG and Ape.

Recently, the enzymes BC1960 (BA1961 homologue) and BC1974 (BA1977 homologue) were cloned, expressed in *E.coli* and crystallized [152 and in preparation respectively]. Further structural studies are essential in order to facilitate the design and synthesis of new inhibitors towards the development of effective antimicrobial agents.

The application of the experimental methods of protein crystallography enhances the ability of understanding the interactions between the inhibitor and the

protein molecular target, leading to optimized inhibitors. The initial design is based on crystal structures of complexes between enzymes and several substrates e.g. GlcNAc oligomers for PG GlcNAc deacetylases. By defining the three dimensional structure of the protein-targets it will subsequently allow us to test a large number of molecules *in silico* (by using available libraries) for their ability to bind and inhibit the enzymes. Using initial hits or hits derived from structure based studies, as ligands, a ligand-based virtual screening will be applied for the identification of hit compounds with improved properties, such as binding affinity. Lead compounds are optimized in terms of the number and type of molecular interactions with the enzyme and filtered for safe pharmacological action.

Consequently, one interesting perspective will be to use a combination of X-ray crystallography, enzymology, mutagenesis, high-throughput screening and iterative structure-driven organic synthesis to define the structure, mechanism and substrate binding of the the PGNG-dacs from *B. anthracis,* presented in this study, to identify inhibitors and study their *in vitro/in vivo* effects of cell wall hydrolysis by mammalian glycosidases.

5.2 Role of BA1961 and BA3679 in regulation of cell wall synthesis

The gram-positive organism *Bacillus subtilis* has three actin-like proteins: MreB, Mbl, and MreBH. It has been shown that all three colocalize, forming a helical structure spanning the length of the cell [153], and that they interact with each other [154]. Formstone *et al* claim that in *B. subtilis*, an *mreB* deletion mutant is lethal under normal growth conditions but viable when the growth medium is supplemented with high concentrations of Mg^{2+} (Fig. 30) [155]. Elevated Mg^{2+} concentrations are known to rescue various other *B. subtilis* mutants, many of which are impaired in cell wall synthesis. For example, growth and the cell shape of a *ponA* (encoding PBP1) mutant are restored by Mg^{2+} [156], and the phenotype of a strain carrying a deletion in *tagO* (resulting in a strain deficient in wall teichoic acid) is ameliorated by high Mg^{2+} concentrations [157]. Also, *mreC* and *mreD* mutants (which both encode proteins with a role in cell elongation) are Mg^{2+} dependent [158].

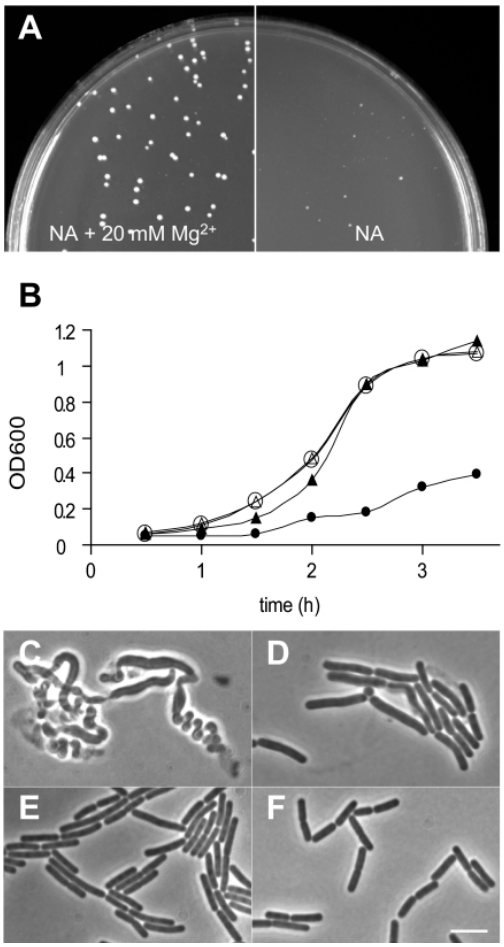

Figure 30: ***B. subtilis Δmbl is Mg^{2+} dependent. (A) Plating efficiency after transformation selecting for deletion of mbl with (left) or without (right) addition of 20 mM Mg2+. (B) Growth curve of B. subtilis wild type (open symbols) and mbl mutant (closed symbols) at 37°C in Difco Antibiotic Medium 3 (PAB) medium without (circles) or with (triangles) addition of 20 mM Mg^{2+}. (C to F) Morphology (phase-contrast microscopy) of B. subtilis Δmbl grown in PAB (C) or in PAB supplemented with 20 mM Mg^{2+} (D) compared to a wild-type strain grown in PAB (E) or in PAB containing 20 mM Mg^{2+} (F) [139].***

ba1961 and *ba3679* deletions produce bacteria with abnormal cell shape, unable both to separate after cell division and sporulate under normal Mg^{2+} concentration (10mM). Moreover, transmission electron microscopy analysis of the

above deletion mutants revealed peptidoglycan thickenings at certain areas of the bacterial cell wall. Noteworthy, although peptidoglycan analysis derived from 7Δ*ba1961* and 7Δ*ba3679 B. anthracis* mutants by HPLC and mass spectrometry confirmed that BA1961 and BA3679 are PGNG-dacs, their deletion mutants were resistant to lysozyme. Almost complete recovery of their abnormal phenotype was derived after decrease of Mg^{2+} concentration to 0.5mM.

Therefore, it will be extremely interesting to investigate possible implications of BA1961 and BA3679 in orchestrating cell wall synthesis by regulating either the targeting or function of the machinery that is adding new peptidoglycan material at the regions that is needed. Protein-protein interaction experiments combined with double deletion mutants of one of the two PGNG-dacs referred at this section and of the MreB-homologue of *B. anthracis* (BA4684) would provide useful information for a possible role of these two enzymes in regulation of cell wall synthesis.

6. REFERENCES

1. Schwartz, M., *Dr. Jekyll and Mr. Hyde: a short history of anthrax.* Mol Aspects Med, 2009. **30**(6): p. 347-55.
2. Dirckx, J.H., *Virgil on anthrax.* Am J Dermatopathol, 1981. **3**(2): p. 191-5.
3. McSherry, J. and R. Kilpatrick, *The plague of Athens.* J R Soc Med, 1992. **85**(11): p. 713.
4. Edwards, K.A., H.A. Clancy, and A.J. Baeumner, *Bacillus anthracis: toxicology, epidemiology and current rapid-detection methods.* Anal Bioanal Chem, 2006. **384**(1): p. 73-84.
5. Hudson, M.J., et al., *Bacillus anthracis: balancing innocent research with dual-use potential.* Int J Med Microbiol, 2008. **298**(5-6): p. 345-64.
6. Inglesby, T.V., et al., *Anthrax as a biological weapon, 2002: updated recommendations for management.* JAMA, 2002. **287**(17): p. 2236-52.
7. Koehler, T.M., *Bacillus anthracis physiology and genetics.* Mol Aspects Med, 2009. **30**(6): p. 386-96.
8. Helgason, E., et al., *Bacillus anthracis, Bacillus cereus, and Bacillus thuringiensis--one species on the basis of genetic evidence.* Appl Environ Microbiol, 2000. **66**(6): p. 2627-30.
9. Dixon, T.C., et al., *Anthrax.* N Engl J Med, 1999. **341**(11): p. 815-26.
10. Fouet, A., *AtxA, a Bacillus anthracis global virulence regulator.* Res Microbiol. **161**(9): p. 735-42.
11. Guidi-Rontani, C., et al., *Germination of Bacillus anthracis spores within alveolar macrophages.* Mol Microbiol, 1999. **31**(1): p. 9-17.
12. Okinaka, R.T., et al., *Sequence and organization of pXO1, the large Bacillus anthracis plasmid harboring the anthrax toxin genes.* J Bacteriol, 1999. **181**(20): p. 6509-15.
13. Candela, T., M. Mock, and A. Fouet, *CapE, a 47-amino-acid peptide, is necessary for Bacillus anthracis polyglutamate capsule synthesis.* J Bacteriol, 2005. **187**(22): p. 7765-72.

14. Candela, T. and A. Fouet, *Bacillus anthracis CapD, belonging to the gamma-glutamyltranspeptidase family, is required for the covalent anchoring of capsule to peptidoglycan.* Mol Microbiol, 2005. **57**(3): p. 717-26.
15. Fouet, A. and M. Mock, *Regulatory networks for virulence and persistence of Bacillus anthracis.* Curr Opin Microbiol, 2006. **9**(2): p. 160-6.
16. Mock, M. and A. Fouet, *Anthrax.* Annu Rev Microbiol, 2001. **55**: p. 647-71.
17. Drysdale, M., et al., *atxA controls Bacillus anthracis capsule synthesis via acpA and a newly discovered regulator, acpB.* J Bacteriol, 2004. **186**(2): p. 307-15.
18. Hugh-Jones, M. and J. Blackburn, *The ecology of Bacillus anthracis.* Mol Aspects Med, 2009. **30**(6): p. 356-67.
19. Weiner, M.A. and P.C. Hanna, *Macrophage-mediated germination of Bacillus anthracis endospores requires the gerH operon.* Infect Immun, 2003. **71**(7): p. 3954-9.
20. Stanley, J.L. and H. Smith, *Purification of factor I and recognition of a third factor of the anthrax toxin.* J Gen Microbiol, 1961. **26**: p. 49-63.
21. Gladstone, G.P., *Immunity to anthrax: protective antigen present in cell-free culture filtrates.* Br J Exp Pathol, 1946. **27**(6): p. 394-418.
22. Mogridge, J., K. Cunningham, and R.J. Collier, *Stoichiometry of anthrax toxin complexes.* Biochemistry, 2002. **41**(3): p. 1079-82.
23. Leppla, S.H., *Anthrax toxin edema factor: a bacterial adenylate cyclase that increases cyclic AMP concentrations of eukaryotic cells.* Proc Natl Acad Sci U S A, 1982. **79**(10): p. 3162-6.
24. Tonello, F. and C. Montecucco, *The anthrax lethal factor and its MAPK kinase-specific metalloprotease activity.* Mol Aspects Med, 2009. **30**(6): p. 431-8.
25. Duesbery, N.S., et al., *Proteolytic inactivation of MAP-kinase-kinase by anthrax lethal factor.* Science, 1998. **280**(5364): p. 734-7.
26. Schleifer, K.H. and O. Kandler, *Peptidoglycan types of bacterial cell walls and their taxonomic implications.* Bacteriol Rev, 1972. **36**(4): p. 407-77.
27. Boneca, I.G., *The role of peptidoglycan in pathogenesis.* Curr Opin Microbiol, 2005. **8**(1): p. 46-53.
28. Barreteau, H., et al., *Cytoplasmic steps of peptidoglycan biosynthesis.* FEMS Microbiol Rev, 2008. **32**(2): p. 168-207.

29. van Heijenoort, J., *Lipid intermediates in the biosynthesis of bacterial peptidoglycan.* Microbiol Mol Biol Rev, 2007. **71**(4): p. 620-35.
30. Mohammadi, T., et al., *Identification of FtsW as a transporter of lipid-linked cell wall precursors across the membrane.* EMBO J. **30**(8): p. 1425-32.
31. Lovering, A.L., M. Gretes, and N.C. Strynadka, *Structural details of the glycosyltransferase step of peptidoglycan assembly.* Curr Opin Struct Biol, 2008. **18**(5): p. 534-43.
32. Sorbara, M.T. and D.J. Philpott, *Peptidoglycan: a critical activator of the mammalian immune system during infection and homeostasis.* Immunol Rev. **243**(1): p. 40-60.
33. Dziarski, R. and D. Gupta, *Review: Mammalian peptidoglycan recognition proteins (PGRPs) in innate immunity.* Innate Immun. **16**(3): p. 168-74.
34. Wang, L., et al., *Sensing of Gram-positive bacteria in Drosophila: GNBP1 is needed to process and present peptidoglycan to PGRP-SA.* EMBO J, 2006. **25**(20): p. 5005-14.
35. Filipe, S.R., A. Tomasz, and P. Ligoxygakis, *Requirements of peptidoglycan structure that allow detection by the Drosophila Toll pathway.* EMBO Rep, 2005. **6**(4): p. 327-33.
36. Inohara, N., et al., *Nod1, an Apaf-1-like activator of caspase-9 and nuclear factor-kappaB.* J Biol Chem, 1999. **274**(21): p. 14560-7.
37. Magalhaes, J.G., et al., *Murine Nod1 but not its human orthologue mediates innate immune detection of tracheal cytotoxin.* EMBO Rep, 2005. **6**(12): p. 1201-7.
38. Ogura, Y., et al., *Nod2, a Nod1/Apaf-1 family member that is restricted to monocytes and activates NF-kappaB.* J Biol Chem, 2001. **276**(7): p. 4812-8.
39. Gutierrez, O., et al., *Induction of Nod2 in myelomonocytic and intestinal epithelial cells via nuclear factor-kappa B activation.* J Biol Chem, 2002. **277**(44): p. 41701-5.
40. Girardin, S.E., et al., *Nod1 detects a unique muropeptide from gram-negative bacterial peptidoglycan.* Science, 2003. **300**(5625): p. 1584-7.
41. Chamaillard, M., et al., *An essential role for NOD1 in host recognition of bacterial peptidoglycan containing diaminopimelic acid.* Nat Immunol, 2003. **4**(7): p. 702-7.

42. Girardin, S.E., et al., *Peptidoglycan molecular requirements allowing detection by Nod1 and Nod2.* J Biol Chem, 2003. **278**(43): p. 41702-8.
43. Travassos, L.H., et al., *Toll-like receptor 2-dependent bacterial sensing does not occur via peptidoglycan recognition.* EMBO Rep, 2004. **5**(10): p. 1000-6.
44. Schroder, N.W., et al., *Lipoteichoic acid (LTA) of Streptococcus pneumoniae and Staphylococcus aureus activates immune cells via Toll-like receptor (TLR)-2, lipopolysaccharide-binding protein (LBP), and CD14, whereas TLR-4 and MD-2 are not involved.* J Biol Chem, 2003. **278**(18): p. 15587-94.
45. Schwandner, R., et al., *Peptidoglycan- and lipoteichoic acid-induced cell activation is mediated by toll-like receptor 2.* J Biol Chem, 1999. **274**(25): p. 17406-9.
46. Asong, J., et al., *Binding and Cellular Activation Studies Reveal That Toll-like Receptor 2 Can Differentially Recognize Peptidoglycan from Gram-positive and Gram-negative Bacteria.* J Biol Chem, 2009. **284**(13): p. 8643-53.
47. Ozinsky, A., et al., *The repertoire for pattern recognition of pathogens by the innate immune system is defined by cooperation between toll-like receptors.* Proc Natl Acad Sci U S A, 2000. **97**(25): p. 13766-71.
48. Vollmer, W., *Structural variation in the glycan strands of bacterial peptidoglycan.* FEMS Microbiol Rev, 2008. **32**(2): p. 287-306.
49. Fukushima, T., T. Kitajima, and J. Sekiguchi, *A polysaccharide deacetylase homologue, PdaA, in Bacillus subtilis acts as an N-acetylmuramic acid deacetylase in vitro.* J Bacteriol, 2005. **187**(4): p. 1287-92.
50. Gilmore, M.E., et al., *Production of muramic delta-lactam in Bacillus subtilis spore peptidoglycan.* J Bacteriol, 2004. **186**(1): p. 80-9.
51. Davis, K.M. and J.N. Weiser, *Modifications to the peptidoglycan backbone help bacteria to establish infection.* Infect Immun. **79**(2): p. 562-70.
52. Freymond, P.P., et al., *Poly(glucosyl-N-acetylgalactosamine 1-phosphate), a wall teichoic acid of Bacillus subtilis 168: its biosynthetic pathway and mode of attachment to peptidoglycan.* Microbiology, 2006. **152**(Pt 6): p. 1709-18.
53. Ward, J.B., *Teichoic and teichuronic acids: biosynthesis, assembly, and location.* Microbiol Rev, 1981. **45**(2): p. 211-43.
54. Read, T.D., et al., *The genome sequence of Bacillus anthracis Ames and comparison to closely related bacteria.* Nature, 2003. **423**(6935): p. 81-6.

55. Fox, A., et al., *Determination of carbohydrate profiles of Bacillus anthracis and Bacillus cereus including identification of O-methyl methylpentoses by using gas chromatography-mass spectrometry.* J Clin Microbiol, 1993. **31**(4): p. 887-94.
56. Ekwunife, F.S., et al., *Isolation and purification of cell wall polysaccharide of Bacillus anthracis (delta Sterne).* FEMS Microbiol Lett, 1991. **66**(3): p. 257-62.
57. Choudhury, B., et al., *The structure of the major cell wall polysaccharide of Bacillus anthracis is species-specific.* J Biol Chem, 2006. **281**(38): p. 27932-41.
58. Leoff, C., et al., *Secondary cell wall polysaccharides of Bacillus anthracis are antigens that contain specific epitopes which cross-react with three pathogenic Bacillus cereus strains that caused severe disease, and other epitopes common to all the Bacillus cereus strains tested.* Glycobiology, 2009. **19**(6): p. 665-73.
59. Forsberg, L.S., et al., *Secondary cell wall polysaccharides from Bacillus cereus strains G9241, 03BB87 and 03BB102 causing fatal pneumonia share similar glycosyl structures with the polysaccharides from Bacillus anthracis.* Glycobiology. **21**(7): p. 934-48.
60. Mesnage, S., et al., *Bacterial SLH domain proteins are non-covalently anchored to the cell surface via a conserved mechanism involving wall polysaccharide pyruvylation.* EMBO J, 2000. **19**(17): p. 4473-84.
61. Forsberg, L.S., et al., *Localization and structural analysis of a conserved pyruvylated epitope in Bacillus anthracis secondary cell wall polysaccharides and characterization of the galactose-deficient wall polysaccharide from avirulent B. anthracis CDC 684.* Glycobiology. **22**(8): p. 1103-17.
62. Schneewind, O. and D.M. Missiakas, *Protein secretion and surface display in Gram-positive bacteria.* Philos Trans R Soc Lond B Biol Sci. **367**(1592): p. 1123-39.
63. Lupas, A., et al., *Domain structure of the Acetogenium kivui surface layer revealed by electron crystallography and sequence analysis.* J Bacteriol, 1994. **176**(5): p. 1224-33.

64. Mignot, T., et al., *Distribution of S-layers on the surface of Bacillus cereus strains: phylogenetic origin and ecological pressure.* Environ Microbiol, 2001. **3**(8): p. 493-501.
65. Mesnage, S., et al., *Molecular characterization of the Bacillus anthracis main S-layer component: evidence that it is the major cell-associated antigen.* Mol Microbiol, 1997. **23**(6): p. 1147-55.
66. Ezzell, J.W., Jr. and T.G. Abshire, *Immunological analysis of cell-associated antigens of Bacillus anthracis.* Infect Immun, 1988. **56**(2): p. 349-56.
67. Etienne-Toumelin, I., et al., *Characterization of the Bacillus anthracis S-layer: cloning and sequencing of the structural gene.* J Bacteriol, 1995. **177**(3): p. 614-20.
68. Mignot, T., et al., *Developmental switch of S-layer protein synthesis in Bacillus anthracis.* Mol Microbiol, 2002. **43**(6): p. 1615-27.
69. Mignot, T., M. Mock, and A. Fouet, *A plasmid-encoded regulator couples the synthesis of toxins and surface structures in Bacillus anthracis.* Mol Microbiol, 2003. **47**(4): p. 917-27.
70. Guignot, J., M. Mock, and A. Fouet, *AtxA activates the transcription of genes harbored by both Bacillus anthracis virulence plasmids.* FEMS Microbiol Lett, 1997. **147**(2): p. 203-7.
71. Ariel, N., et al., *Genome-based bioinformatic selection of chromosomal Bacillus anthracis putative vaccine candidates coupled with proteomic identification of surface-associated antigens.* Infect Immun, 2003. **71**(8): p. 4563-79.
72. Mesnage, S. and A. Fouet, *Plasmid-encoded autolysin in Bacillus anthracis: modular structure and catalytic properties.* J Bacteriol, 2002. **184**(1): p. 331-4.
73. Green, B.D., et al., *Demonstration of a capsule plasmid in Bacillus anthracis.* Infect Immun, 1985. **49**(2): p. 291-7.
74. Uchida, I., et al., *Identification of a novel gene, dep, associated with depolymerization of the capsular polymer in Bacillus anthracis.* Mol Microbiol, 1993. **9**(3): p. 487-96.
75. Richter, S., et al., *Capsule anchoring in Bacillus anthracis occurs by a transpeptidation reaction that is inhibited by capsidin.* Mol Microbiol, 2009. **71**(2): p. 404-20.

76. Wang, T.T. and A.H. Lucas, *The capsule of Bacillus anthracis behaves as a thymus-independent type 2 antigen.* Infect Immun, 2004. **72**(9): p. 5460-3.
77. Glomski, I.J., et al., *Primary involvement of pharynx and peyer's patch in inhalational and intestinal anthrax.* PLoS Pathog, 2007. **3**(6): p. e76.
78. Keppie, J., H. Smith, and P.W. Harris-Smith, *The chemical basis of the virulence of bacillus anthracis. II. Some biological properties of bacterial products.* Br J Exp Pathol, 1953. **34**(5): p. 486-96.
79. Makino, S., et al., *Molecular characterization and protein analysis of the cap region, which is essential for encapsulation in Bacillus anthracis.* J Bacteriol, 1989. **171**(2): p. 722-30.
80. Candela, T., et al., *Cell-wall preparation containing poly-gamma-D-glutamate covalently linked to peptidoglycan, a straightforward extractable molecule, protects mice against experimental anthrax infection.* Vaccine. **31**(1): p. 171-5.
81. Caufrier, F., et al., *Carbohydrate esterase family 4 enzymes: substrate specificity.* Carbohydr Res, 2003. **338**(7): p. 687-92.
82. Tsigos, I., et al., *Chitin deacetylases: new, versatile tools in biotechnology.* Trends Biotechnol, 2000. **18**(7): p. 305-12.
83. Kafetzopoulos, D., A. Martinou, and V. Bouriotis, *Bioconversion of chitin to chitosan: purification and characterization of chitin deacetylase from Mucor rouxii.* Proc Natl Acad Sci U S A, 1993. **90**(7): p. 2564-8.
84. Vollmer, W. and A. Tomasz, *The pgdA gene encodes for a peptidoglycan N-acetylglucosamine deacetylase in Streptococcus pneumoniae.* J Biol Chem, 2000. **275**(27): p. 20496-501.
85. Psylinakis, E., et al., *Peptidoglycan N-acetylglucosamine deacetylases from Bacillus cereus, highly conserved proteins in Bacillus anthracis.* J Biol Chem, 2005. **280**(35): p. 30856-63.
86. Boneca, I.G., et al., *A critical role for peptidoglycan N-deacetylation in Listeria evasion from the host innate immune system.* Proc Natl Acad Sci U S A, 2007. **104**(3): p. 997-1002.
87. Meyrand, M., et al., *Peptidoglycan N-acetylglucosamine deacetylation decreases autolysis in Lactococcus lactis.* Microbiology, 2007. **153**(Pt 10): p. 3275-85.

88. Fittipaldi, N., et al., *Significant contribution of the pgdA gene to the virulence of Streptococcus suis.* Mol Microbiol, 2008. **70**(5): p. 1120-35.
89. Kaoukab-Raji, A., et al., *Characterization of SfPgdA, a Shigella flexneri peptidoglycan deacetylase required for bacterial persistence within polymorphonuclear neutrophils.* Microbes Infect. **14**(7-8): p. 619-27.
90. Kobayashi, K., et al., *Identification and characterization of a novel polysaccharide deacetylase C (PdaC) from Bacillus subtilis.* J Biol Chem. **287**(13): p. 9765-76.
91. Deng, D.M., et al., *Streptococcus mutans SMU.623c codes for a functional, metal-dependent polysaccharide deacetylase that modulates interactions with salivary agglutinin.* J Bacteriol, 2009. **191**(1): p. 394-402.
92. Milani, C.J., et al., *The novel polysaccharide deacetylase homologue Pdi contributes to virulence of the aquatic pathogen Streptococcus iniae.* Microbiology. **156**(Pt 2): p. 543-54.
93. Vuong, C., et al., *A crucial role for exopolysaccharide modification in bacterial biofilm formation, immune evasion, and virulence.* J Biol Chem, 2004. **279**(52): p. 54881-6.
94. Blair, D.E. and D.M. van Aalten, *Structures of Bacillus subtilis PdaA, a family 4 carbohydrate esterase, and a complex with N-acetyl-glucosamine.* FEBS Lett, 2004. **570**(1-3): p. 13-9.
95. Blair, D.E., et al., *Structure and metal-dependent mechanism of peptidoglycan deacetylase, a streptococcal virulence factor.* Proc Natl Acad Sci U S A, 2005. **102**(43): p. 15429-34.
96. Oberbarnscheidt, L., et al., *Structure of a carbohydrate esterase from Bacillus anthracis.* Proteins, 2007. **66**(1): p. 250-2.
97. Deckers, D., et al., *Periplasmic lysozyme inhibitor contributes to lysozyme resistance in Escherichia coli.* Cell Mol Life Sci, 2004. **61**(10): p. 1229-37.
98. Fernie-King, B.A., et al., *Streptococcal inhibitor of complement inhibits two additional components of the mucosal innate immune system: secretory leukocyte proteinase inhibitor and lysozyme.* Infect Immun, 2002. **70**(9): p. 4908-16.
99. Masschalck, B. and C.W. Michiels, *Antimicrobial properties of lysozyme in relation to foodborne vegetative bacteria.* Crit Rev Microbiol, 2003. **29**(3): p. 191-214.

100. Nash, J.A., et al., *The peptidoglycan-degrading property of lysozyme is not required for bactericidal activity in vivo.* J Immunol, 2006. **177**(1): p. 519-26.
101. George, J. and L. Claflin, *Selection of B cell clones and memory B cells.* Semin Immunol, 1992. **4**(1): p. 11-7.
102. Cross, M., et al., *Mouse lysozyme M gene: isolation, characterization, and expression studies.* Proc Natl Acad Sci U S A, 1988. **85**(17): p. 6232-6.
103. Cole, A.M., et al., *Decreased clearance of Pseudomonas aeruginosa from airways of mice deficient in lysozyme M.* J Leukoc Biol, 2005. **78**(5): p. 1081-5.
104. Shimada, J., et al., *Lysozyme M deficiency leads to an increased susceptibility to Streptococcus pneumoniae-induced otitis media.* BMC Infect Dis, 2008. **8**: p. 134.
105. Ganz, T., et al., *Increased inflammation in lysozyme M-deficient mice in response to Micrococcus luteus and its peptidoglycan.* Blood, 2003. **101**(6): p. 2388-92.
106. Rae, C.S., et al., *Mutations of the Listeria monocytogenes peptidoglycan N-deacetylase and O-acetylase result in enhanced lysozyme sensitivity, bacteriolysis, and hyperinduction of innate immune pathways.* Infect Immun. **79**(9): p. 3596-606.
107. Markart, P., et al., *Comparison of the microbicidal and muramidase activities of mouse lysozyme M and P.* Biochem J, 2004. **380**(Pt 2): p. 385-92.
108. Vollmer, W. and A. Tomasz, *Peptidoglycan N-acetylglucosamine deacetylase, a putative virulence factor in Streptococcus pneumoniae.* Infect Immun, 2002. **70**(12): p. 7176-8.
109. Davis, K.M., et al., *Resistance to mucosal lysozyme compensates for the fitness deficit of peptidoglycan modifications by Streptococcus pneumoniae.* PLoS Pathog, 2008. **4**(12): p. e1000241.
110. Hebert, L., et al., *Enterococcus faecalis constitutes an unusual bacterial model in lysozyme resistance.* Infect Immun, 2007. **75**(11): p. 5390-8.
111. Chateau, A., et al., *CodY regulation is required for full virulence and heme iron acquisition in Bacillus anthracis.* FASEB J. **25**(12): p. 4445-56.
112. Sambrook, J. and M.J. Gething, *Protein structure. Chaperones, paperones.* Nature, 1989. **342**(6247): p. 224-5.

113. Trieu-Cuot, P., Carlier, C., Martin, P., and Courvalin, P., *Plasmid transfer by conjugation from Escherichia coli to*

Gram-positive bacteria. FEMS Microbiol Lett, 1987. **48**: p. 289-294.

114. Pezard, C., P. Berche, and M. Mock, *Contribution of individual toxin components to virulence of Bacillus anthracis.* Infect Immun, 1991. **59**(10): p. 3472-7.

115. Gimenez, A.P., et al., *High bactericidal efficiency of type iia phospholipase A2 against Bacillus anthracis and inhibition of its secretion by the lethal toxin.* J Immunol, 2004. **173**(1): p. 521-30.

116. Brossier, F., M. Levy, and M. Mock, *Anthrax spores make an essential contribution to vaccine efficacy.* Infect Immun, 2002. **70**(2): p. 661-4.

117. Trieu-Cuot, P., et al., *Shuttle vectors containing a multiple cloning site and a lacZ alpha gene for conjugal transfer of DNA from Escherichia coli to gram-positive bacteria.* Gene, 1991. **102**(1): p. 99-104.

118. Namy, O., M. Mock, and A. Fouet, *Co-existence of clpB and clpC in the Bacillaceae.* FEMS Microbiol Lett, 1999. **173**(2): p. 297-302.

119. Fortinea, N., et al., *Optimization of green fluorescent protein expression vectors for in vitro and in vivo detection of Listeria monocytogenes.* Res Microbiol, 2000. **151**(5): p. 353-60.

120. Araki, Y., et al., *Enzymatic deacetylation of N-acetylglucosamine residues in cell wall peptidoglycan.* J Biochem, 1980. **88**(2): p. 469-79.

121. Antignac, A., et al., *Detailed structural analysis of the peptidoglycan of the human pathogen Neisseria meningitidis.* J Biol Chem, 2003. **278**(34): p. 31521-8.

122. Flouret, B., D. Mengin-Lecreulx, and J. van Heijenoort, *Reverse-phase high-pressure liquid chromatography of uridine diphosphate N-acetylmuramyl peptide precursors of bacterial cell wall peptidoglycan.* Anal Biochem, 1981. **114**(1): p. 59-63.

123. Murphy, E., *Nucleotide sequence of a spectinomycin adenyltransferase AAD(9) determinant from Staphylococcus aureus and its relationship to AAD(3") (9).* Mol Gen Genet, 1985. **200**(1): p. 33-9.

124. Qian, H., et al., *Plasmid transfer from Escherichia coli to coryneform bacteria by conjugation.* Chin J Biotechnol, 1994. **10**(1): p. 55-60.

125. Mesnage, S., E. Tosi-Couture, and A. Fouet, *Production and cell surface anchoring of functional fusions between the SLH motifs of the Bacillus anthracis S-layer proteins and the Bacillus subtilis levansucrase.* Mol Microbiol, 1999. **31**(3): p. 927-36.
126. Popham, D.L., et al., *Analysis of the peptidoglycan structure of Bacillus subtilis endospores.* J Bacteriol, 1996. **178**(22): p. 6451-8.
127. Ristroph, J.D. and B.E. Ivins, *Elaboration of Bacillus anthracis antigens in a new, defined culture medium.* Infect Immun, 1983. **39**(1): p. 483-6.
128. Guillouard, I., et al., *Identification of Bacillus subtilis CysL, a regulator of the cysJI operon, which encodes sulfite reductase.* J Bacteriol, 2002. **184**(17): p. 4681-9.
129. Foster, S.J., *Analysis of the autolysins of Bacillus subtilis 168 during vegetative growth and differentiation by using renaturing polyacrylamide gel electrophoresis.* J Bacteriol, 1992. **174**(2): p. 464-70.
130. Markart, P., et al., *Mouse lysozyme M is important in pulmonary host defense against Klebsiella pneumoniae infection.* Am J Respir Crit Care Med, 2004. **169**(4): p. 454-8.
131. Reed, L.J., Muenc493–497h, H. , *A simple method of estimating fifty percent endpoints. The American Journal of Hygiene*, 1938. **27**: p. 493-497.
132. Bergman, N.H., et al., *Transcriptional profiling of the Bacillus anthracis life cycle in vitro and an implied model for regulation of spore formation.* J Bacteriol, 2006. **188**(17): p. 6092-100.
133. Kern, J., et al., *Bacillus anthracis surface-layer proteins assemble by binding to the secondary cell wall polysaccharide in a manner that requires csaB and tagO.* J Mol Biol. **401**(5): p. 757-75.
134. Severin, A., K. Tabei, and A. Tomasz, *The structure of the cell wall peptidoglycan of Bacillus cereus RSVF1, a strain closely related to Bacillus anthracis.* Microb Drug Resist, 2004. **10**(2): p. 77-82.
135. Bera, A., et al., *Why are pathogenic staphylococci so lysozyme resistant? The peptidoglycan O-acetyltransferase OatA is the major determinant for lysozyme resistance of Staphylococcus aureus.* Mol Microbiol, 2005. **55**(3): p. 778-87.
136. Hayashi, H., Y. Araki, and E. Ito, *Occurrence of glucosamine residues with free amino groups in cell wall peptidoglycan from bacilli as a factor responsible for resistance to lysozyme.* J Bacteriol, 1973. **113**(2): p. 592-8.

137. Bui, N.K., et al., *Development of screening assays and discovery of initial inhibitors of pneumococcal peptidoglycan deacetylase PgdA.* Biochem Pharmacol. **82**(1): p. 43-52.
138. Potluri, L.P., M.A. de Pedro, and K.D. Young, *Escherichia coli low-molecular-weight penicillin-binding proteins help orient septal FtsZ, and their absence leads to asymmetric cell division and branching.* Mol Microbiol. **84**(2): p. 203-24.
139. Schirner, K. and J. Errington, *The cell wall regulator {sigma}I specifically suppresses the lethal phenotype of mbl mutants in Bacillus subtilis.* J Bacteriol, 2009. **191**(5): p. 1404-13.
140. Chitlaru, T., et al., *Differential proteomic analysis of the Bacillus anthracis secretome: distinct plasmid and chromosome CO2-dependent cross talk mechanisms modulate extracellular proteolytic activities.* J Bacteriol, 2006. **188**(10): p. 3551-71.
141. Garner, E.C., et al., *Coupled, circumferential motions of the cell wall synthesis machinery and MreB filaments in B. subtilis.* Science. **333**(6039): p. 222-5.
142. Daniel, R.A. and J. Errington, *Control of cell morphogenesis in bacteria: two distinct ways to make a rod-shaped cell.* Cell, 2003. **113**(6): p. 767-76.
143. Kern, V.J., et al., *Surface-Layer (S-Layer) Proteins Sap and EA1 Govern the Binding of the S-Layer-Associated Protein BslO at the Cell Septa of Bacillus anthracis.* J Bacteriol. **194**(15): p. 3833-40.
144. Drysdale, M., et al., *Capsule synthesis by Bacillus anthracis is required for dissemination in murine inhalation anthrax.* EMBO J, 2005. **24**(1): p. 221-7.
145. Bourgogne, A., et al., *Global effects of virulence gene regulators in a Bacillus anthracis strain with both virulence plasmids.* Infect Immun, 2003. **71**(5): p. 2736-43.
146. Antelmann, H., et al., *The extracellular and cytoplasmic proteomes of the non-virulent Bacillus anthracis strain UM23C1-2.* Proteomics, 2005. **5**(14): p. 3684-95.
147. Hanna, M.L., T.M. Tarasow, and J. Perkins, *Mechanistic differences between in vitro assays for hydrazone-based small molecule inhibitors of anthrax lethal factor.* Bioorg Chem, 2007. **35**(1): p. 50-8.
148. Klebe, G., *Virtual ligand screening: strategies, perspectives and limitations.* Drug Discov Today, 2006. **11**(13-14): p. 580-94.

149. Ripphausen, P., et al., *Quo vadis, virtual screening? A comprehensive survey of prospective applications.* J Med Chem. **53**(24): p. 8461-7.
150. Simmons, K.J., I. Chopra, and C.W. Fishwick, *Structure-based discovery of antibacterial drugs.* Nat Rev Microbiol. **8**(7): p. 501-10.
151. Pfeffer, J.M. and A.J. Clarke, *Identification of the first known inhibitors of O-acetylpeptidoglycan esterase: a potential new antibacterial target.* Chembiochem. **13**(5): p. 722-31.
152. Tsalafouta, A., et al., *Purification, crystallization and preliminary X-ray analysis of the peptidoglycan N-acetylglucosamine deacetylase BC1960 from Bacillus cereus in the presence of its substrate (GlcNAc)6.* Acta Crystallogr Sect F Struct Biol Cryst Commun, 2008. **64**(Pt 3): p. 203-5.
153. Carballido-Lopez, R., et al., *Actin homolog MreBH governs cell morphogenesis by localization of the cell wall hydrolase LytE.* Dev Cell, 2006. **11**(3): p. 399-409.
154. Defeu Soufo, H.J. and P.L. Graumann, *Dynamic localization and interaction with other Bacillus subtilis actin-like proteins are important for the function of MreB.* Mol Microbiol, 2006. **62**(5): p. 1340-56.
155. Formstone, A. and J. Errington, *A magnesium-dependent mreB null mutant: implications for the role of mreB in Bacillus subtilis.* Mol Microbiol, 2005. **55**(6): p. 1646-57.
156. Murray, T., D.L. Popham, and P. Setlow, *Bacillus subtilis cells lacking penicillin-binding protein 1 require increased levels of divalent cations for growth.* J Bacteriol, 1998. **180**(17): p. 4555-63.
157. D'Elia, M.A., et al., *Wall teichoic acid polymers are dispensable for cell viability in Bacillus subtilis.* J Bacteriol, 2006. **188**(23): p. 8313-6.
158. Leaver, M. and J. Errington, *Roles for MreC and MreD proteins in helical growth of the cylindrical cell wall in Bacillus subtilis.* Mol Microbiol, 2005. **57**(5): p. 1196-209.